

Supplementary Material: A Biophysically-Based Model of the Optical Properties of Skin Aging

Jose A. Iglesias-Guitian

Carlos Aliaga

Adrian Jarabo

Diego Gutierrez

Universidad de Zaragoza

Contents

The supplementary material includes the formulas used to model the absorption of the chromophores used in our model (Table 1), the formulas to model the total absorption of each layer (Table 2), based on the absorption of each chromophore and their concentration, and the detailed description of how the sebum is modeled in our specular reflectance model (Section A). Finally, we include the database of simulated results for different types of skin, and different ages t , and degrees of skin care ξ , including with a sum-of-Gaussians fit [dL07] for each diffusion profile.

Appendix A: Modelling of sebum

We include the effect of skin surface sebum in the specular reflection, by assuming that the skin is composed of consecutive pyramidal holes whose edges' length and slope are defined by the microfacet properties derived for the surface roughness. Then we fill the holes with a certain volume of sebum. As humans age, sebaceous glands become less active. The thickness of the sebum film can vary between up to $3 \mu\text{m}$ in young skin to $1.69 \mu\text{m}$ in the elderly [PSD79]. Thus, the new value for α is computed as

$$\alpha' = \psi_s \alpha_{sr} \quad (1)$$

with $\psi_s = 1 - a_s/a_t$, a_t is the projected area of a facet of the pyramidal hole, and a_s is the portion of that area covered by sebum. Using trigonometry, we get:

$$\frac{a_s}{a_t} = \frac{l_s^2}{l^2} \quad (2)$$

with l the length of the skin profile scan, and

$$l_s = \sqrt[3]{\frac{3V_s}{2\tan\alpha_{sr}}} \quad (3)$$

where V_s is the volume of sebum computed for an specific age, based on the data of Pochi and colleagues [PSD79].

References

- [DJ06] DONNER C., JENSEN H. W.: A spectral bssrdf for shading human skin. In *EGSR '06* (2006). 1
- [dL07] D'EON E., LUEBKE D.: Advanced techniques for realistic real-time skin rendering. In *GPU Gems 3*. Addison Wesley, 2007, ch. 14. 1

Chromophore	Absorption coefficient
Eumelanin	$\mu_a^{em}(\lambda) = 6.6 \times 10^{10} \times \lambda^{-3.33}$
Pheomelanin	$\mu_a^{pm}(\lambda) = 2.9 \times 10^{14} \times \lambda^{-4.75}$
Oxy-Hb	$\mu_a^{HbO_2}(\lambda) = \frac{\epsilon_{HbO_2}(\lambda)}{66500(\text{g/mole})}$
Deoxy-Hb	$\mu_a^{Hb}(\lambda) = \frac{\epsilon_{Hb}(\lambda)}{66500(\text{g/mole})}$
Carotene	$\mu_a^{car}(\lambda) = \frac{\epsilon_{car}(\lambda)}{537(\text{g/mole})}$
Bilirubin	$\mu_a^{bil}(\lambda) = \frac{\epsilon_{bil}(\lambda)}{585(\text{g/mole})}$
Water	$\mu_a^{H_2O}(\lambda) = \epsilon_{H_2O}(\lambda)$
Baseline	$\mu_a^{base}(\lambda) = 7.84 \cdot 10^7 \cdot \lambda^{-3.255}$

Table 1: The partial contribution of each chromophore to the final spectral absorption coefficient $\mu_a^l(\lambda)$ of a given layer, is obtained by multiplying the spectral extinction coefficient $\epsilon(\lambda)$ of the chromophore, generally measured in $(\text{cm}^{-1}\text{M}^{-1})$, by its concentration c_i in that layer. Chromophore absorptions are obtained from both measured data and previous empirical fits. For μ_a^{em} and μ_a^{pm} , we use empirical fits from [DJ06]. For $\mu_a^{HbO_2}$, μ_a^{Hb} , μ_a^{car} and μ_a^{bil} we use equations from the BioSpec model [KB04]. Last, we employ measured values for $\mu_a^{H_2O}$ taken from [PF97] and baseline absorption for depigmented skin from Saidi [Sai92].

- [KB04] KRISHNASWAMY A., BARANOSKI G. V.: A biophysically-based spectral model of light interaction with human skin. *Computer Graphics Forum* 23, 3 (2004). 1, 2
- [MM02] MEGLINSKI I. V., MATCHER S. J.: Quantitative assessment of skin layers absorption and skin reflectance spectra simulation in the visible and near-infrared spectral regions. *Physiological measurement* 23, 4 (2002). 2

Skin layer absorption coefficient	Reformulated absorption equation
$\mu_a^{sc}(\lambda)$	$[(0.1 - 0.3 \times 10^{-4}\lambda) + 0.125\frac{\lambda}{10} \times \mu_a^{base}(\lambda)] \times (1 - f_{H_2O}) + \mu_a^{H_2O}(\lambda)$
$\mu_a^{le}(\lambda)$	$[v_m \times (\mu_a^{eu}(\lambda) + \mu_a^{ph}(\lambda)) + (1 - v_m) \times (\mu_a^{car}(\lambda) + (1 - c_{car}) \times \mu_a^{base}(\lambda))] \times (1 - f_{H_2O}) + \mu_a^{H_2O}(\lambda)$
$\mu_a^{pd}(\lambda)$	$[v_{Hb}^{pd} \times (\mu_a^{oxy-Hb}(\lambda) + \mu_a^{deoxy-Hb}(\lambda) + \mu_a^{bil}(\lambda) + \mu_a^{car}(\lambda)) + (1 - v_{Hb}) \times \mu_a^{base}(\lambda)] \times (1 - f_{H_2O}) + \mu_a^{H_2O}(\lambda)$
$\mu_a^{rd}(\lambda)$	$[v_{Hb}^{rd} \times (\mu_a^{oxy-Hb}(\lambda) + \mu_a^{deoxy-Hb}(\lambda) + \mu_a^{bil}(\lambda) + \mu_a^{car}(\lambda)) + (1 - v_{Hb}) \times \mu_a^{base}(\lambda)] \times (1 - f_{H_2O}) + \mu_a^{H_2O}(\lambda)$
$\mu_a^{hd}(\lambda)$	$\mu_a^{H_2O}(\lambda)$

Table 2: Wavelength-dependent absorption equations for each layer of our skin model. All equations fit data absorption in mm^{-1} . Different volume fractions v_p and v_r of blood present in tissue are estimated for the papillary and reticular dermis respectively (adapted from [MM02, KB04]).

[PF97] POPE R. M., FRY E. S.: Absorption spectrum (380–700 nm) of pure water. ii. integrating cavity measurements. *Applied optics* 36, 33 (1997). 1

[PSD79] POCHE P. E., STRAUSS J. S., DOWNING D. T.: Age-related changes in sebaceous gland activity. *Journal of Investigative Dermatology* 73, 1 (1979). 1

[Sai92] SAIDI I. S.: *Transcutaneous optical measurement of hyperbilirubinemia in neonates*. PhD thesis, Rice, University, 1992. <http://hdl.handle.net/1911/19082>. 1

Female Age 30 $\xi = 0$ v_m 10 v_{Hb} 5

Gender	Age	ξ	v_m	v_{Hb}	c_{bil}	c_{car}	Skin roughness
Female	30	0	10	5	0.05	2.1e-4	0.081579

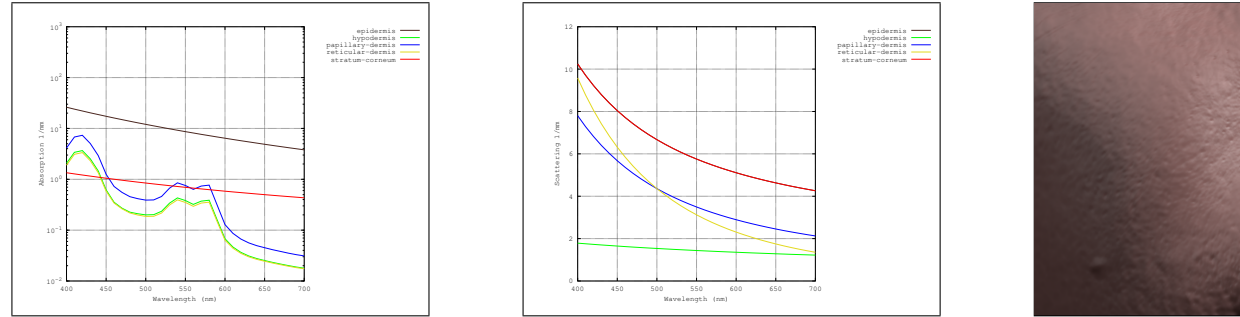


Figure 1: Top row: Full skin phantom description and skin closeup image. Bottom row, from left to right: Absorption and scattering coefficients per-wavelength for each skin layer, and result on a human cheek.

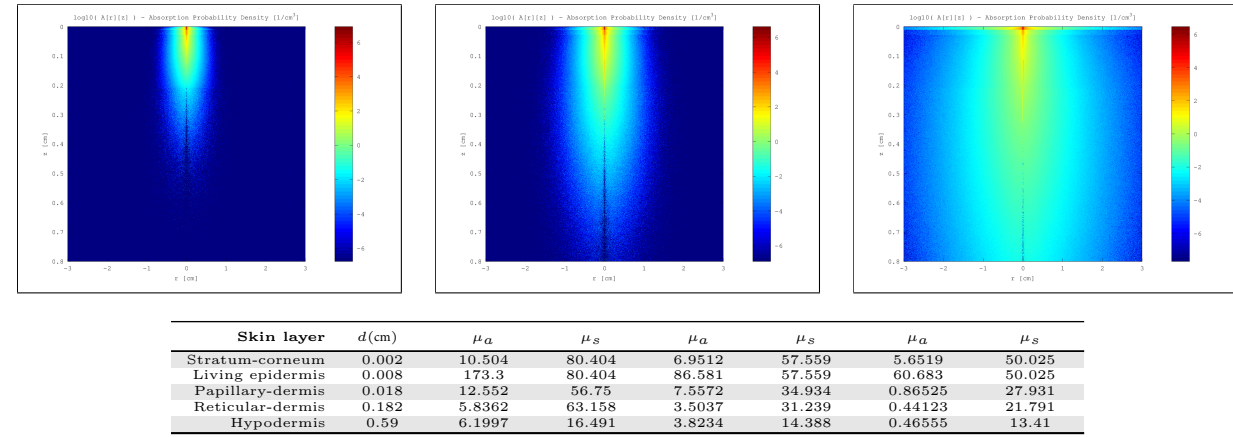
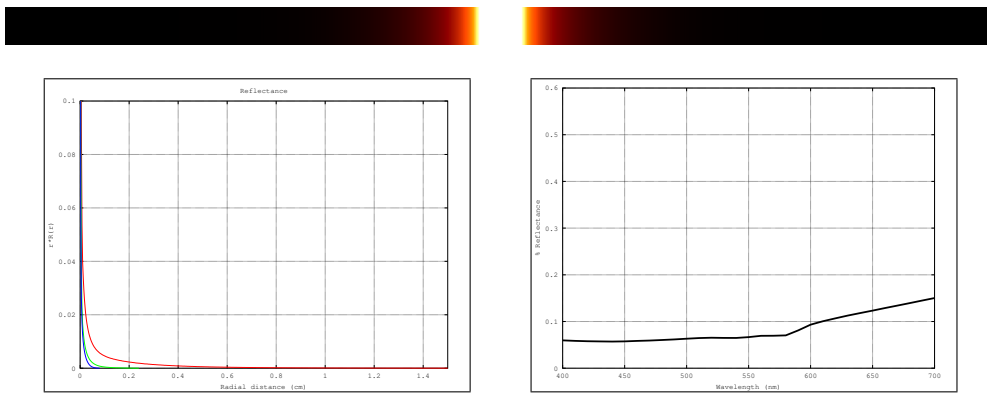


Figure 2: Top row: MonteCarlo simulations for 450nm, 550nm and 610nm. Bottom row: Resultant optical parameters (d , μ_a , μ'_s) applying our skin aging model.



Fitting	R	G	B
w_i v_i RMS,AMAX	(664.116, 46.467, 4.154, 0.714, 0.091, 0.012) (0.500, 2.537, 17.788, 110.758, 900.240, 8447.149) 2.03e-13, 1e-04f	(319.824, 212.952, 26.166, 1.742, 0.190, -7.845) (0.267, 0.581, 2.690, 19.809, 156.189, 2.636) 1.23e-10, 2e-03f	(352.099, 242.769, 28.853, 4.028, 1.011, 0.205) (0.295, 0.414, 1.309, 4.950, 18.779, 69.196) 3.37e-10, 3e-03f

Figure 3: Top row: Diffusion profile response for a pencil light-beam. Middle-row: RGB-profiles and reflectance-per-wavelength. Bottom row: Result of fitting the RGB-profile with 6 weighted Gaussians.

Gender	Age	ξ	v_m	v_{Hb}	c_{bil}	c_{car}	Skin roughness
Female	55	0	10	5	0.05	2.1e-4	0.12802

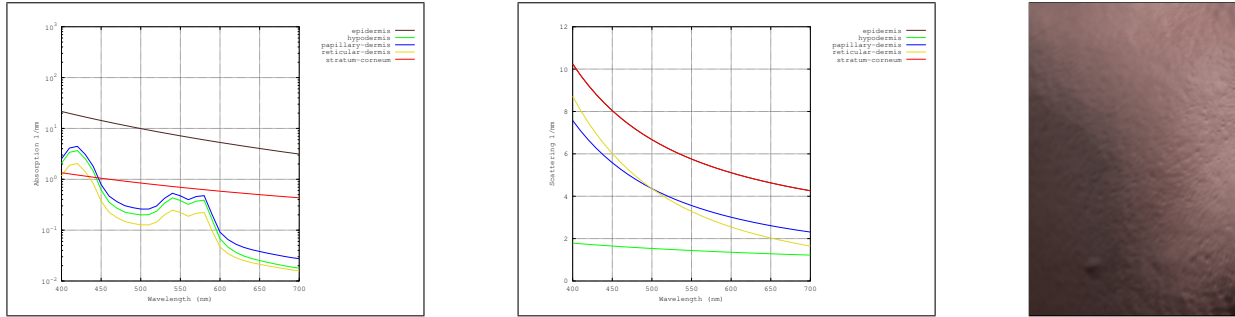


Figure 4: Top row: Full skin phantom description and skin closeup image. Bottom row, from left to right: Absorption and scattering coefficients per-wavelength for each skin layer, and result on a human cheek.

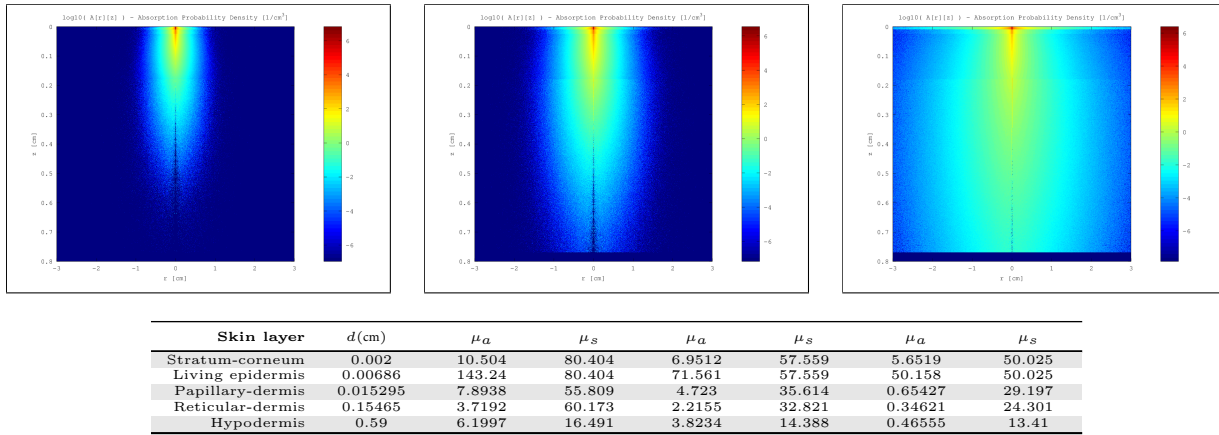
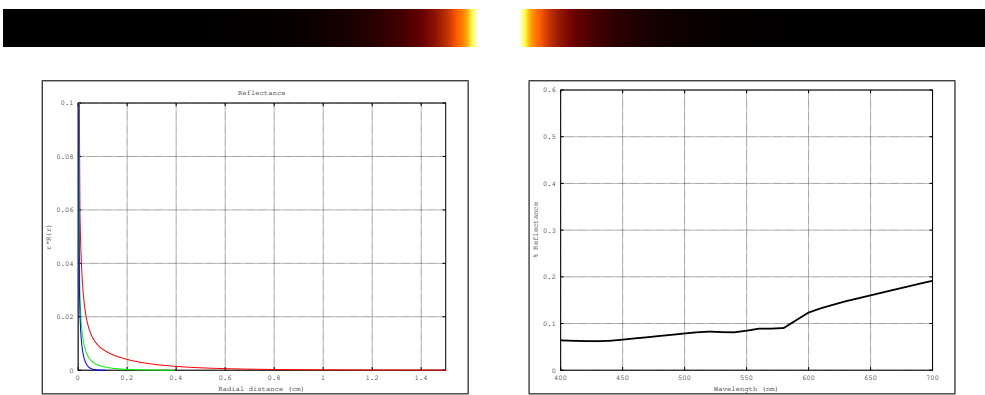


Figure 5: Top row: MonteCarlo simulations for 450nm, 550nm and 610nm. Bottom row: Resultant optical parameters (d , μ_a , μ'_s) applying our skin aging model.



Fitting	R	G	B
w_i v_i RMS,AMAX	(670.886, 53.509, 5.047, 0.906, 0.139, 0.019) (0.492, 2.306, 17.780, 120.470, 998.124, 8405.643) 2.71e-12, 5e-04f	(408.487, 35.095, 3.352, 0.778, 0.150, 0.018) (0.436, 1.790, 9.785, 43.955, 211.079, 1372.135) 1.32e-09, 6e-03f	(2.203, 2.175, 2.170, 2.169, 2.168, -0.063) (1.271, 1.216, 1.193, 1.306, 1.257, 0.538) 9.15e-01, 2e+02f

Figure 6: Top row: Diffusion profile response for a pencil light-beam. Middle-row: RGB-profiles and reflectance-per-wavelength. Bottom row: Result of fitting the RGB-profile with 6 weighted Gaussians.

Gender	Age	ξ	v_m	v_{Hb}	c_{bil}	c_{car}	Skin roughness
Female	80	0	10	5	0.05	2.1e-4	0.18059

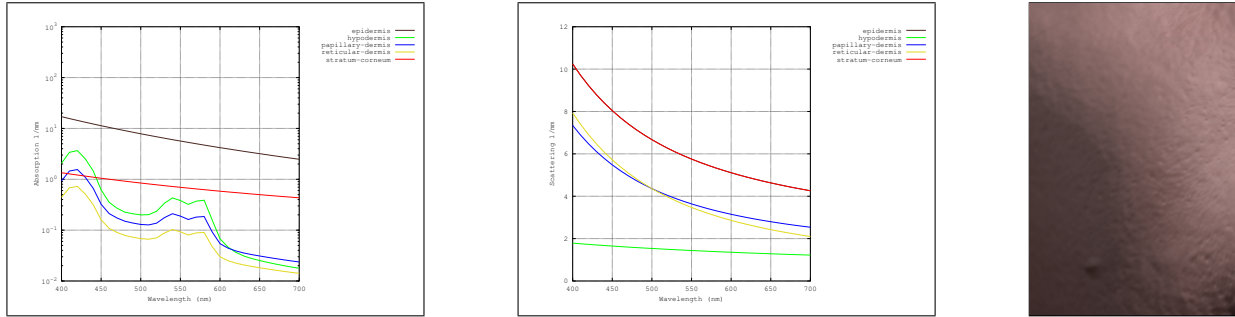


Figure 7: Top row: Full skin phantom description and skin closeup image. Bottom row, from left to right: Absorption and scattering coefficients per-wavelength for each skin layer, and result on a human cheek.

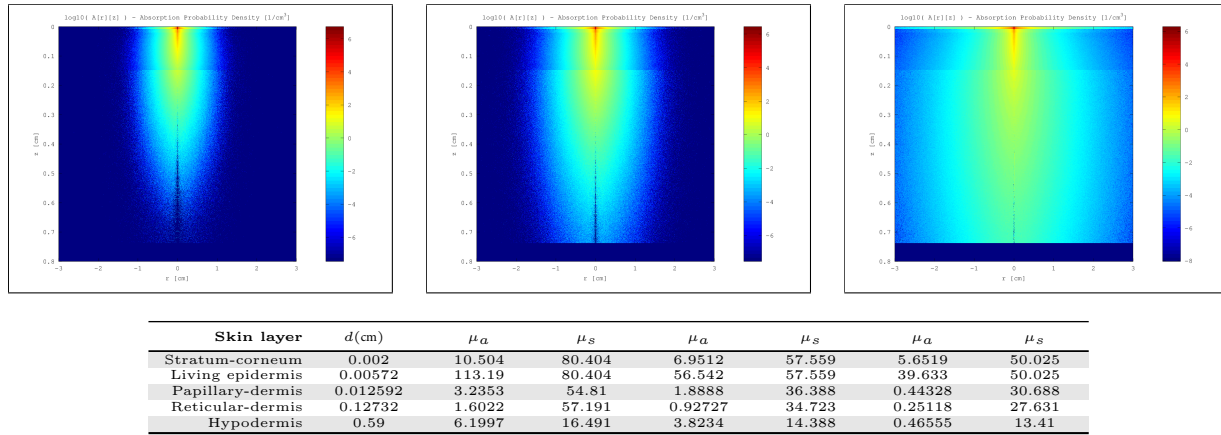


Figure 8: Top row: MonteCarlo simulations for 450nm, 550nm and 610nm. Bottom row: Resultant optical parameters (d , μ_a , μ'_s) applying our skin aging model.

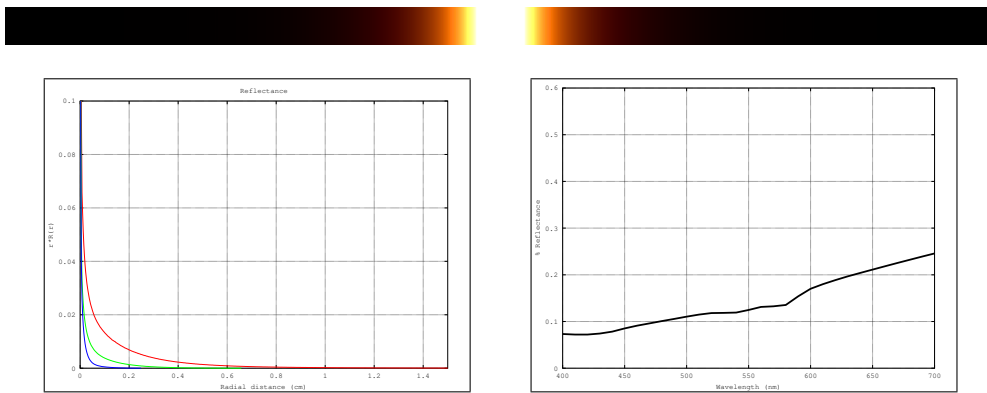


Figure 9: Top row: Diffusion profile response for a pencil light-beam. Middle-row: RGB-profiles and reflectance-per-wavelength. Bottom row: Result of fitting the RGB-profile with 6 weighted Gaussians.

Gender	Age	ξ	v_m	v_{Hb}	c_{bil}	c_{car}	Skin roughness
Female	30	1	10	5	0.05	2.1e-4	0.069549

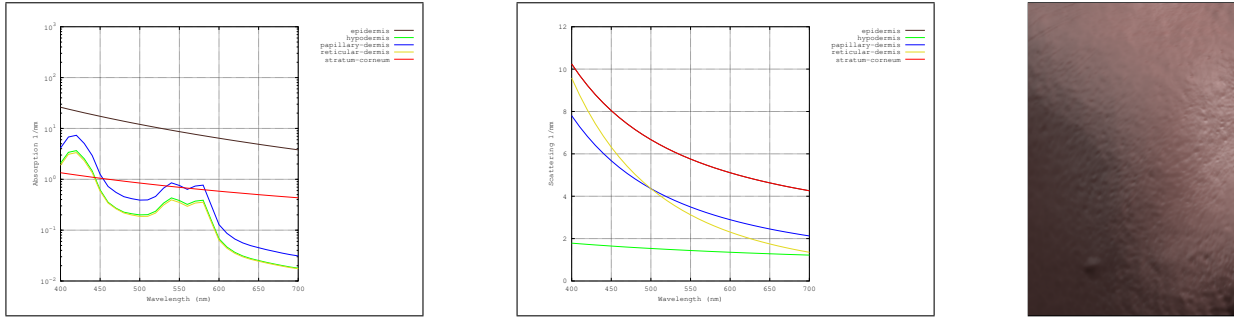


Figure 10: Top row: Full skin phantom description and skin closeup image. Bottom row, from left to right: Absorption and scattering coefficients per-wavelength for each skin layer, and result on a human cheek.

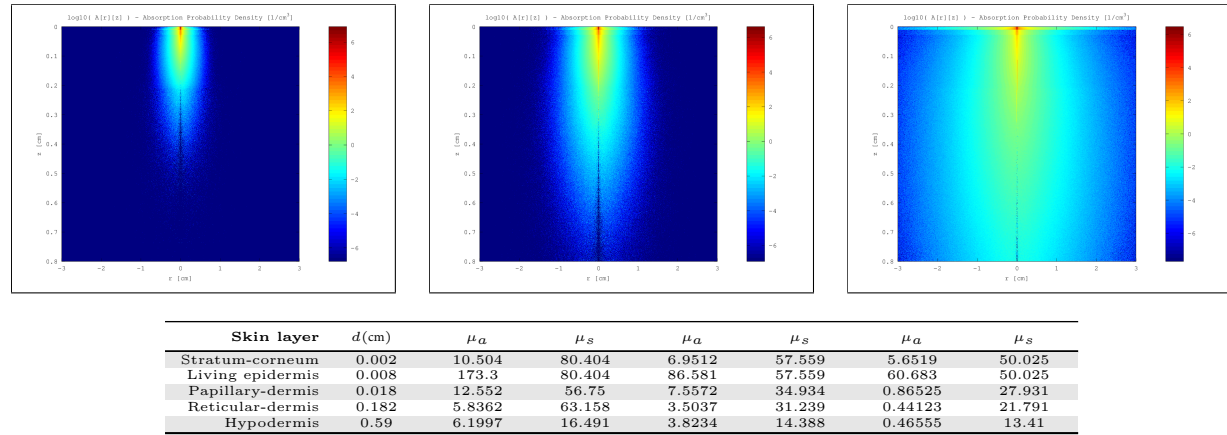
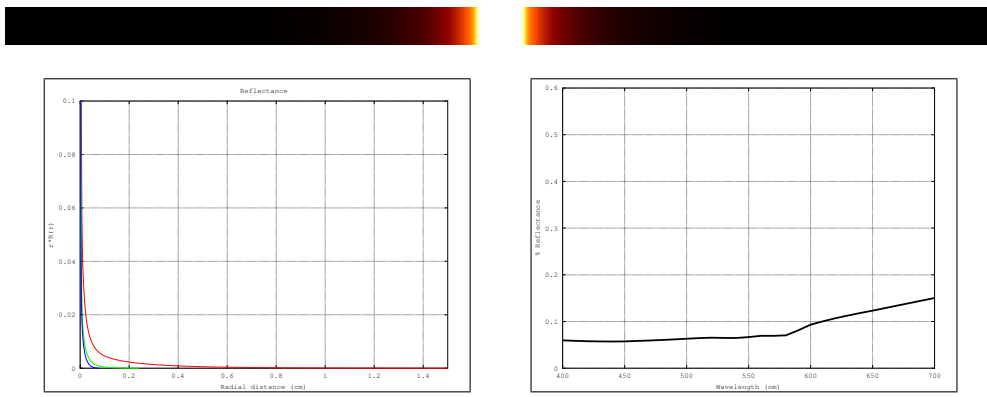


Figure 11: Top row: MonteCarlo simulations for 450nm, 550nm and 610nm. Bottom row: Resultant optical parameters (d , μ_a , μ'_s) applying our skin aging model.



Fitting	R	G	B
w_i v_i RMS,AMAX	(667.196, 48.133, 4.220, 0.725, 0.093, 0.012) (0.495, 2.487, 17.498, 109.109, 884.029, 8363.333) 2.08e-13, 1e-04f	(218.600, 212.586, 35.751, 1.707, 0.187, -17.680) (0.343, 0.572, 2.703, 20.168, 157.685, 2.658) 1.65e-09, 6e-03f	(422.316, 205.908, 28.145, 3.917, 1.002, 0.204) (0.285, 0.431, 1.336, 5.014, 18.911, 69.250) 4.93e-10, 4e-03f

Figure 12: Top row: Diffusion profile response for a pencil light-beam. Middle-row: RGB-profiles and reflectance-per-wavelength. Bottom row: Result of fitting the RGB-profile with 6 weighted Gaussians.

Gender	Age	ξ	v_m	v_{Hb}	c_{bil}	c_{car}	Skin roughness
Female	55	1	10	5	0.05	2.1e-4	0.099683

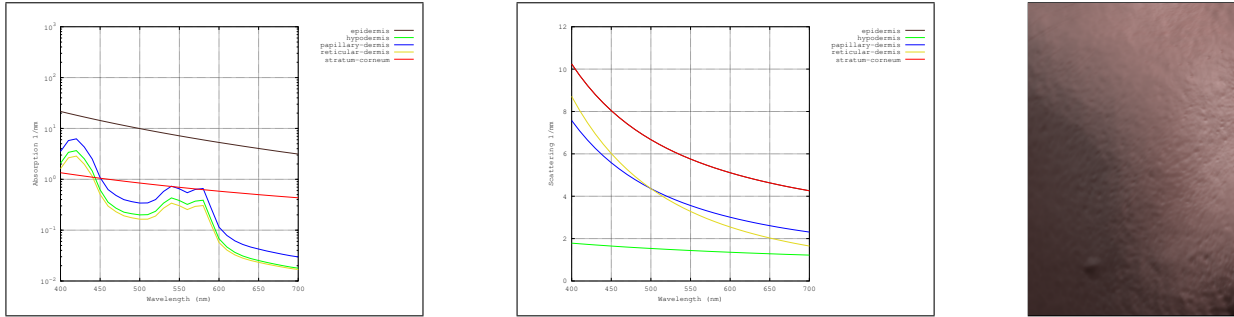


Figure 13: Top row: Full skin phantom description and skin closeup image. Bottom row, from left to right: Absorption and scattering coefficients per-wavelength for each skin layer, and result on a human cheek.

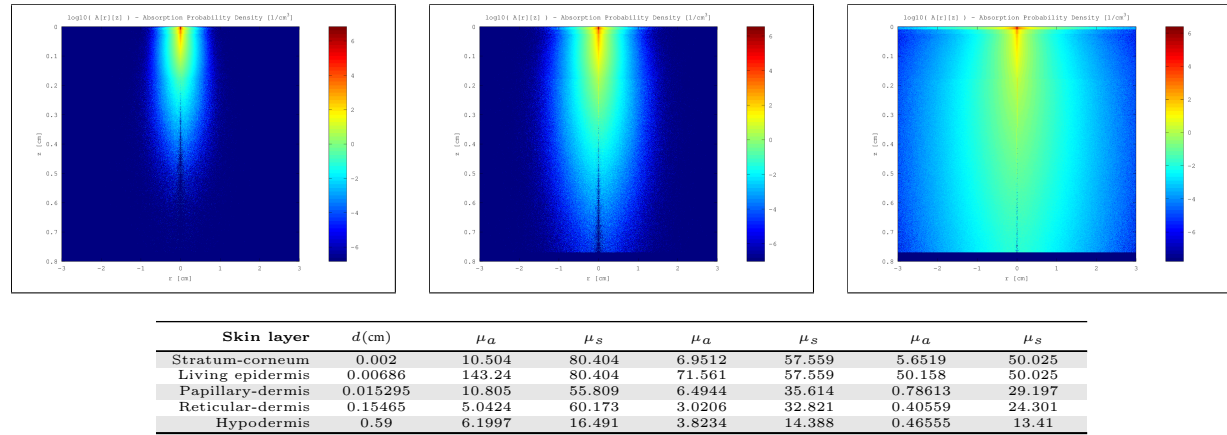
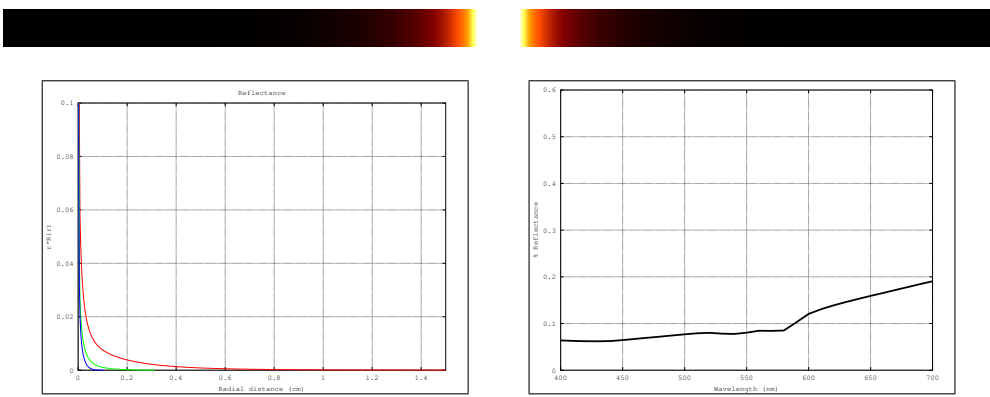


Figure 14: Top row: MonteCarlo simulations for 450nm, 550nm and 610nm. Bottom row: Resultant optical parameters (d , μ_a , μ'_s) applying our skin aging model.



Fitting	R	G	B
w_i v_i RMS,AMAX	(672.321, 54.642, 5.128, 0.921, 0.140, 0.019) (0.490, 2.273, 17.367, 116.808, 960.373, 8158.612) 2.29e-12, 4e-04f	(444.419, 45.453, 9.447, 2.302, 0.423, 0.040) (0.380, 1.268, 3.208, 16.079, 91.135, 681.992) 9.41e-10, 5e-03f	(2.207, 2.175, 2.169, 2.165, -0.062) (1.270, 1.215, 1.193, 1.305, 1.256, 0.537) 9.15e-01, 2e+02f

Figure 15: Top row: Diffusion profile response for a pencil light-beam. Middle-row: RGB-profiles and reflectance-per-wavelength. Bottom row: Result of fitting the RGB-profile with 6 weighted Gaussians.

Gender	Age	ξ	v_m	v_{Hb}	c_{bil}	c_{car}	Skin roughness
Female	80	1	10	5	0.05	2.1e-4	0.14797

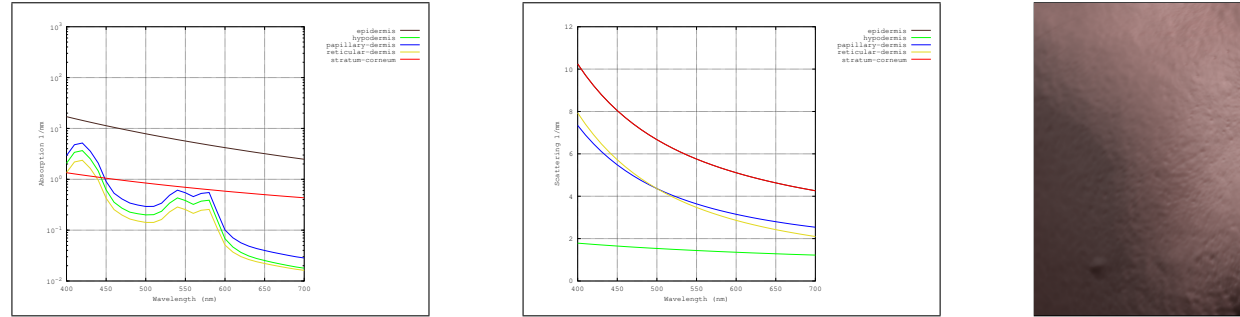


Figure 16: Top row: Full skin phantom description and skin closeup image. Bottom row, from left to right: Absorption and scattering coefficients per-wavelength for each skin layer, and result on a human cheek.

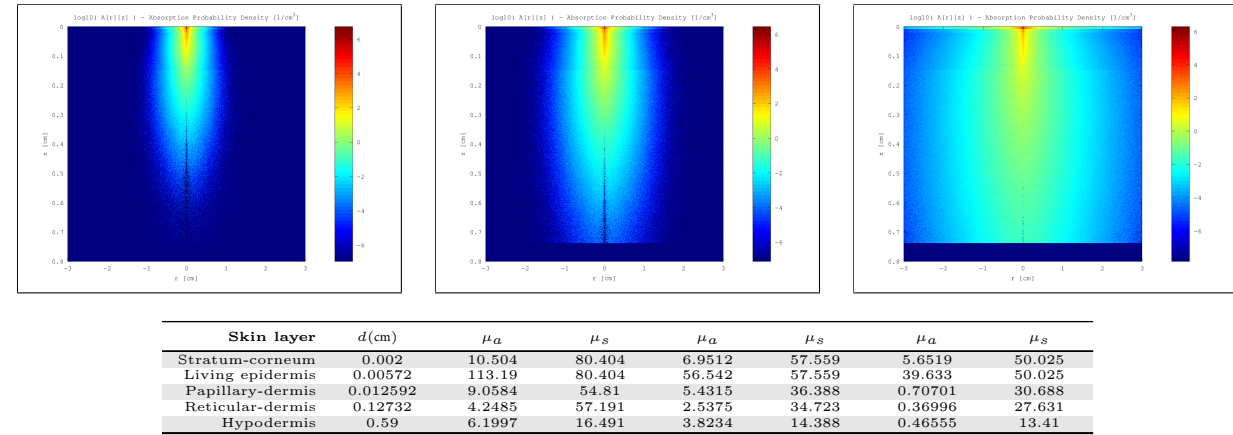
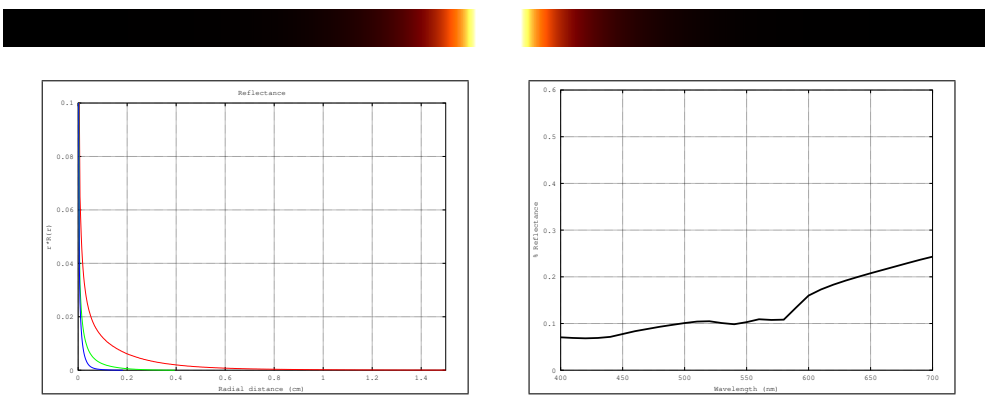


Figure 17: Top row: MonteCarlo simulations for 450nm, 550nm and 610nm. Bottom row: Resultant optical parameters (d , μ_a , μ'_s) applying our skin aging model.



Fitting	R	G	B
w_i v_i RMS,AMAX	(2077.740, 125.577, 7.550, 1.424, 0.253, 0.036) (0.212, 1.460, 13.665, 101.680, 843.909, 6916.234) 1.29e-08, 3e-02f	(137.296, 95.203, 84.042, 51.686, 3.942, 0.325) (0.432, 0.735, 0.931, 0.391, 14.094, 0.057) 1.06e-03, 5e+00f	(478.496, 136.175, 16.869, 3.266, 0.680, 0.055) (0.309, 0.642, 2.236, 9.837, 42.952, 233.925) 3.66e-09, 1e-02f

Figure 18: Top row: Diffusion profile response for a pencil light-beam. Middle-row: RGB-profiles and reflectance-per-wavelength. Bottom row: Result of fitting the RGB-profile with 6 weighted Gaussians.

Female Age 30 $\xi = 0$ v_m 15 v_{Hb} 5

Gender	Age	ξ	v_m	v_{Hb}	c_{bil}	c_{car}	Skin roughness
Female	30	0	15	5	0.05	2.1e-4	0.081579

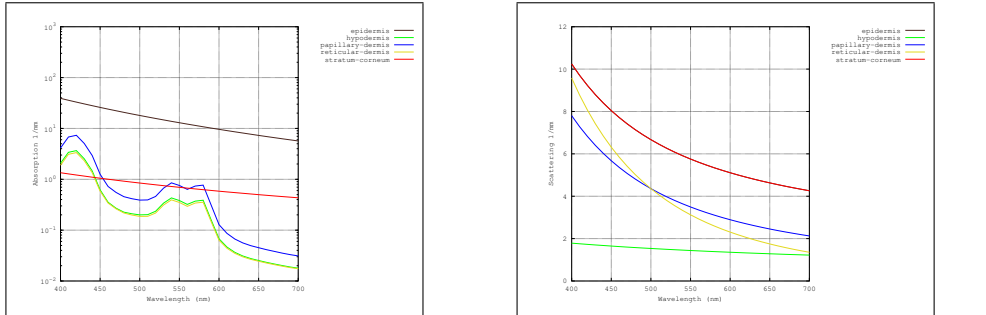


Figure 19: Top row: Full skin phantom description and skin closeup image. Bottom row, from left to right: Absorption and scattering coefficients per-wavelength for each skin layer, and result on a human cheek.

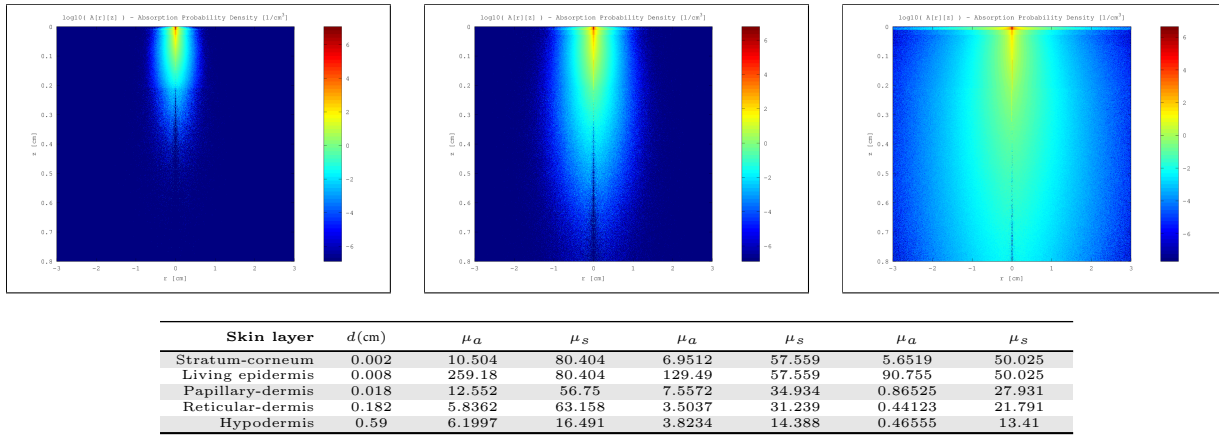
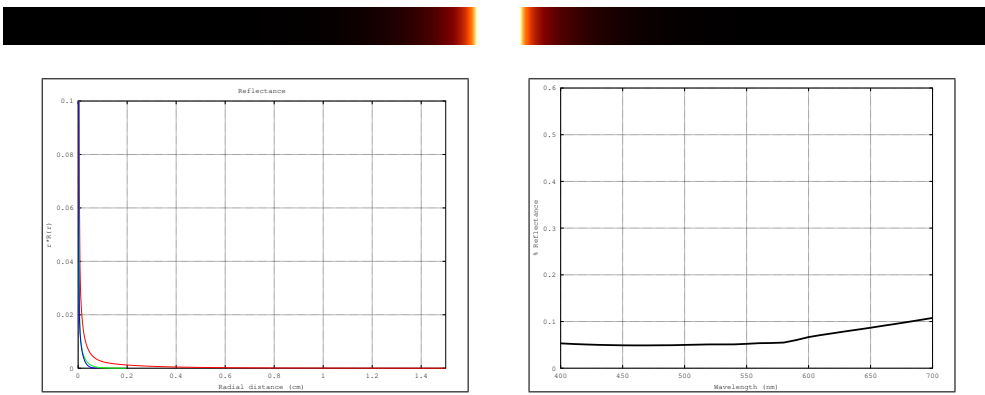


Figure 20: Top row: MonteCarlo simulations for 450nm, 550nm and 610nm. Bottom row: Resultant optical parameters (d , μ_a , μ_s') applying our skin aging model.



Fitting	R	G	B
w_i v_i RMS,AMAX	(667.106, 36.646, 3.130, 0.547, 0.061, 0.007) (0.486, 2.442, 15.952, 96.113, 731.241, 7683.410) 4.48e-14, 6e-05f	(349.940, 124.105, 14.625, 1.603, 0.354, 0.044) (0.335, 0.599, 2.230, 10.991, 52.405, 246.059) 1.71e-10, 2e-03f	(304.844, 269.051, 90.778, 6.451, 1.342, 0.282) (0.266, 0.317, 0.607, 2.809, 13.175, 57.667) 2.91e-09, 8e-03f

Figure 21: Top row: Diffusion profile response for a pencil light-beam. Middle-row: RGB-profiles and reflectance-per-wavelength. Bottom row: Result of fitting the RGB-profile with 6 weighted Gaussians.

Gender	Age	ξ	v_m	v_{Hb}	c_{bil}	c_{car}	Skin roughness
Female	55	0	15	5	0.05	2.1e-4	0.12802

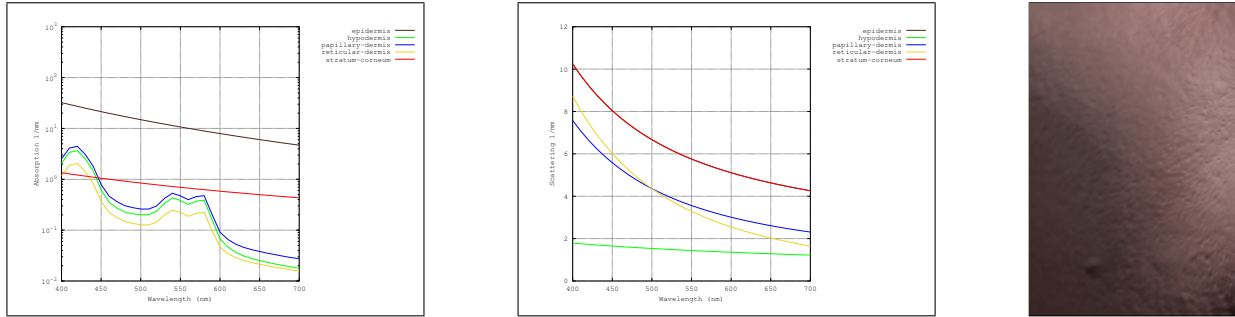


Figure 22: Top row: Full skin phantom description and skin closeup image. Bottom row, from left to right: Absorption and scattering coefficients per-wavelength for each skin layer, and result on a human cheek.

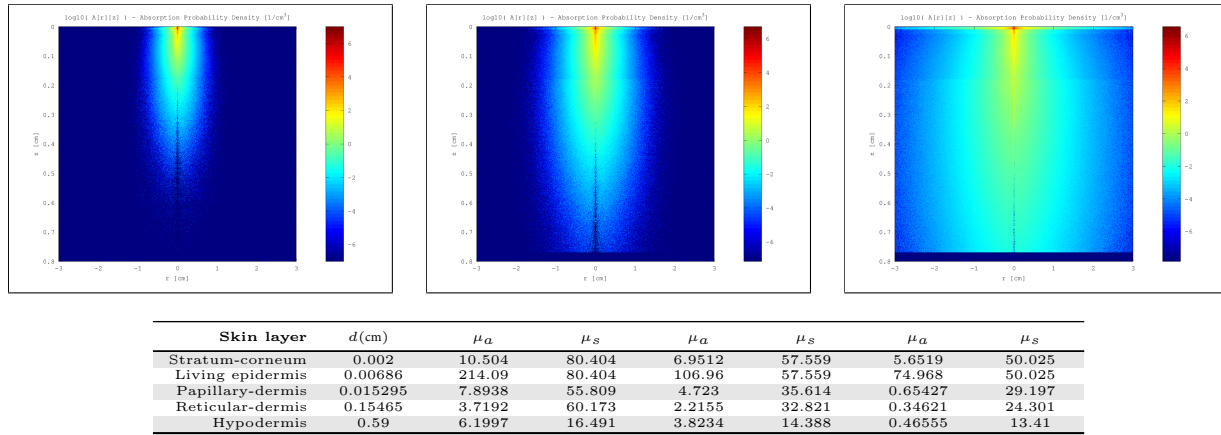
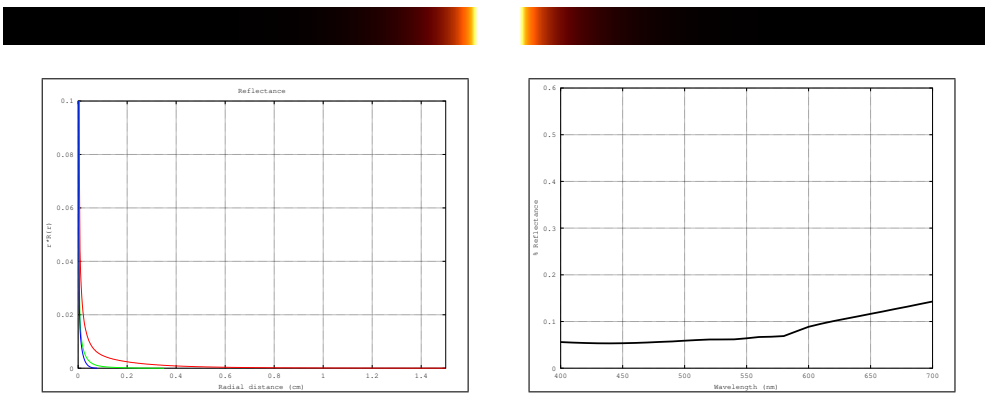


Figure 23: Top row: MonteCarlo simulations for 450nm, 550nm and 610nm. Bottom row: Resultant optical parameters (d , μ_a , μ_s') applying our skin aging model.



Fitting	R	G	B
w_i v_i RMS,AMAX	(676.077, 45.931, 4.137, 0.723, 0.098, 0.013) (0.477, 2.187, 15.807, 104.123, 852.442, 7719.352) 2.54e-12, 4e-04f	(2.159, 2.130, 2.129, 2.118, 2.113, -0.012) (1.292, 1.192, 1.225, 1.283, 1.336, 0.392) 9.07e-01, 1e+02f	(380.403, 258.112, 49.122, 6.195, 1.299, 0.259) (0.271, 0.347, 0.837, 3.246, 14.760, 62.008) 7.14e-09, 1e-02f

Figure 24: Top row: Diffusion profile response for a pencil light-beam. Middle-row: RGB-profiles and reflectance-per-wavelength. Bottom row: Result of fitting the RGB-profile with 6 weighted Gaussians.

Gender	Age	ξ	v_m	v_{Hb}	c_{bil}	c_{car}	Skin roughness
Female	80	0	15	5	0.05	2.1e-4	0.18059

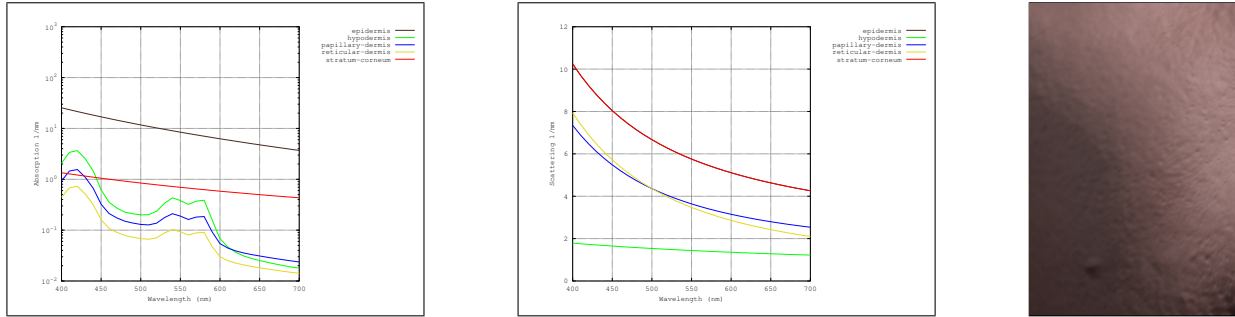


Figure 25: Top row: Full skin phantom description and skin closeup image. Bottom row, from left to right: Absorption and scattering coefficients per-wavelength for each skin layer, and result on a human cheek.

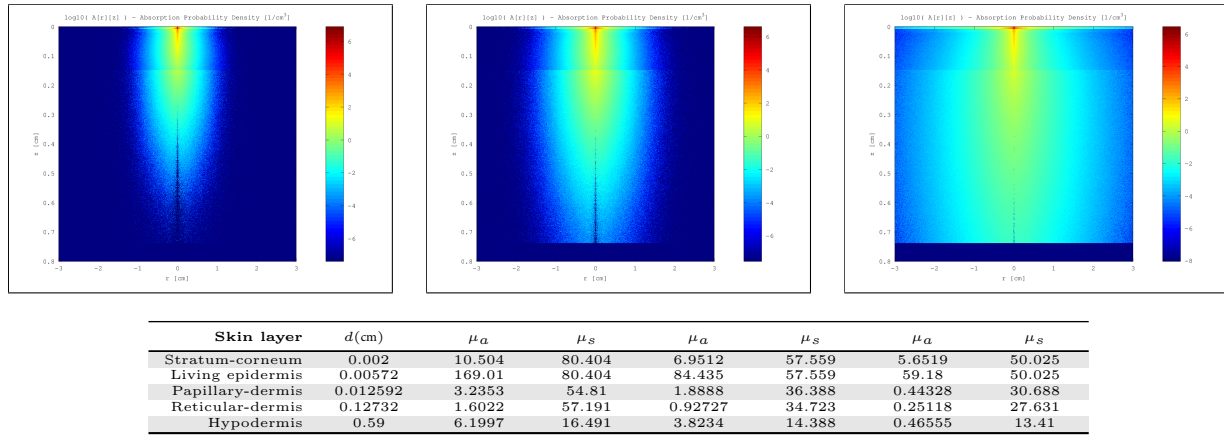


Figure 26: Top row: MonteCarlo simulations for 450nm, 550nm and 610nm. Bottom row: Resultant optical parameters (d , μ_a , μ'_s) applying our skin aging model.

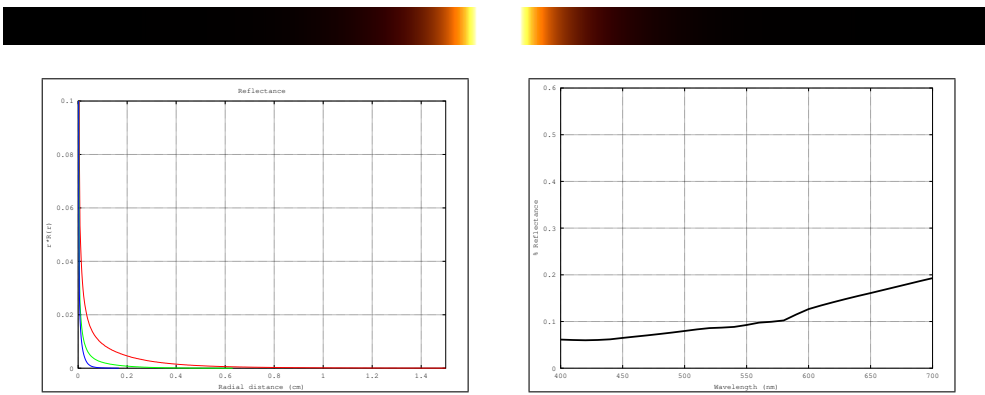


Figure 27: Top row: Diffusion profile response for a pencil light-beam. Middle-row: RGB-profiles and reflectance-per-wavelength. Bottom row: Result of fitting the RGB-profile with 6 weighted Gaussians.

Gender	Age	ξ	v_m	v_{Hb}	c_{bil}	c_{car}	Skin roughness
Female	30	1	15	5	0.05	2.1e-4	0.069549

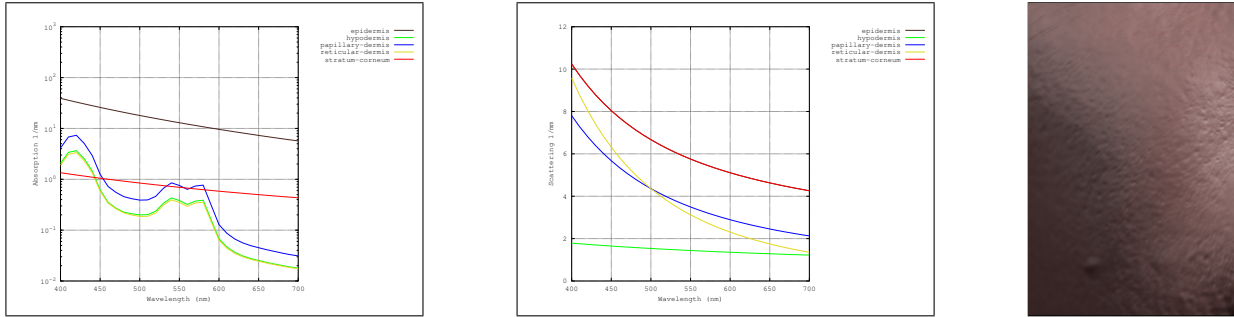


Figure 28: Top row: Full skin phantom description and skin closeup image. Bottom row, from left to right: Absorption and scattering coefficients per-wavelength for each skin layer, and result on a human cheek.

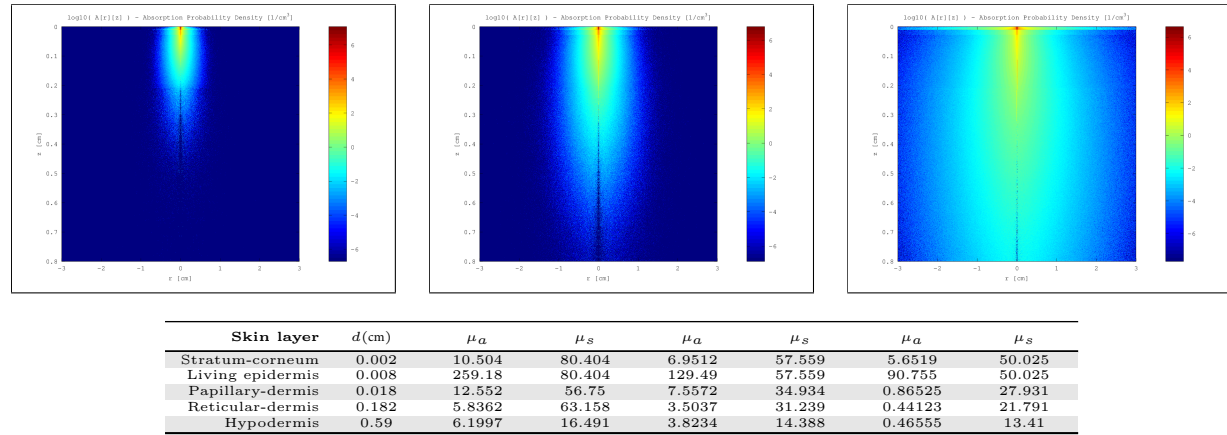
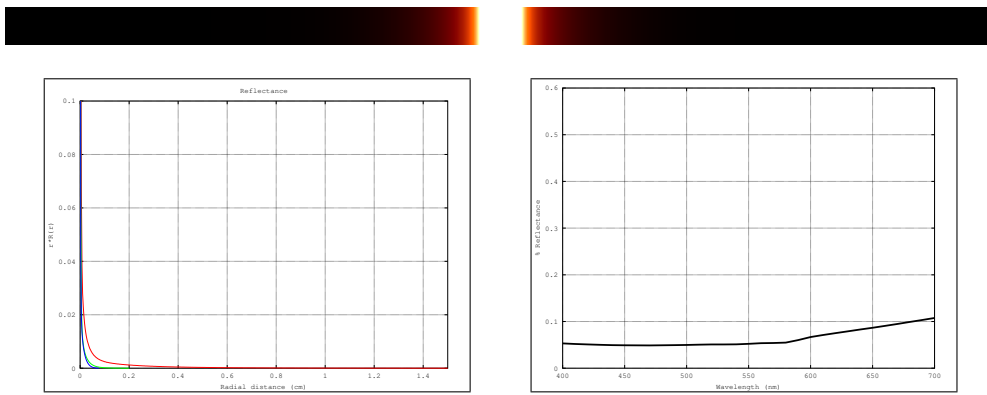


Figure 29: Top row: MonteCarlo simulations for 450nm, 550nm and 610nm. Bottom row: Resultant optical parameters (d , μ_a , μ'_s) applying our skin aging model.



Fitting	R	G	B
w_i v_i RMS,AMAX	(673.470, 38.581, 3.279, 0.599, 0.074, 0.008) (0.479, 2.355, 14.873, 85.484, 602.253, 6675.745) 8.90e-11, 3e-03f	(375.005, 140.397, 14.250, 1.566, 0.341, 0.041) (0.303, 0.596, 2.264, 11.343, 54.232, 253.184) 1.52e-10, 2e-03f	(296.158, 280.654, 103.185, 6.807, 1.339, 0.277) (0.269, 0.296, 0.587, 2.737, 13.329, 57.976) 5.91e-09, 1e-02f

Figure 30: Top row: Diffusion profile response for a pencil light-beam. Middle-row: RGB-profiles and reflectance-per-wavelength. Bottom row: Result of fitting the RGB-profile with 6 weighted Gaussians.

Gender	Age	ξ	v_m	v_{Hb}	c_{bil}	c_{car}	Skin roughness
Female	55	1	15	5	0.05	2.1e-4	0.099683

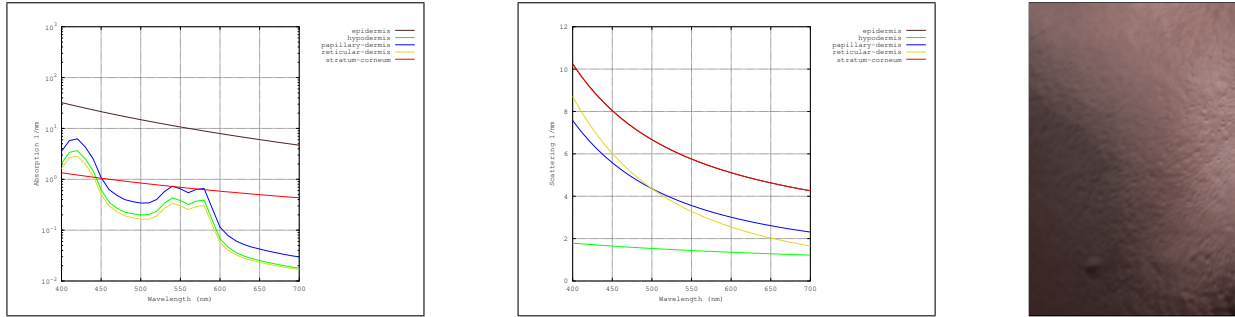


Figure 31: Top row: Full skin phantom description and skin closeup image. Bottom row, from left to right: Absorption and scattering coefficients per-wavelength for each skin layer, and result on a human cheek.

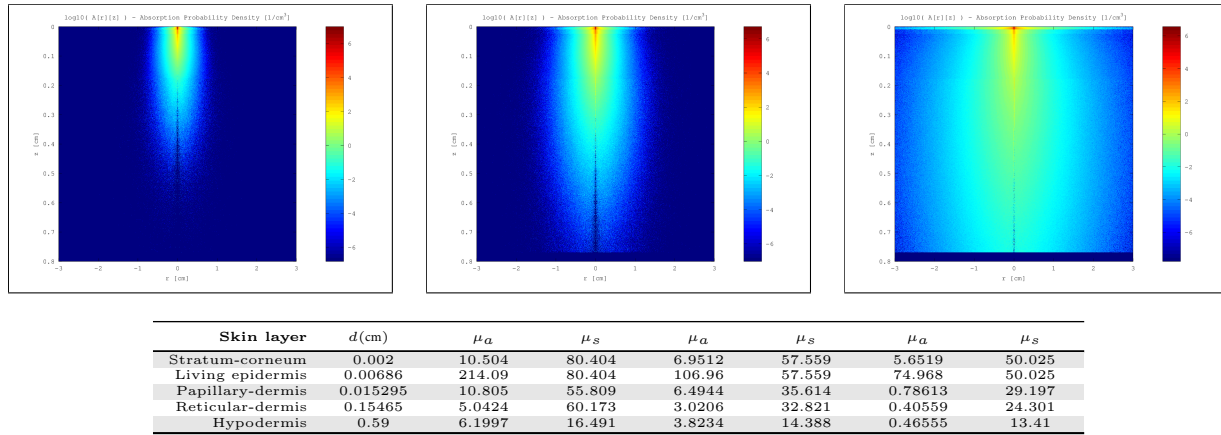


Figure 32: Top row: MonteCarlo simulations for 450nm, 550nm and 610nm. Bottom row: Resultant optical parameters (d , μ_a , μ_s') applying our skin aging model.

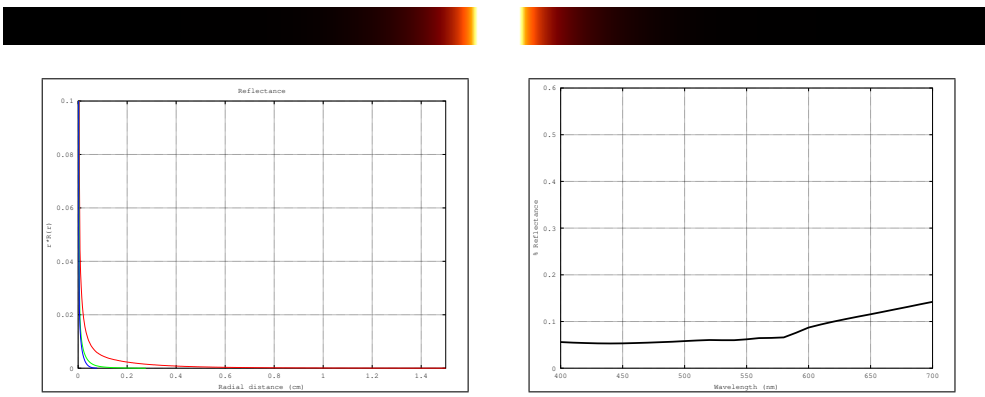


Figure 33: Top row: Diffusion profile response for a pencil light-beam. Middle-row: RGB-profiles and reflectance-per-wavelength. Bottom row: Result of fitting the RGB-profile with 6 weighted Gaussians.

Gender	Age	ξ	v_m	v_{Hb}	c_{bil}	c_{car}	Skin roughness
Female	80	1	15	5	0.05	2.1e-4	0.14797

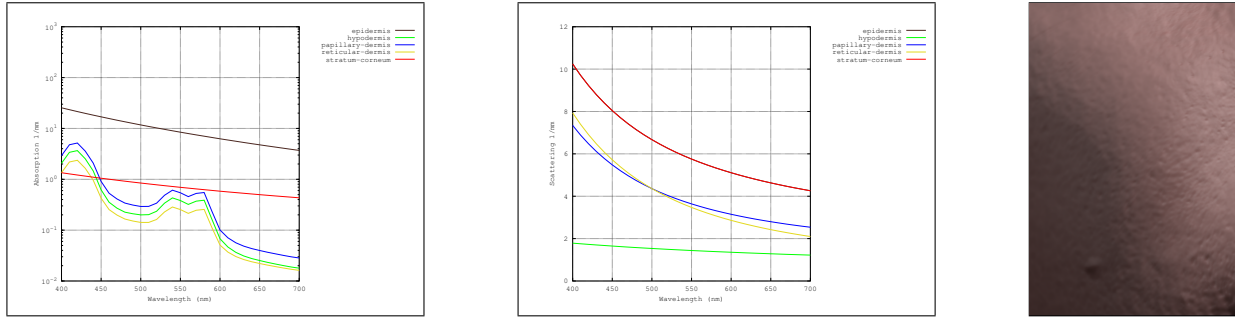


Figure 34: Top row: Full skin phantom description and skin closeup image. Bottom row, from left to right: Absorption and scattering coefficients per-wavelength for each skin layer, and result on a human cheek.

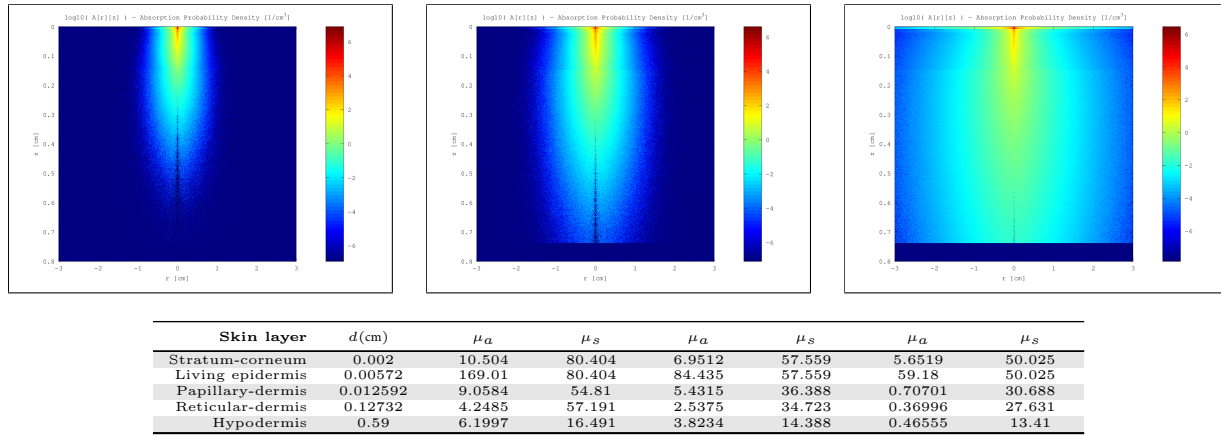
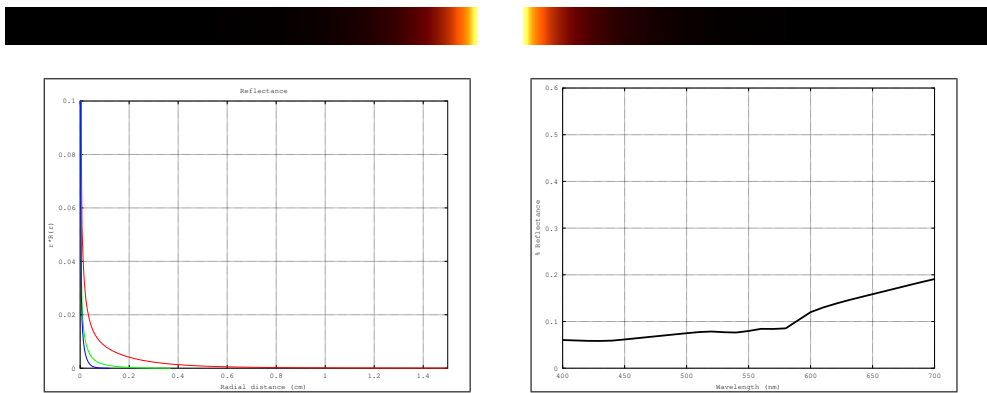


Figure 35: Top row: MonteCarlo simulations for 450nm, 550nm and 610nm. Bottom row: Resultant optical parameters (d , μ_a , μ'_s) applying our skin aging model.



Fitting	R	G	B
w_i v_i RMS,AMAX	(1.794, 1.744, 1.739, -0.031, -0.091, -0.098) (1.280, 1.420, 1.182, 0.586, 0.705, 0.774) 9.76e-01, 3e+02f	(2.008, 1.928, 1.909, 0.049, 0.008, -0.002) (1.101, 1.221, 1.217, 0.555, 0.873, 0.572) 9.51e-01, 2e+02f	(372.093, 299.433, 39.460, 4.256, 1.029, 0.162) (0.263, 0.364, 1.172, 5.255, 21.853, 91.549) 3.33e-09, 9e-03f

Figure 36: Top row: Diffusion profile response for a pencil light-beam. Middle-row: RGB-profiles and reflectance-per-wavelength. Bottom row: Result of fitting the RGB-profile with 6 weighted Gaussians.

Female Age 30 $\xi = 0$ v_m 1 v_{Hb} 5

Gender	Age	ξ	v_m	v_{Hb}	c_{bil}	c_{car}	Skin roughness
Female	30	0	1	5	0.05	2.1e-4	0.081579

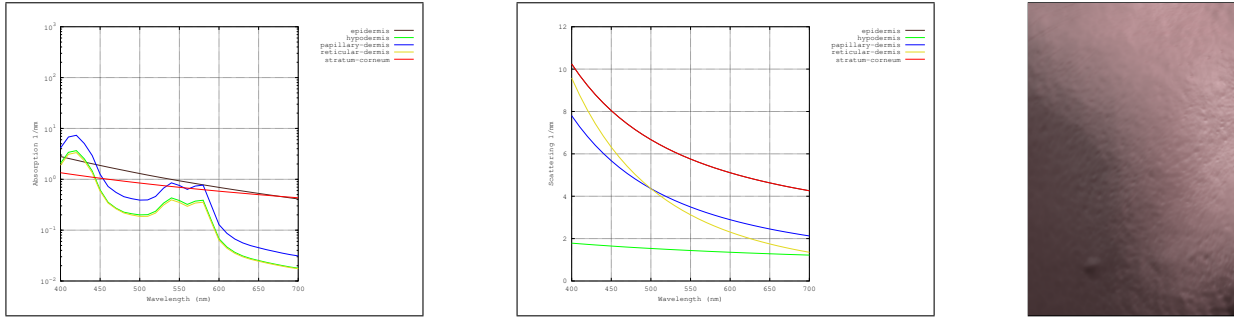


Figure 37: Top row: Full skin phantom description and skin closeup image. Bottom row, from left to right: Absorption and scattering coefficients per-wavelength for each skin layer, and result on a human cheek.

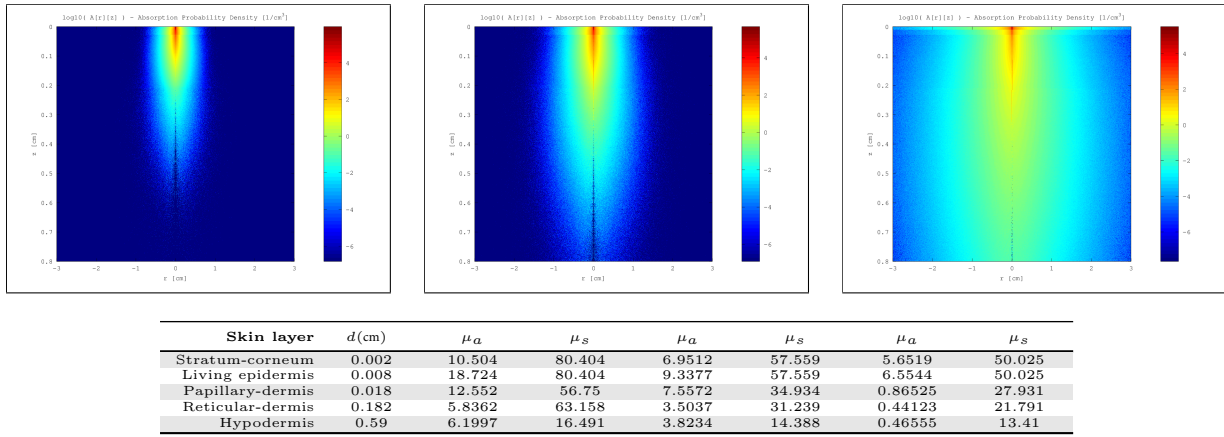
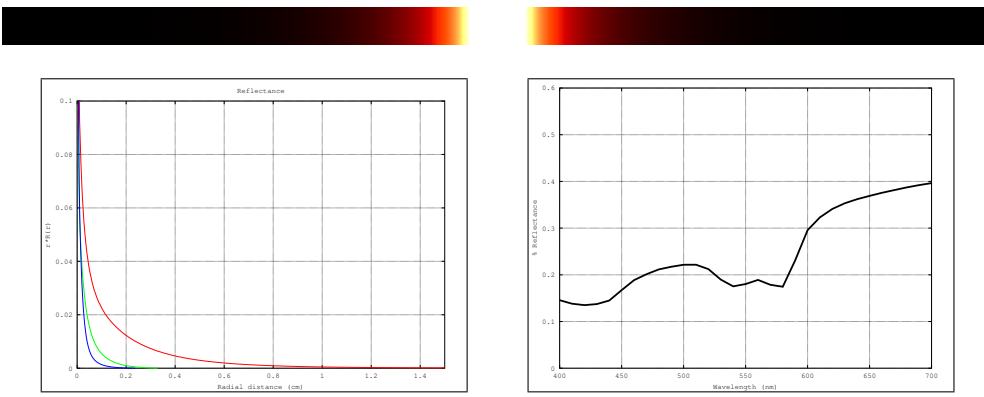


Figure 38: Top row: MonteCarlo simulations for 450nm, 550nm and 610nm. Bottom row: Resultant optical parameters (d , μ_a , μ_s') applying our skin aging model.



Fitting	R	G	B
w_i v_i RMS,AMAX	(651.641, 68.357, 7.286, 1.511, 0.280, 0.041) (0.546, 2.971, 26.045, 182.768, 1465.997, 11165.793) 5.91e-12, 8e-04f	(381.727, 43.519, 5.270, 1.719, 0.451, 0.072) (0.513, 2.526, 14.615, 60.846, 253.440, 1210.122) 2.89e-14, 3e-05f	(450.700, 44.670, 7.516, 2.482, 0.506, 0.052) (0.504, 2.385, 10.401, 35.256, 125.002, 596.212) 4.19e-15, 1e-05f

Figure 39: Top row: Diffusion profile response for a pencil light-beam. Middle-row: RGB-profiles and reflectance-per-wavelength. Bottom row: Result of fitting the RGB-profile with 6 weighted Gaussians.

Female Age 55 $\xi = 0$ v_m 1 v_{Hb} 5

Gender	Age	ξ	v_m	v_{Hb}	c_{bil}	c_{car}	Skin roughness
Female	55	0	1	5	0.05	2.1e-4	0.12802

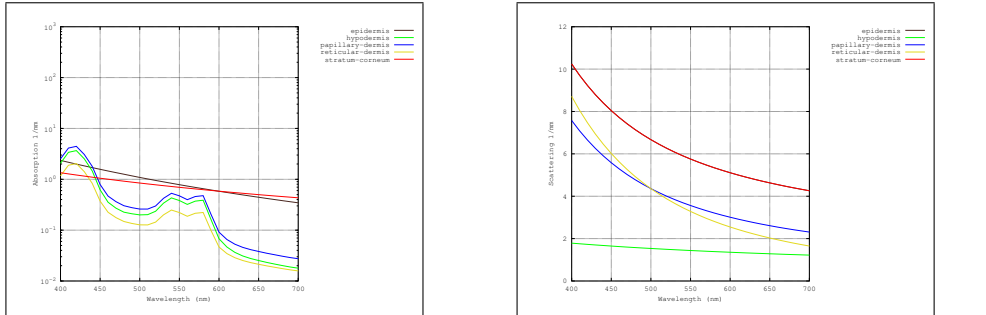


Figure 40: Top row: Full skin phantom description and skin closeup image. Bottom row, from left to right: Absorption and scattering coefficients per-wavelength for each skin layer, and result on a human cheek.

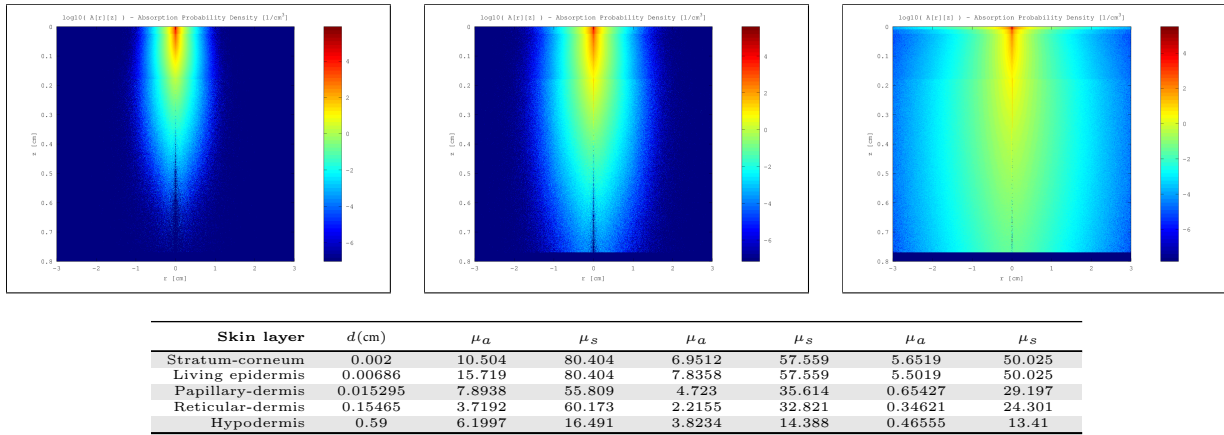
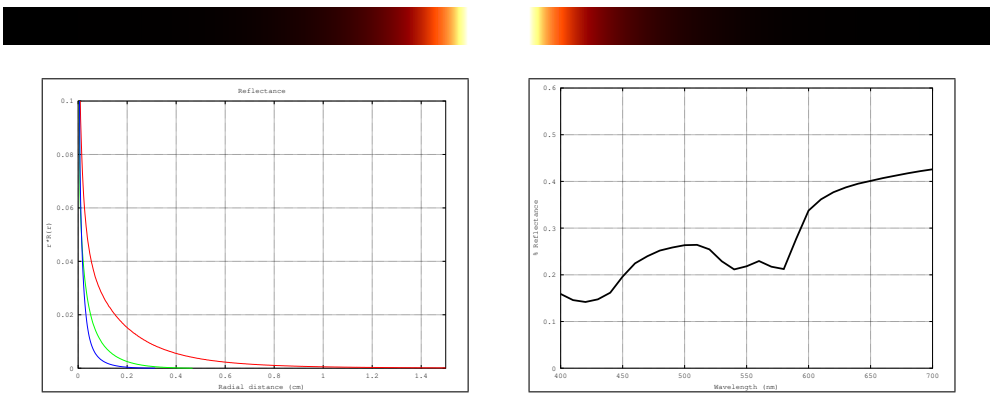


Figure 41: Top row: MonteCarlo simulations for 450nm, 550nm and 610nm. Bottom row: Resultant optical parameters (d , μ_a , μ'_s) applying our skin aging model.



Fitting	R	G	B
w_i v_i RMS,AMAX	(652.215, 67.226, 7.628, 1.604, 0.336, 0.051) (0.541, 2.698, 24.647, 185.516, 1487.447, 10773.621) 2.07e-11, 1e-03f	(392.611, 50.433, 5.811, 1.702, 0.426, 0.070) (0.478, 2.140, 14.440, 73.537, 371.514, 1963.968) 5.18e-12, 4e-04f	(465.038, 53.620, 8.550, 2.621, 0.520, 0.062) (0.470, 2.029, 10.018, 39.251, 162.873, 852.639) 1.66e-12, 3e-04f

Figure 42: Top row: Diffusion profile response for a pencil light-beam. Middle-row: RGB-profiles and reflectance-per-wavelength. Bottom row: Result of fitting the RGB-profile with 6 weighted Gaussians.

Female Age 80 $\xi = 0$ v_m 1 v_{Hb} 5

Gender	Age	ξ	v_m	v_{Hb}	c_{bil}	c_{car}	Skin roughness
Female	80	0	1	5	0.05	2.1e-4	0.18059

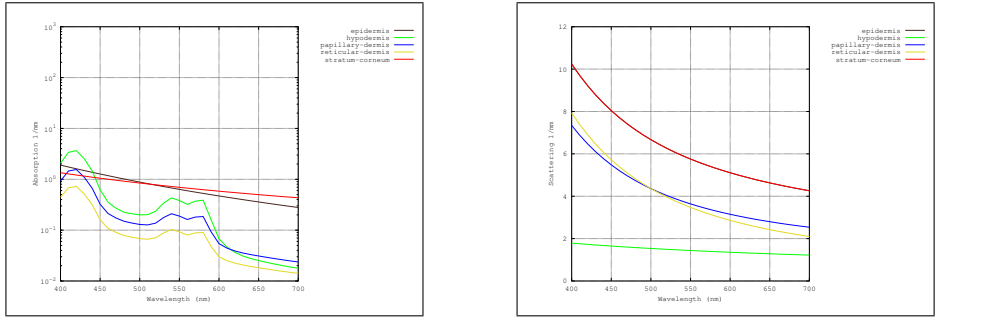


Figure 43: Top row: Full skin phantom description and skin closeup image. Bottom row, from left to right: Absorption and scattering coefficients per-wavelength for each skin layer, and result on a human cheek.

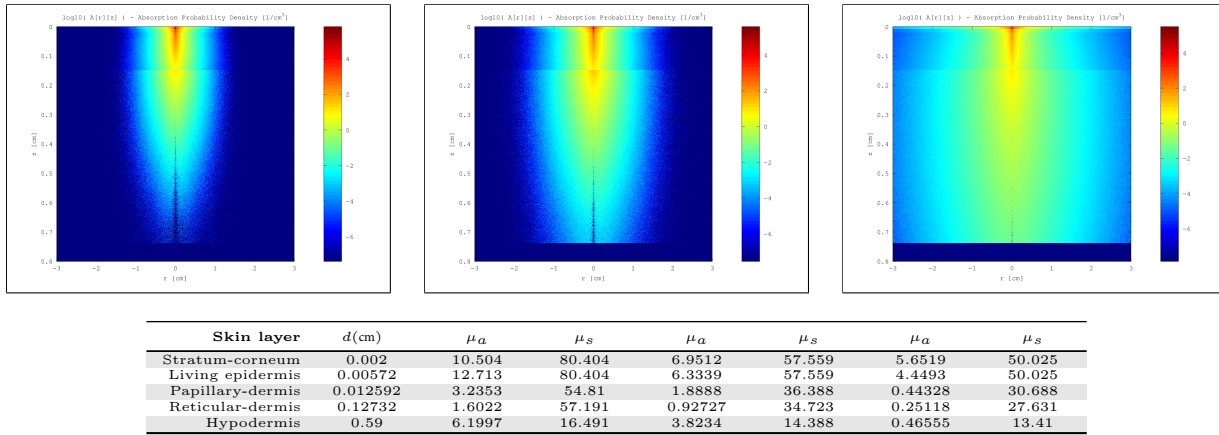
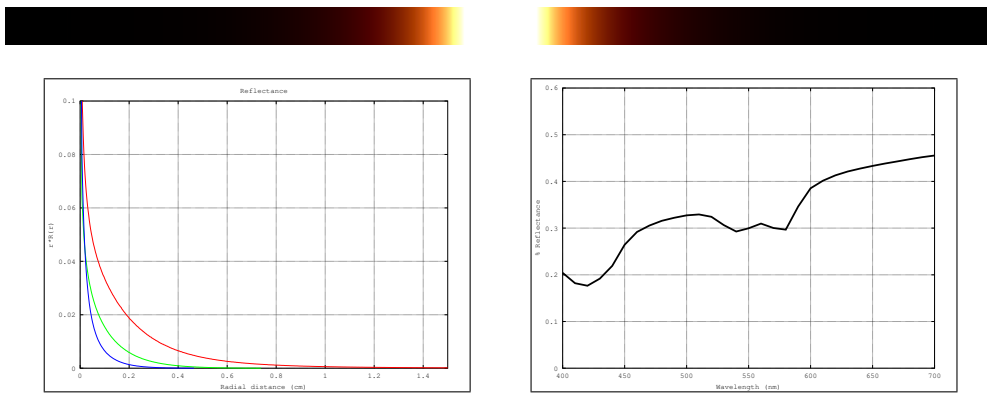


Figure 44: Top row: MonteCarlo simulations for 450nm, 550nm and 610nm. Bottom row: Resultant optical parameters (d , μ_a , μ'_s) applying our skin aging model.



Fitting	R	G	B
w_i v_i RMS,AMAX	(637.944, 42.313, 6.830, 1.546, 0.381, 0.059) (0.594, 3.270, 28.130, 216.673, 1622.700, 10801.508) 1.39e-10, 4e-03f	(371.998, 32.793, 5.256, 1.446, 0.387, 0.069) (0.549, 2.479, 17.682, 106.313, 625.044, 3448.074) 2.17e-11, 9e-04f	(443.657, 40.747, 8.078, 2.335, 0.519, 0.074) (0.520, 2.241, 12.035, 54.409, 261.989, 1394.286) 8.46e-12, 6e-04f

Figure 45: Top row: Diffusion profile response for a pencil light-beam. Middle-row: RGB-profiles and reflectance-per-wavelength. Bottom row: Result of fitting the RGB-profile with 6 weighted Gaussians.

Female Age 30 $\xi = 1$ v_m 1 v_{Hb} 5

Gender	Age	ξ	v_m	v_{Hb}	c_{bil}	c_{car}	Skin roughness
Female	30	1	1	5	0.05	2.1e-4	0.069549

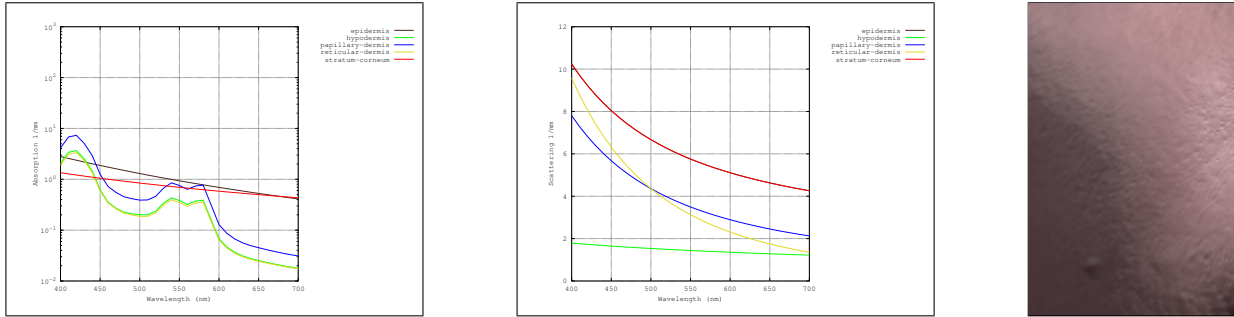


Figure 46: Top row: Full skin phantom description and skin closeup image. Bottom row, from left to right: Absorption and scattering coefficients per-wavelength for each skin layer, and result on a human cheek.

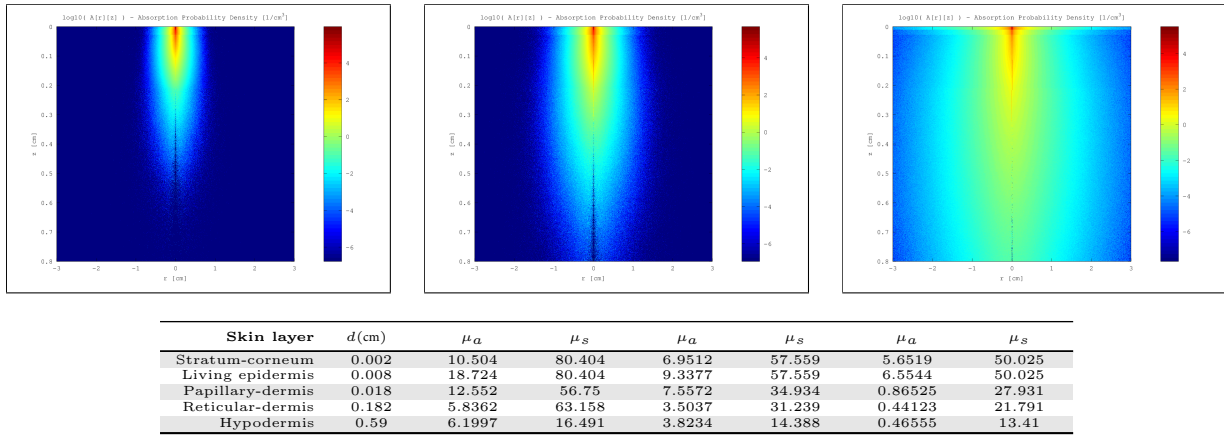
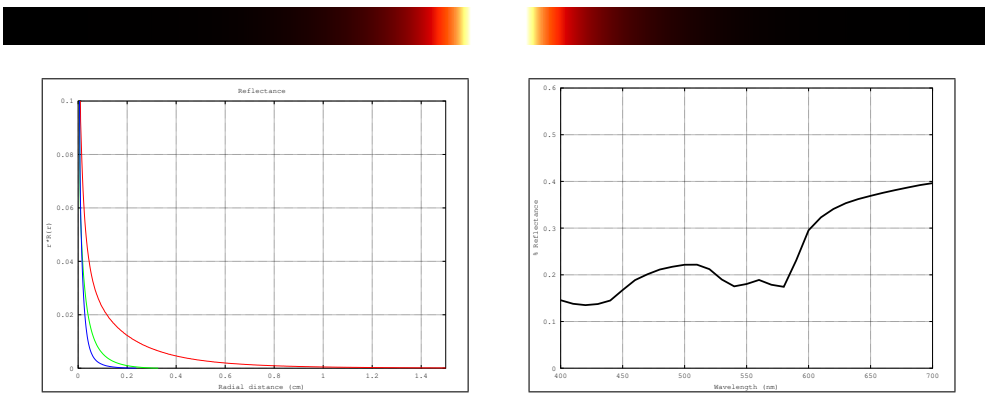


Figure 47: Top row: MonteCarlo simulations for 450nm, 550nm and 610nm. Bottom row: Resultant optical parameters (d , μ_a , μ_s') applying our skin aging model.



Fitting	R	G	B
w_i v_i RMS,AMAX	(654.092, 68.839, 7.309, 1.521, 0.283, 0.041) (0.542, 2.955, 25.854, 180.716, 1446.558, 11067.703) 5.36e-12, 8e-04f	(384.807, 45.049, 5.359, 1.717, 0.442, 0.070) (0.505, 2.480, 14.520, 61.400, 257.355, 1220.962) 2.39e-14, 3e-05f	(450.143, 45.128, 7.624, 2.508, 0.499, 0.052) (0.503, 2.360, 10.274, 35.343, 126.039, 599.606) 9.68e-16, 7e-06f

Figure 48: Top row: Diffusion profile response for a pencil light-beam. Middle-row: RGB-profiles and reflectance-per-wavelength. Bottom row: Result of fitting the RGB-profile with 6 weighted Gaussians.

Female Age 55 $\xi = 1$ v_m 1 v_{Hb} 5

Gender	Age	ξ	v_m	v_{Hb}	c_{bil}	c_{car}	Skin roughness
Female	55	1	1	5	0.05	2.1e-4	0.099683

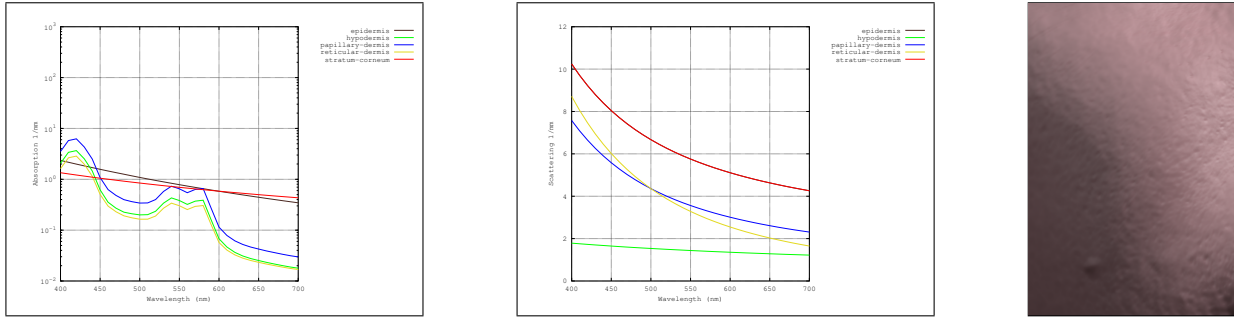


Figure 49: Top row: Full skin phantom description and skin closeup image. Bottom row, from left to right: Absorption and scattering coefficients per-wavelength for each skin layer, and result on a human cheek.

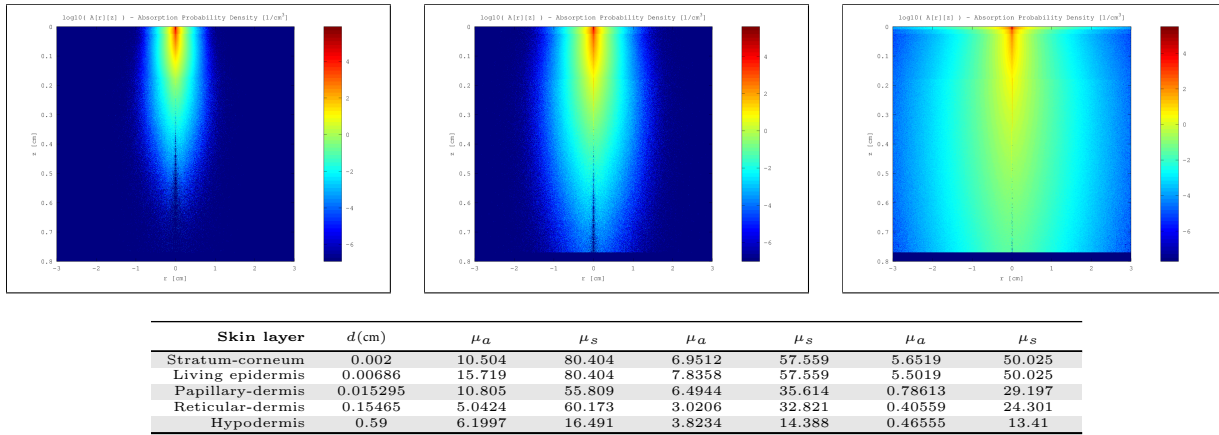


Figure 50: Top row: MonteCarlo simulations for 450nm, 550nm and 610nm. Bottom row: Resultant optical parameters (d , μ_a , μ'_s) applying our skin aging model.

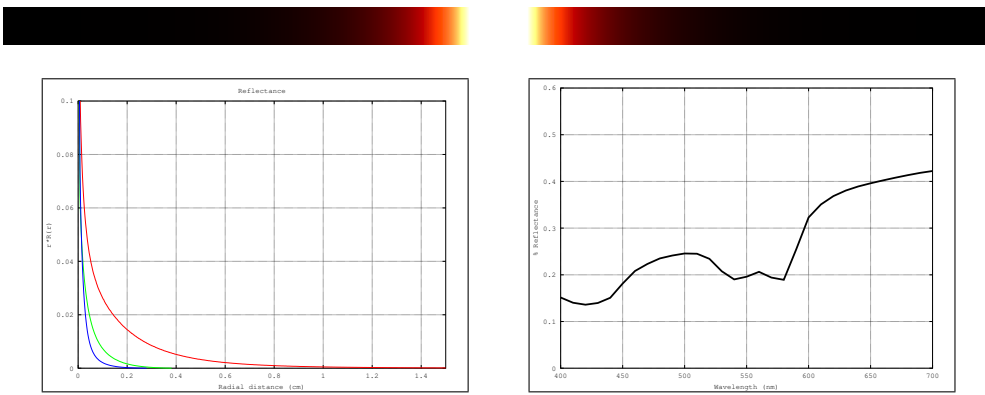


Figure 51: Top row: Diffusion profile response for a pencil light-beam. Middle-row: RGB-profiles and reflectance-per-wavelength. Bottom row: Result of fitting the RGB-profile with 6 weighted Gaussians.

Female Age 80 $\xi = 1$ v_m 1 v_{Hb} 5

Gender	Age	ξ	v_m	v_{Hb}	c_{bil}	c_{car}	Skin roughness
Female	80	1	1	5	0.05	2.1e-4	0.14797

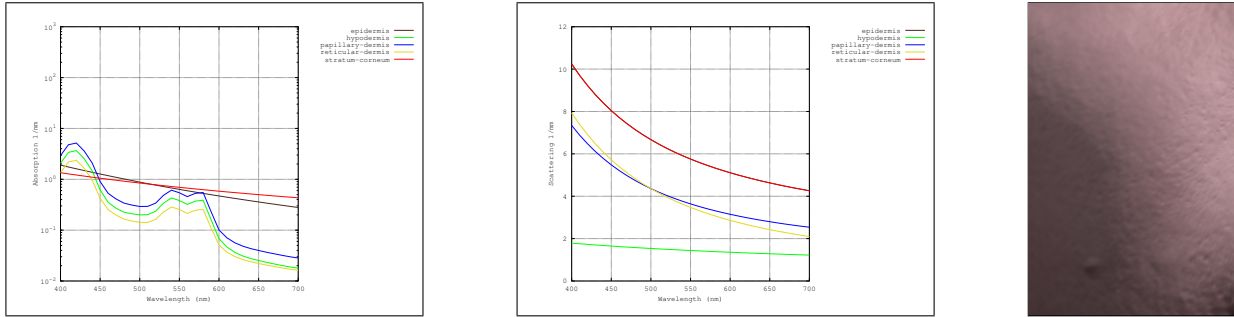


Figure 52: Top row: Full skin phantom description and skin closeup image. Bottom row, from left to right: Absorption and scattering coefficients per-wavelength for each skin layer, and result on a human cheek.

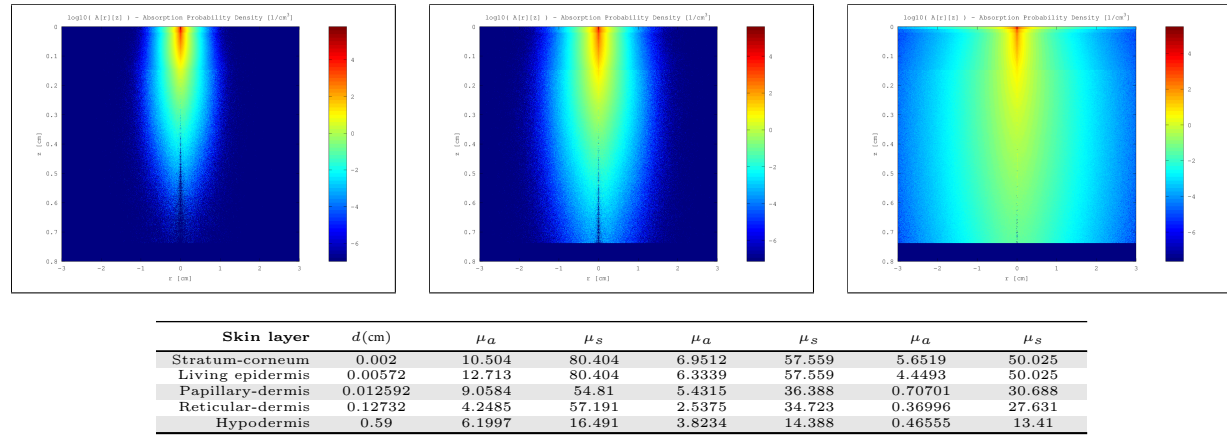
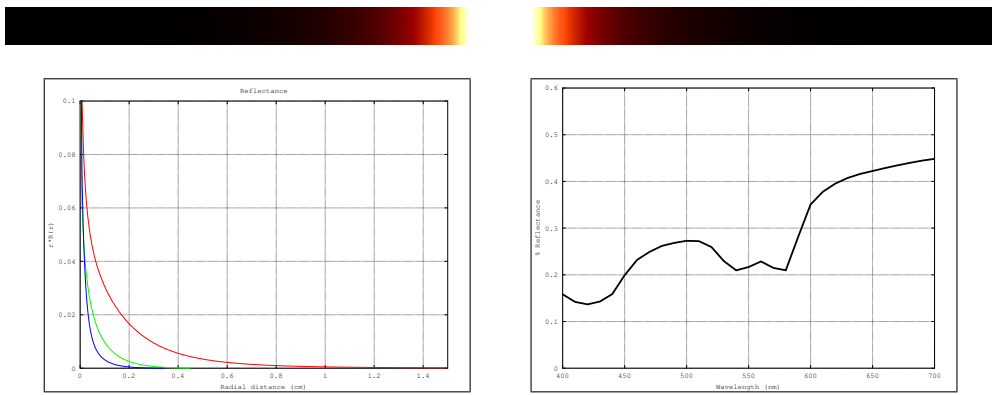


Figure 53: Top row: MonteCarlo simulations for 450nm, 550nm and 610nm. Bottom row: Resultant optical parameters (d , μ_a , μ'_s) applying our skin aging model.



Fitting	R	G	B
w_i v_i RMS,AMAX	(639.991, 44.999, 7.028, 1.566, 0.376, 0.056) (0.586, 3.079, 26.072, 198.217, 1480.200, 10012.531) 9.13e-11, 3e-03f	(380.213, 43.964, 5.916, 1.762, 0.473, 0.082) (0.505, 2.007, 13.277, 69.121, 352.005, 1825.367) 4.34e-11, 1e-03f	(1055.429, 96.734, 10.312, 3.126, 0.642, 0.076) (0.240, 1.403, 7.936, 33.676, 149.853, 843.852) 2.19e-10, 3e-03f

Figure 54: Top row: Diffusion profile response for a pencil light-beam. Middle-row: RGB-profiles and reflectance-per-wavelength. Bottom row: Result of fitting the RGB-profile with 6 weighted Gaussians.

Gender	Age	ξ	v_m	v_{Hb}	c_{bil}	c_{car}	Skin roughness
Female	30	0	20	5	0.05	2.1e-4	0.081579

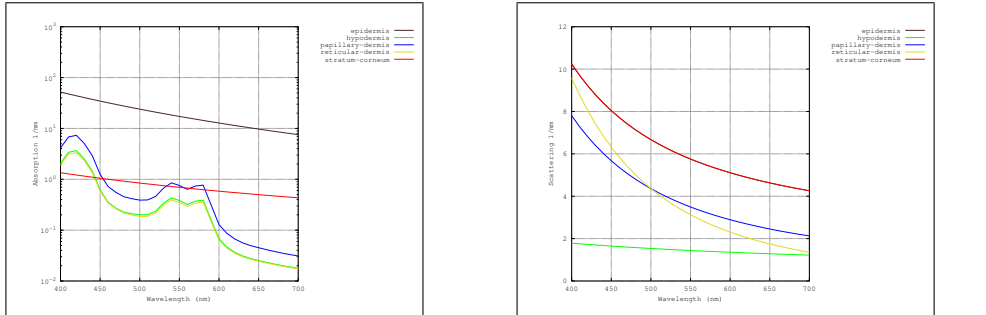


Figure 55: Top row: Full skin phantom description and skin closeup image. Bottom row, from left to right: Absorption and scattering coefficients per-wavelength for each skin layer, and result on a human cheek.

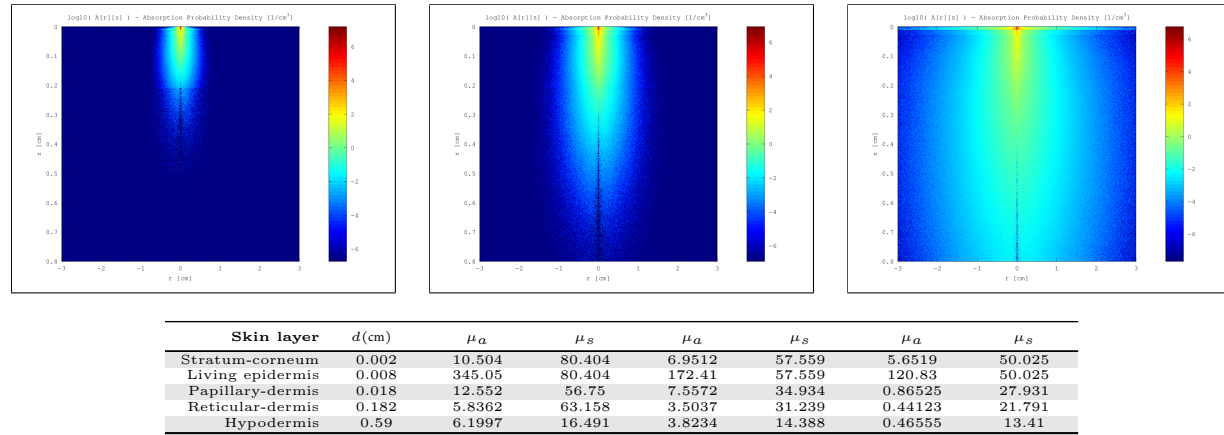
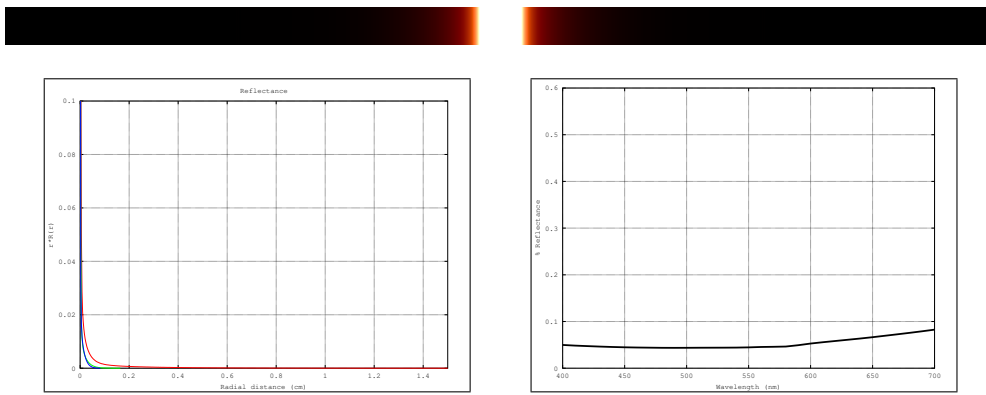


Figure 56: Top row: MonteCarlo simulations for 450nm, 550nm and 610nm. Bottom row: Resultant optical parameters (d , μ_a , μ'_s) applying our skin aging model.



Fitting	R	G	B
w_i v_i RMS,AMAX	(773.254, 58.238, 5.032, 1.050, 0.164, 0.009) (0.386, 1.521, 6.727, 36.107, 229.422, 3857.959) 2.37e-08, 4e-02f	(395.159, 193.480, 27.413, 2.241, 0.471, 0.086) (0.263, 0.414, 1.329, 6.277, 32.042, 147.176) 8.10e-09, 1e-02f	(465.463, 189.426, 4.878, 1.108, 0.232, 0.128) (0.263, 0.470, 3.101, 15.186, 62.393, 0.016) 1.05e-10, 1e-03f

Figure 57: Top row: Diffusion profile response for a pencil light-beam. Middle-row: RGB-profiles and reflectance-per-wavelength. Bottom row: Result of fitting the RGB-profile with 6 weighted Gaussians.

Gender	Age	ξ	v_m	v_{Hb}	c_{bil}	c_{car}	Skin roughness
Female	55	0	20	5	0.05	2.1e-4	0.12802

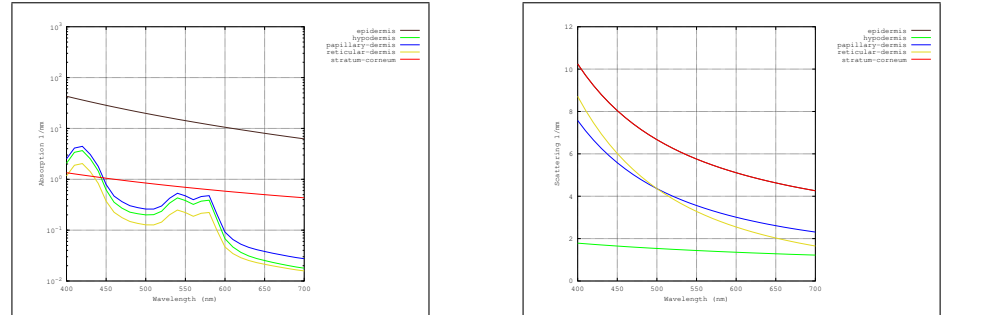


Figure 58: Top row: Full skin phantom description and skin closeup image. Bottom row, from left to right: Absorption and scattering coefficients per-wavelength for each skin layer, and result on a human cheek.

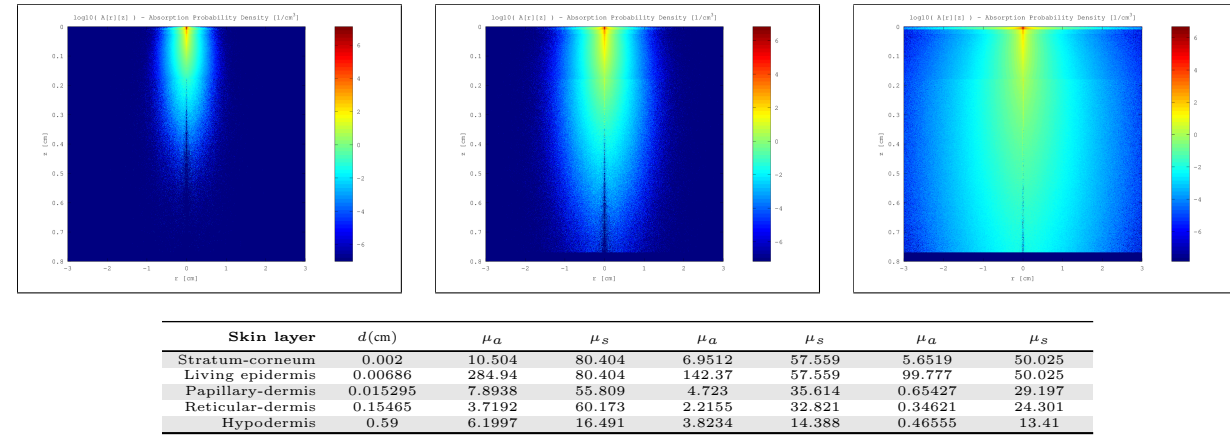
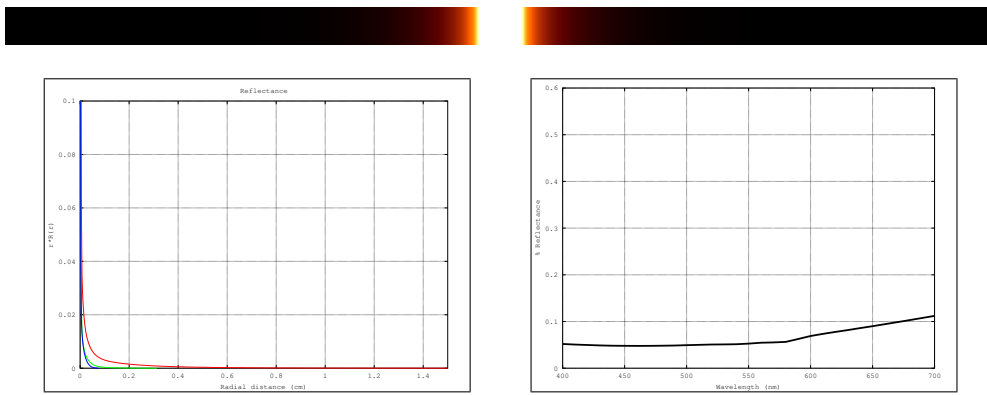


Figure 59: Top row: MonteCarlo simulations for 450nm, 550nm and 610nm. Bottom row: Resultant optical parameters (d , μ_a , μ'_s) applying our skin aging model.



Fitting	R	G	B
w_i v_i RMS,AMAX	(677.325, 37.295, 3.306, 0.580, 0.073, 0.009) (0.470, 2.176, 15.023, 96.056, 747.636, 7255.097) 5.16e-13, 2e-04f	(459.625, 34.660, 4.061, 0.984, 0.223, 0.016) (0.363, 1.190, 3.942, 17.655, 87.261, 577.259) 8.28e-09, 1e-02f	(110.910, 103.924, 97.155, 59.496, 35.627, 0.470) (0.484, 0.421, 0.455, 0.520, 0.828, 0.039) 1.84e-05, 6e-01f

Figure 60: Top row: Diffusion profile response for a pencil light-beam. Middle-row: RGB-profiles and reflectance-per-wavelength. Bottom row: Result of fitting the RGB-profile with 6 weighted Gaussians.

Gender	Age	ξ	v_m	v_{Hb}	c_{bil}	c_{car}	Skin roughness
Female	80	0	20	5	0.05	2.1e-4	0.18059

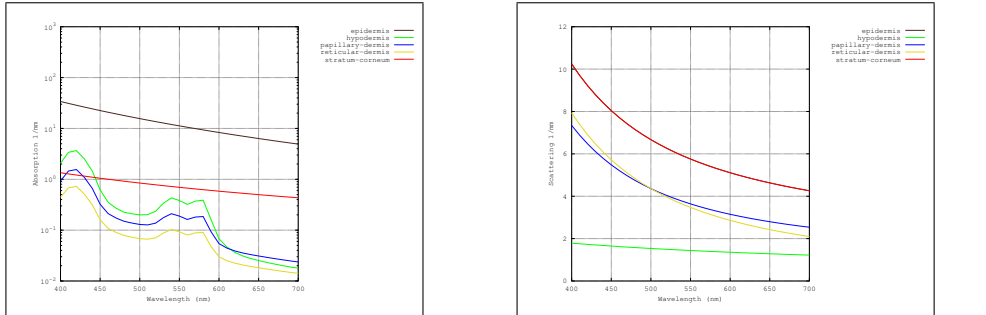


Figure 61: Top row: Full skin phantom description and skin closeup image. Bottom row, from left to right: Absorption and scattering coefficients per-wavelength for each skin layer, and result on a human cheek.

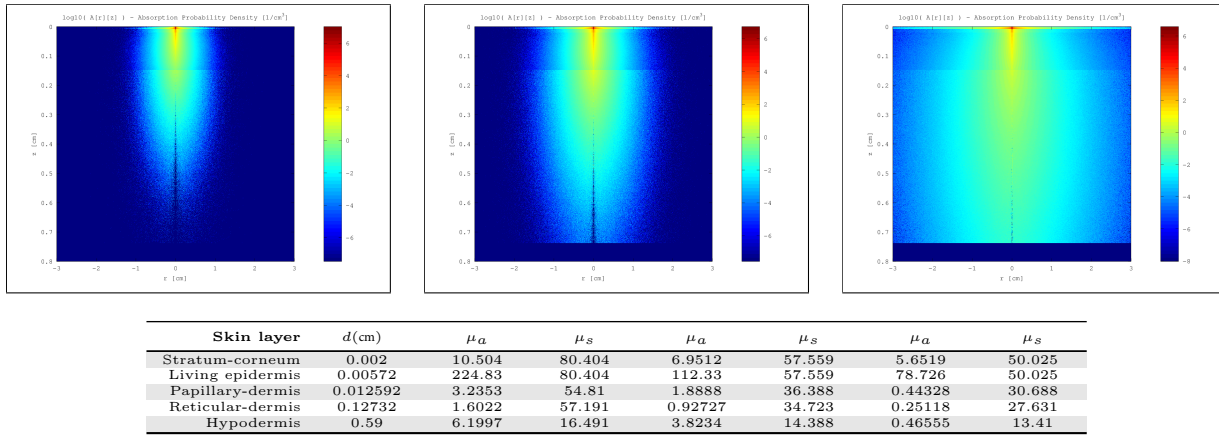
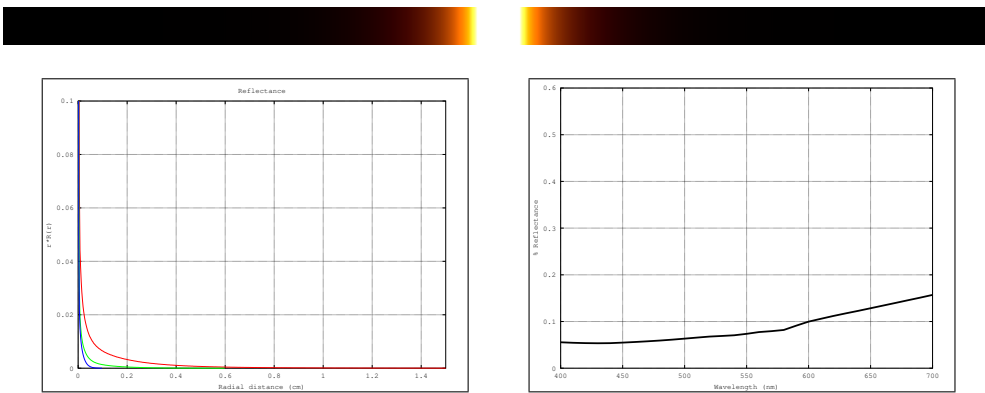


Figure 62: Top row: MonteCarlo simulations for 450nm, 550nm and 610nm. Bottom row: Resultant optical parameters (d , μ_a , μ'_s) applying our skin aging model.



Fitting	R	G	B
w_i v_i RMS,AMAX	(301.379, 183.434, 116.391, 41.326, 4.978, -0.121) (0.525, 0.498, 0.671, 1.608, 25.012, 1.678) 2.44e-05, 1e+00f	(388.433, 16.918, 2.217, 0.491, 0.081, 0.010) (0.468, 2.023, 11.045, 56.887, 310.193, 2313.919) 3.21e-12, 3e-04f	(114.675, 93.116, 83.356, 57.724, 48.026, 0.000) (0.421, 0.599, 0.325, 0.647, 0.717, 0.088) 4.00e-03, 1e+01f

Figure 63: Top row: Diffusion profile response for a pencil light-beam. Middle-row: RGB-profiles and reflectance-per-wavelength. Bottom row: Result of fitting the RGB-profile with 6 weighted Gaussians.

Gender	Age	ξ	v_m	v_{Hb}	c_{bil}	c_{car}	Skin roughness
Female	30	1	20	5	0.05	2.1e-4	0.069549

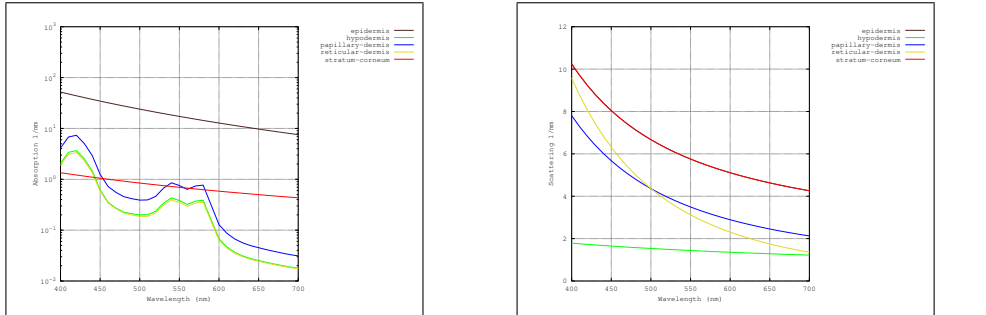


Figure 64: Top row: Full skin phantom description and skin closeup image. Bottom row, from left to right: Absorption and scattering coefficients per-wavelength for each skin layer, and result on a human cheek.

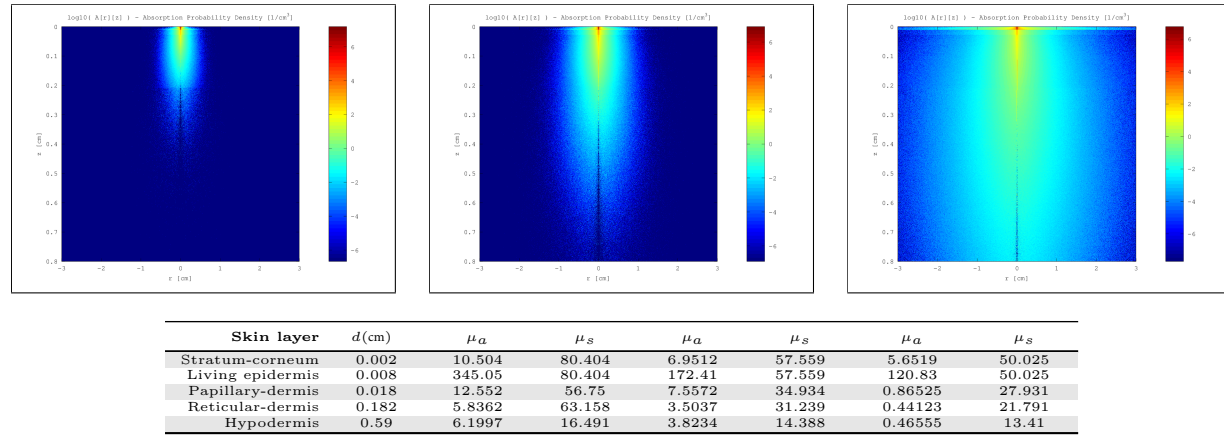
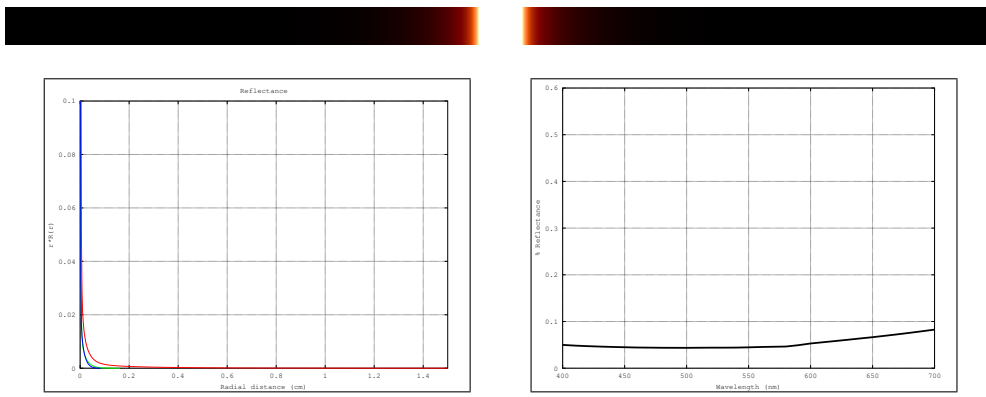


Figure 65: Top row: MonteCarlo simulations for 450nm, 550nm and 610nm. Bottom row: Resultant optical parameters (d , μ_a , μ'_s) applying our skin aging model.



Fitting	R	G	B
w_i v_i RMS,AMAX	(752.335, 75.005, 16.961, 1.866, 0.263, 0.012) (0.374, 1.006, 3.139, 22.094, 165.172, 3114.466) 5.19e-07, 2e-01f	(365.687, 208.633, 21.766, 2.087, 0.463, 0.084) (0.258, 0.444, 1.450, 6.527, 32.716, 148.721) 7.75e-09, 1e-02f	(309.233, 289.090, 95.278, 4.768, 1.111, 0.239) (0.256, 0.294, 0.552, 3.130, 14.925, 61.662) 2.45e-11, 7e-04f

Figure 66: Top row: Diffusion profile response for a pencil light-beam. Middle-row: RGB-profiles and reflectance-per-wavelength. Bottom row: Result of fitting the RGB-profile with 6 weighted Gaussians.

Gender	Age	ξ	v_m	v_{Hb}	c_{bil}	c_{car}	Skin roughness
Female	55	1	20	5	0.05	2.1e-4	0.099683

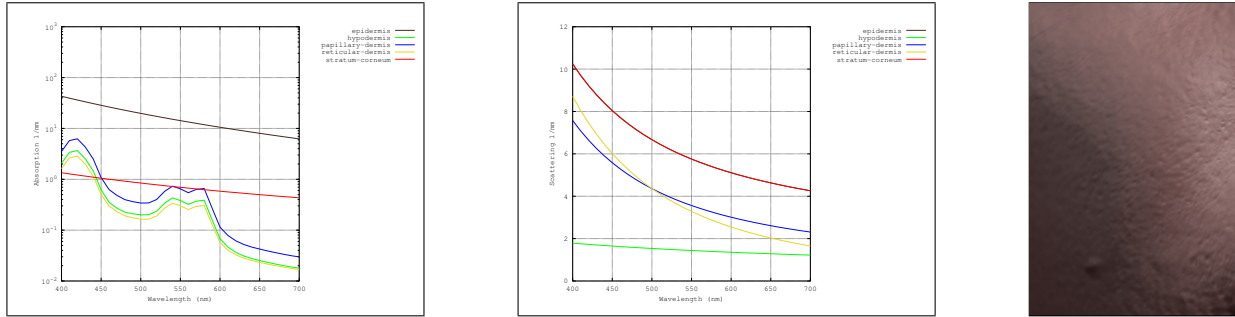


Figure 67: Top row: Full skin phantom description and skin closeup image. Bottom row, from left to right: Absorption and scattering coefficients per-wavelength for each skin layer, and result on a human cheek.

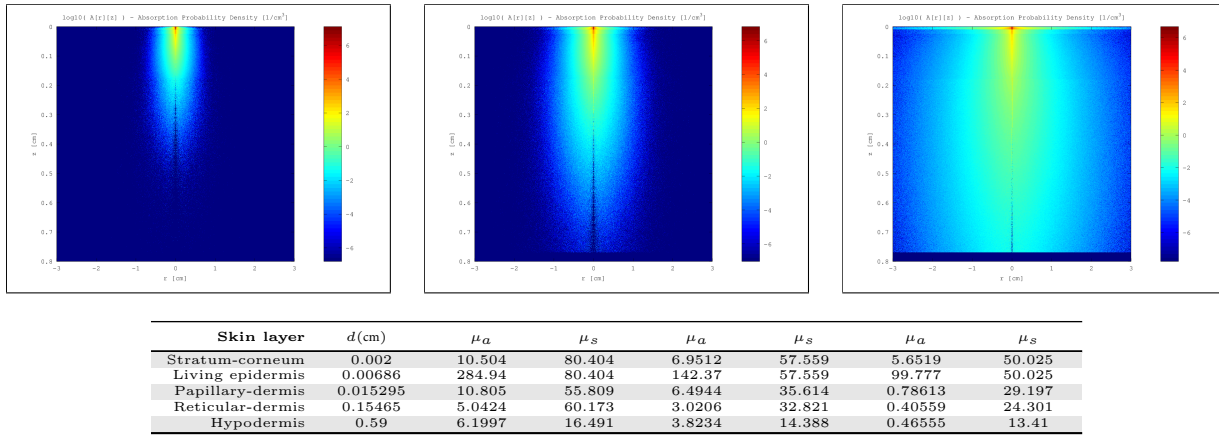
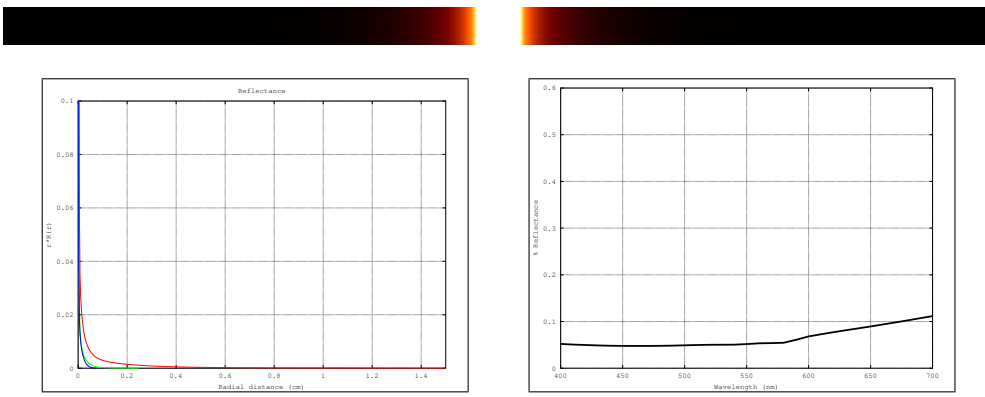


Figure 68: Top row: MonteCarlo simulations for 450nm, 550nm and 610nm. Bottom row: Resultant optical parameters (d , μ_a , μ_s') applying our skin aging model.



Fitting	R	G	B
w_i v_i RMS,AMAX	(187.947, 183.836, 145.651, 138.714, 6.944, -0.012) (0.568, 0.422, 0.737, 0.427, 11.405, 0.058) 1.25e-03, 9e+00f	(322.531, 179.637, 20.301, 1.937, 0.403, 0.045) (0.299, 0.495, 1.712, 9.266, 49.933, 276.495) 1.55e-08, 2e-02f	(104.232, 102.594, 102.324, 69.773, 49.004, -0.102) (0.484, 0.306, 0.524, 0.474, 0.731, 0.214) 4.21e-05, 1e+00f

Figure 69: Top row: Diffusion profile response for a pencil light-beam. Middle-row: RGB-profiles and reflectance-per-wavelength. Bottom row: Result of fitting the RGB-profile with 6 weighted Gaussians.

Gender	Age	ξ	v_m	v_{Hb}	c_{bil}	c_{car}	Skin roughness
Female	80	1	20	5	0.05	2.1e-4	0.14797

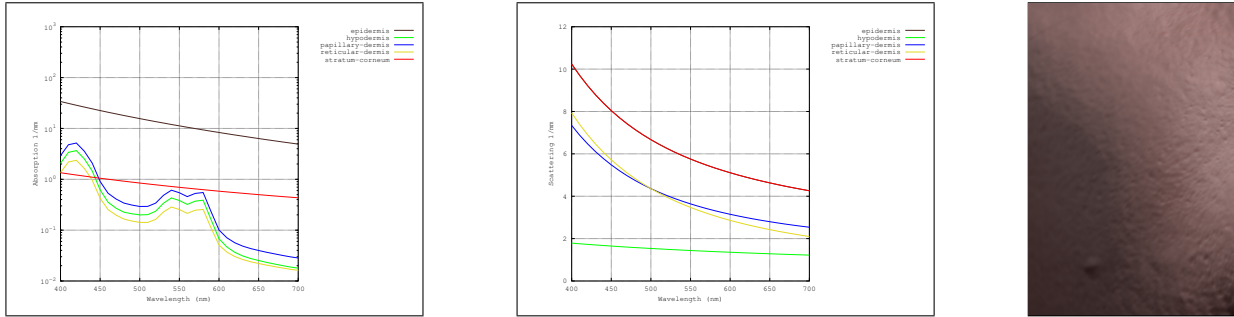


Figure 70: Top row: Full skin phantom description and skin closeup image. Bottom row, from left to right: Absorption and scattering coefficients per-wavelength for each skin layer, and result on a human cheek.

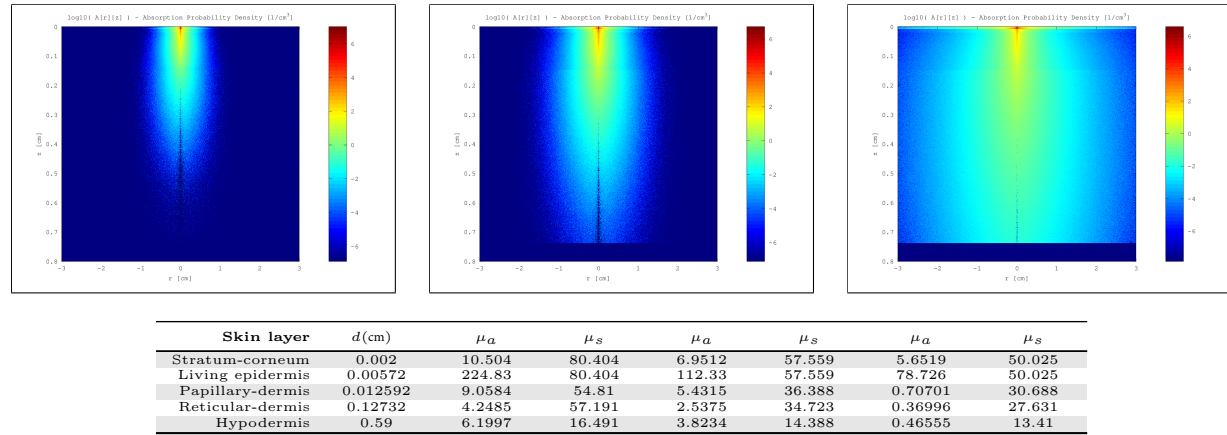
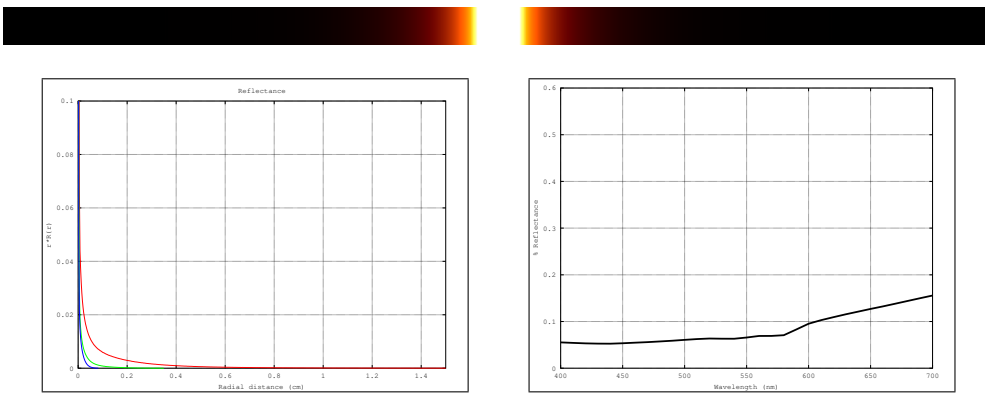


Figure 71: Top row: MonteCarlo simulations for 450nm, 550nm and 610nm. Bottom row: Resultant optical parameters (d , μ_a , μ'_s) applying our skin aging model.



Fitting	R	G	B
w_i v_i RMS,AMAX	(658.158, 33.218, 4.098, 0.766, 0.121, 0.017) (0.503, 2.336, 16.328, 109.755, 861.222, 7063.385) 2.81e-12, 5e-04f	(450.497, 37.602, 2.954, 0.685, 0.148, 0.015) (0.377, 1.375, 7.704, 35.009, 160.793, 1086.794) 1.55e-08, 2e-02f	(103.862, 100.245, 76.648, 73.804, 50.136, -0.329) (0.515, 0.582, 0.450, 0.382, 0.724, 0.816) 1.03e-04, 2e+00f

Figure 72: Top row: Diffusion profile response for a pencil light-beam. Middle-row: RGB-profiles and reflectance-per-wavelength. Bottom row: Result of fitting the RGB-profile with 6 weighted Gaussians.

Gender	Age	ξ	v_m	v_{Hb}	c_{bil}	c_{car}	Skin roughness
Female	30	0	25	5	0.05	2.1e-4	0.081579

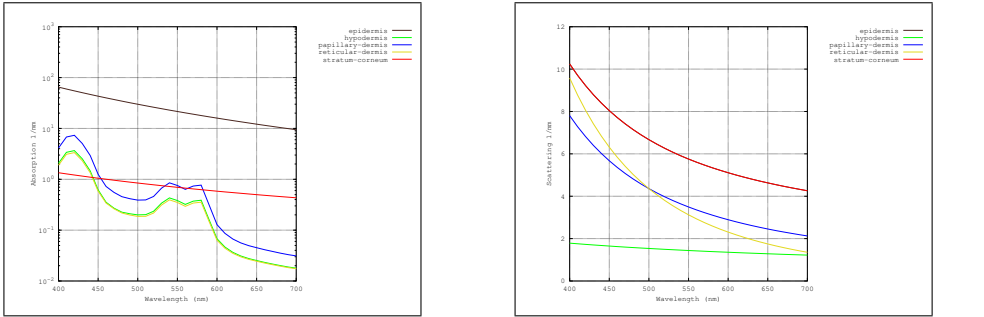


Figure 73: Top row: Full skin phantom description and skin closeup image. Bottom row, from left to right: Absorption and scattering coefficients per-wavelength for each skin layer, and result on a human cheek.

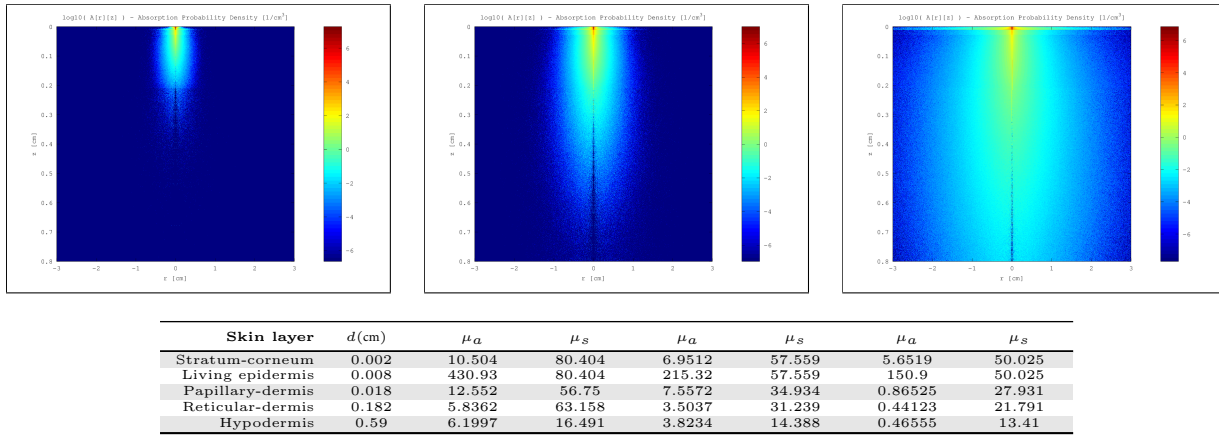
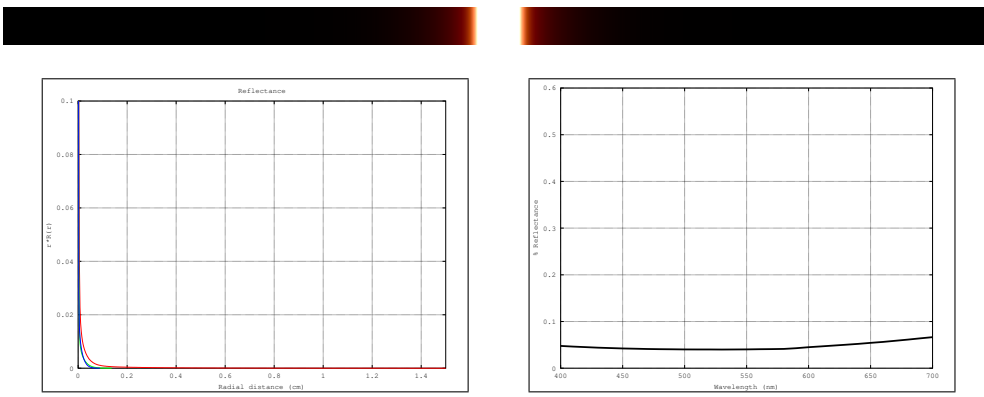


Figure 74: Top row: MonteCarlo simulations for 450nm, 550nm and 610nm. Bottom row: Resultant optical parameters (d , μ_a , μ'_s) applying our skin aging model.



Fitting	R	G	B
w_i v_i RMS,AMAX	(776.315, 95.144, 15.028, 1.578, 0.253, 0.009) (0.345, 0.849, 2.955, 20.214, 140.629, 2503.792) 1.17e-07, 9.e-02f	(110.000, 71.221, 57.758, 53.557, 52.966, 1.502) (0.550, 0.497, 0.649, 0.710, 0.345, 0.070) 9.54e-04, 4e+00f	(100.492, 91.483, 91.420, 79.708, 57.341, 33.101) (0.401, 0.639, 0.470, 0.362, 0.331, 0.014) 5.31e-06, 3e-01f

Figure 75: Top row: Diffusion profile response for a pencil light-beam. Middle-row: RGB-profiles and reflectance-per-wavelength. Bottom row: Result of fitting the RGB-profile with 6 weighted Gaussians.

Gender	Age	ξ	v_m	v_{Hb}	c_{bil}	c_{car}	Skin roughness
Female	55	0	25	5	0.05	2.1e-4	0.12802

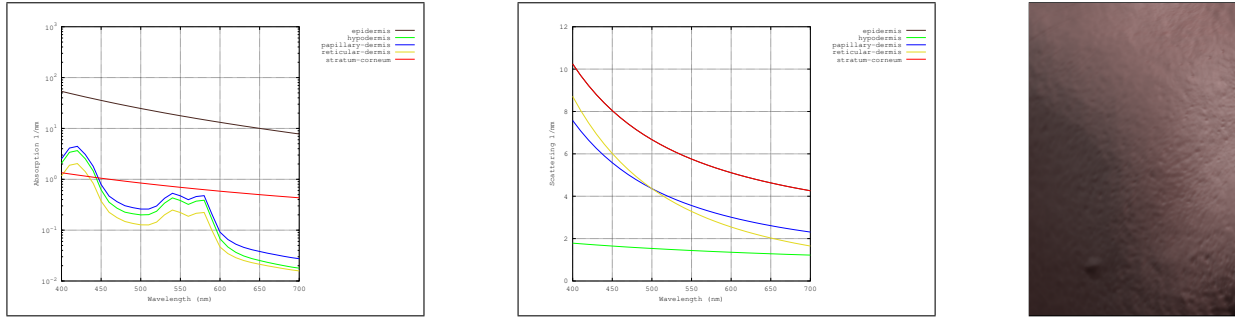


Figure 76: Top row: Full skin phantom description and skin closeup image. Bottom row, from left to right: Absorption and scattering coefficients per-wavelength for each skin layer, and result on a human cheek.

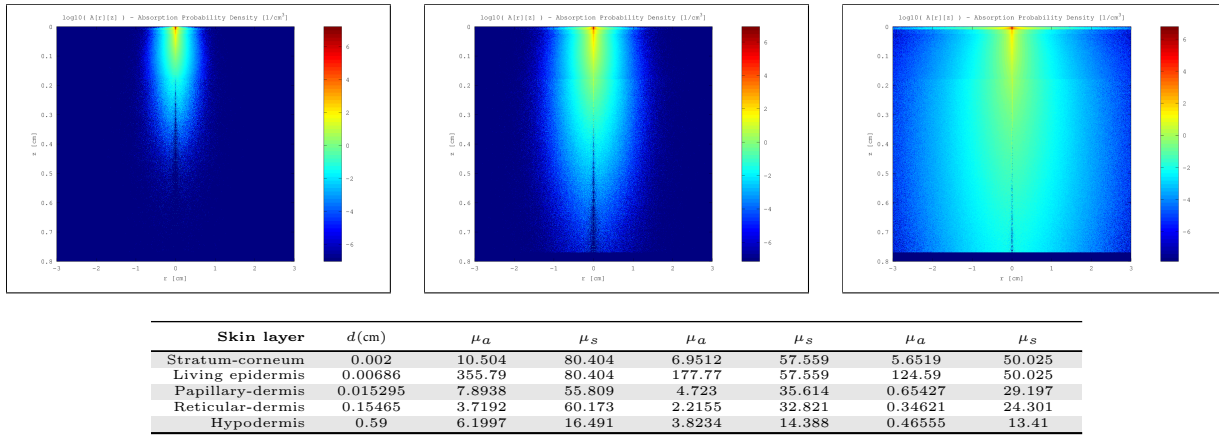
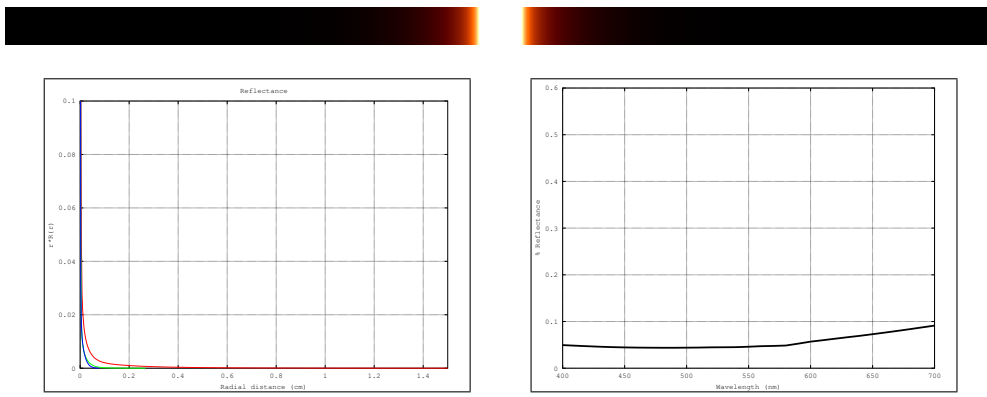


Figure 77: Top row: MonteCarlo simulations for 450nm, 550nm and 610nm. Bottom row: Resultant optical parameters (d , μ_a , μ_s') applying our skin aging model.



Fitting	R	G	B
w_i v_i RMS,AMAX	(683.152, 31.500, 2.807, 0.523, 0.062, 0.007) (0.459, 2.115, 13.737, 84.471, 605.365, 6520.480) 1.06e-12, 3e-04f	(351.924, 185.303, 20.770, 1.887, 0.406, 0.052) (0.281, 0.450, 1.463, 7.702, 42.887, 220.839) 1.80e-08, 2e-02f	(140.791, 120.906, 116.824, 91.769, 3.187, -0.536) (0.388, 0.516, 0.368, 0.357, 12.162, 11.343) 5.21e-08, 3e-02f

Figure 78: Top row: Diffusion profile response for a pencil light-beam. Middle-row: RGB-profiles and reflectance-per-wavelength. Bottom row: Result of fitting the RGB-profile with 6 weighted Gaussians.

Gender	Age	ξ	v_m	v_{Hb}	c_{bil}	c_{car}	Skin roughness
Female	80	0	25	5	0.05	2.1e-4	0.18059

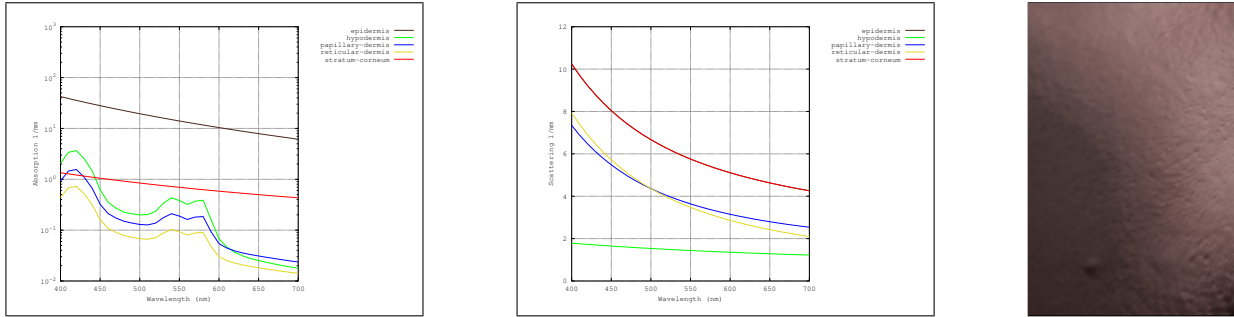


Figure 79: Top row: Full skin phantom description and skin closeup image. Bottom row, from left to right: Absorption and scattering coefficients per-wavelength for each skin layer, and result on a human cheek.

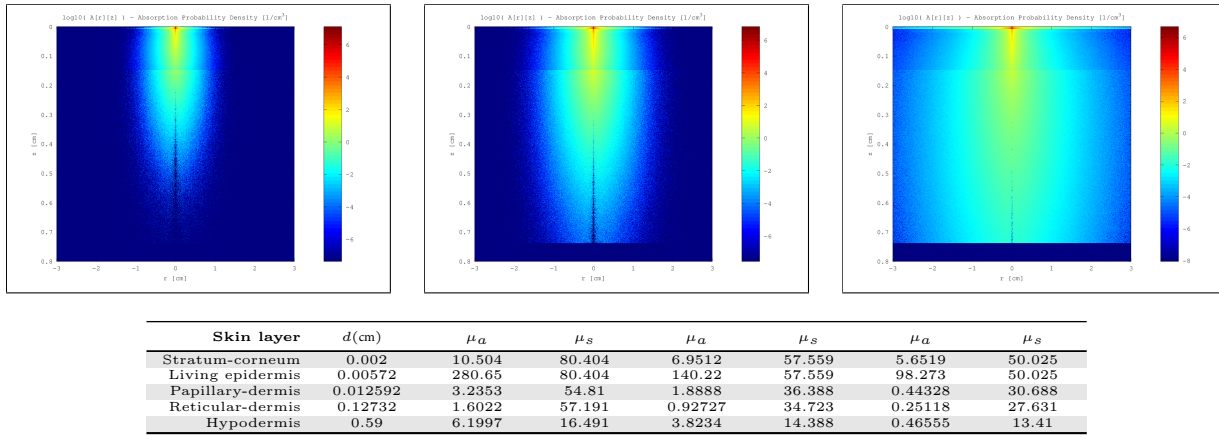
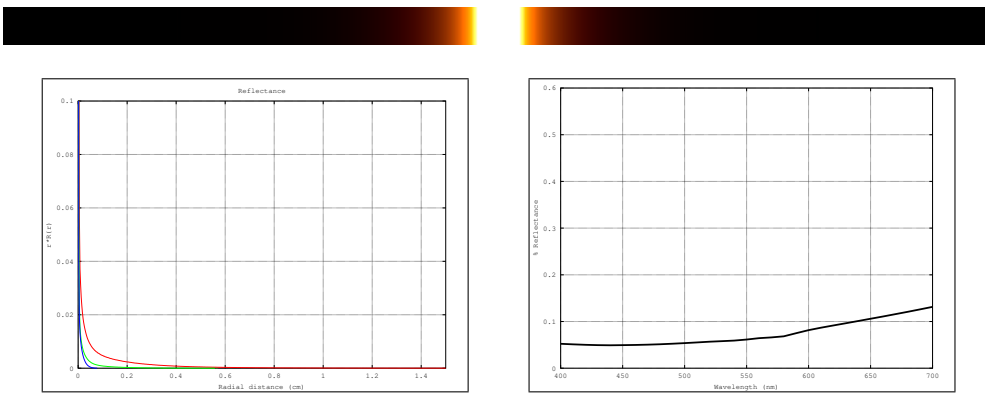


Figure 80: Top row: MonteCarlo simulations for 450nm, 550nm and 610nm. Bottom row: Resultant optical parameters (d , μ_a , μ'_s) applying our skin aging model.



Fitting	R	G	B
w_i v_i RMS,AMAX	(661.166, 28.140, 3.470, 0.649, 0.097, 0.013) (0.493, 2.353, 15.982, 107.012, 850.800, 7189.440) 1.83e-12, 4e-04f	(471.203, 34.185, 2.557, 0.568, 0.103, 0.009) (0.359, 1.313, 7.514, 38.639, 198.381, 1811.636) 2.86e-09, 8e-03f	(737.577, 162.312, 107.367, 103.934, 98.145, 4.249) (0.025, 0.374, 0.392, 0.396, 0.550, 8.028) 9.76e-05, 1e+00f

Figure 81: Top row: Diffusion profile response for a pencil light-beam. Middle-row: RGB-profiles and reflectance-per-wavelength. Bottom row: Result of fitting the RGB-profile with 6 weighted Gaussians.

Gender	Age	ξ	v_m	v_{Hb}	c_{bil}	c_{car}	Skin roughness
Female	30	1	25	5	0.05	2.1e-4	0.069549

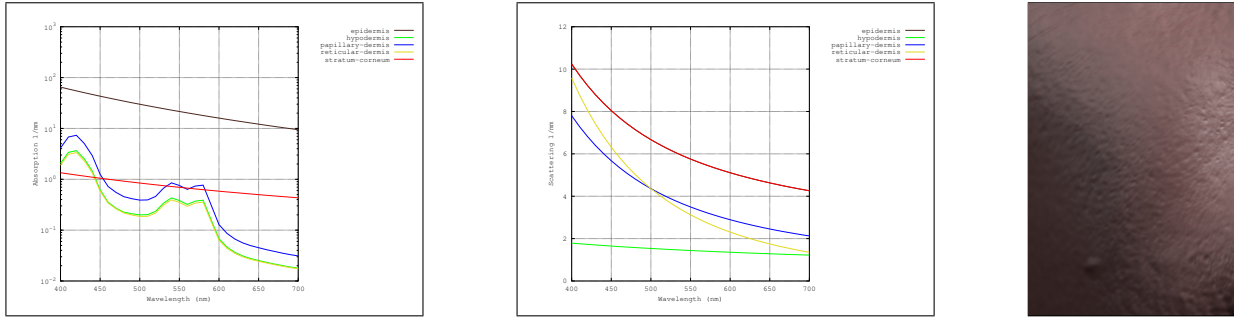


Figure 82: Top row: Full skin phantom description and skin closeup image. Bottom row, from left to right: Absorption and scattering coefficients per-wavelength for each skin layer, and result on a human cheek.

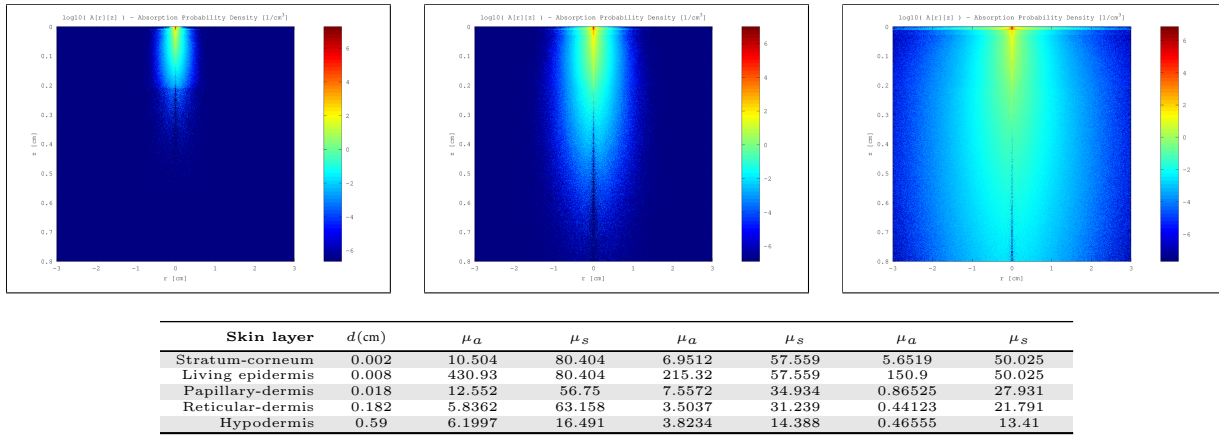
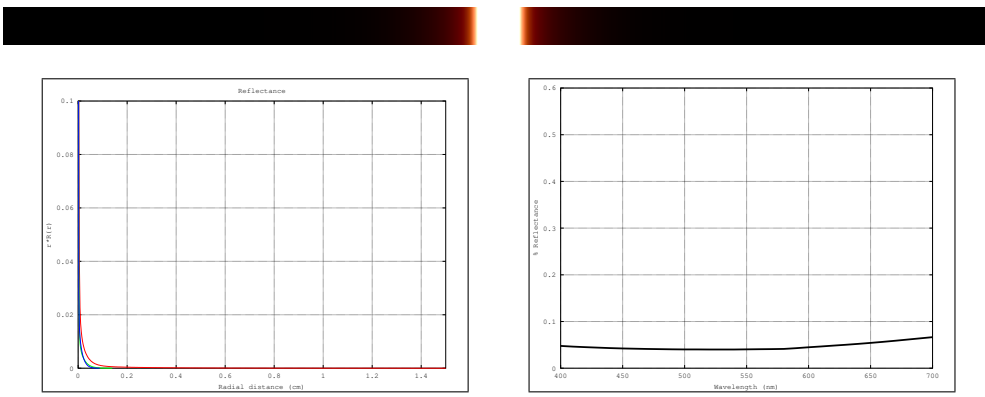


Figure 83: Top row: MonteCarlo simulations for 450nm, 550nm and 610nm. Bottom row: Resultant optical parameters (d , μ_a , μ'_s) applying our skin aging model.



Fitting	R	G	B
w_i v_i RMS,AMAX	(774.315, 63.117, 10.314, 1.409, 0.227, 0.008) (0.368, 1.085, 3.503, 22.472, 151.952, 2725.174) 1.34e-07, 9e-02f	(327.500, 210.492, 20.682, 1.881, 0.443, 0.090) (0.279, 0.404, 1.290, 5.943, 30.176, 133.754) 4.49e-09, 9e-03f	(112.079, 93.069, 71.569, 71.469, 66.218, 1.308) (0.459, 0.377, 0.388, 0.384, 0.706, 0.069) 1.33e-05, 5e-01f

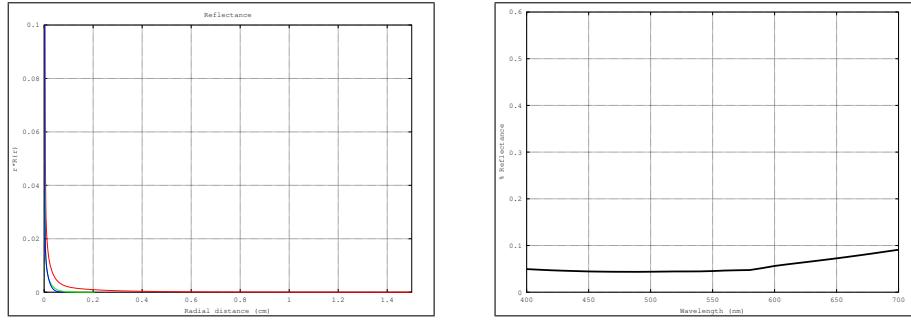
Figure 84: Top row: Diffusion profile response for a pencil light-beam. Middle-row: RGB-profiles and reflectance-per-wavelength. Bottom row: Result of fitting the RGB-profile with 6 weighted Gaussians.

Gender	Age	ξ	v_m	v_{Hb}	c_{bil}	c_{car}	Skin roughness
Female	55	1	25	5	0.05	2.1e-4	0.099683

Figure 85: Top row: Full skin phantom description and skin closeup image. Bottom row, from left to right: Absorption and scattering coefficients per-wavelength for each skin layer, and result on a human cheek.

Skin layer	$d(\text{cm})$	μ_a	μ_s	μ_a	μ_s	μ_a	μ_s
Stratum-corneum	0.002	10.504	80.404	6.9512	57.559	5.6519	50.025
Living epidermis	0.00686	355.79	80.404	177.77	57.559	124.59	50.025
Papillary-dermis	0.015295	10.805	55.809	6.4944	35.614	0.78613	29.197
Reticular-dermis	0.15465	5.0424	60.173	3.0206	32.821	0.40559	24.301
Hypodermis	0.59	6.1997	16.491	3.8234	14.388	0.46555	13.41

Figure 86: Top row: MonteCarlo simulations for 450nm, 550nm and 610nm. Bottom row: Resultant optical parameters (d , μ_a , μ'_s) applying our skin aging model.



Fitting	R	G	B
w_i v_i RMS,AMAX	(681.863, 31.034, 2.774, 0.532, 0.064, 0.007) (0.460, 2.131, 13.667, 82.371, 575.219, 6308.924) 6.50e-13, 2e-04f	(427.234, 129.085, 13.201, 1.522, 0.368, 0.052) (0.285, 0.544, 1.813, 8.913, 44.561, 206.730) 3.69e-09, 8e-03f	(302.836, 297.445, 107.451, 4.796, 1.113, 0.242) (0.260, 0.275, 0.531, 3.083, 14.804, 60.547) 3.27e-10, 3e-03f

Figure 87: Top row: Diffusion profile response for a pencil light-beam. Middle-row: RGB-profiles and reflectance-per-wavelength. Bottom row: Result of fitting the RGB-profile with 6 weighted Gaussians.

Gender	Age	ξ	v_m	v_{Hb}	c_{bil}	c_{car}	Skin roughness
Female	80	1	25	5	0.05	2.1e-4	0.14797

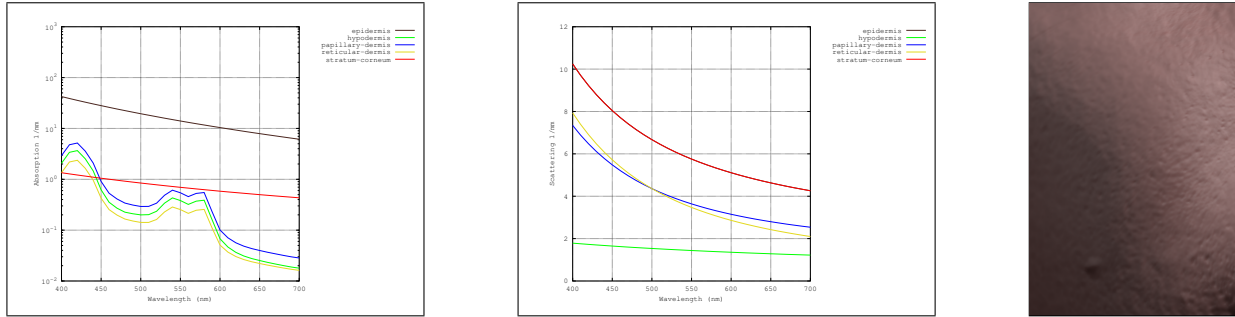


Figure 88: Top row: Full skin phantom description and skin closeup image. Bottom row, from left to right: Absorption and scattering coefficients per-wavelength for each skin layer, and result on a human cheek.

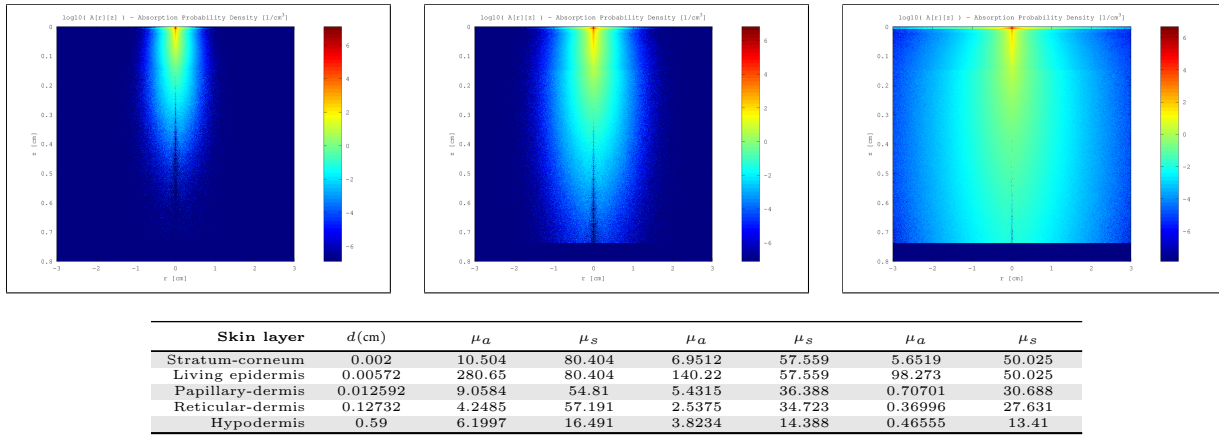
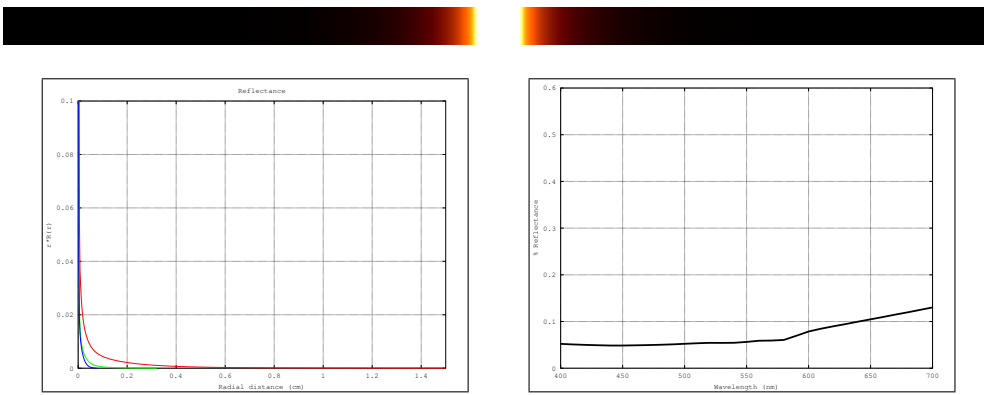


Figure 89: Top row: MonteCarlo simulations for 450nm, 550nm and 610nm. Bottom row: Resultant optical parameters (d , μ_a , μ'_s) applying our skin aging model.



Fitting	R	G	B
w_i v_i RMS,AMAX	(662.594, 29.480, 3.541, 0.664, 0.098, 0.013) (0.490, 2.282, 15.500, 101.538, 788.812, 6736.604) 1.53e-12, 3e-04f	(422.518, 85.898, 8.559, 1.364, 0.282, 0.022) (0.328, 0.717, 2.718, 14.966, 84.103, 628.511) 2.16e-08, 2e-02f	(116.431, 97.634, 83.524, 77.835, 44.363, 37.538) (0.429, 0.540, 0.495, 0.326, 0.801, 0.094) 1.97e-05, 7e-01f

Figure 90: Top row: Diffusion profile response for a pencil light-beam. Middle-row: RGB-profiles and reflectance-per-wavelength. Bottom row: Result of fitting the RGB-profile with 6 weighted Gaussians.

Female Age 30 $\xi = 0$ v_m 2 v_{Hb} 5

Gender	Age	ξ	v_m	v_{Hb}	c_{bil}	c_{car}	Skin roughness
Female	30	0	2	5	0.05	2.1e-4	0.081579

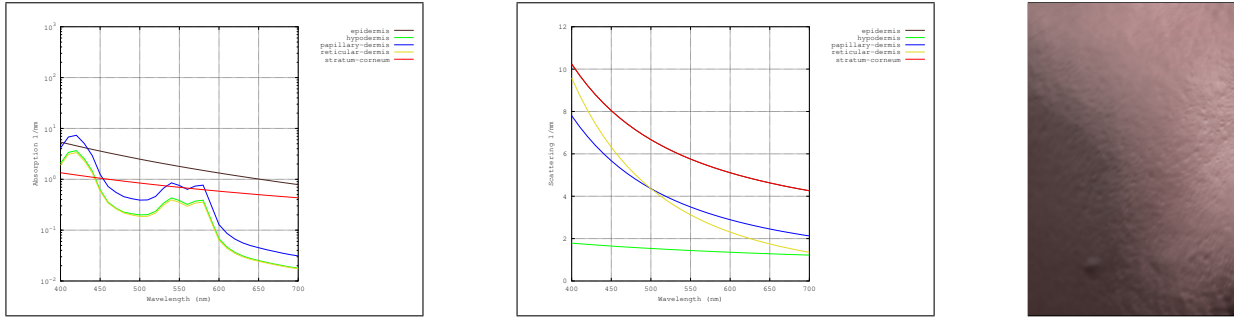


Figure 91: Top row: Full skin phantom description and skin closeup image. Bottom row, from left to right: Absorption and scattering coefficients per-wavelength for each skin layer, and result on a human cheek.

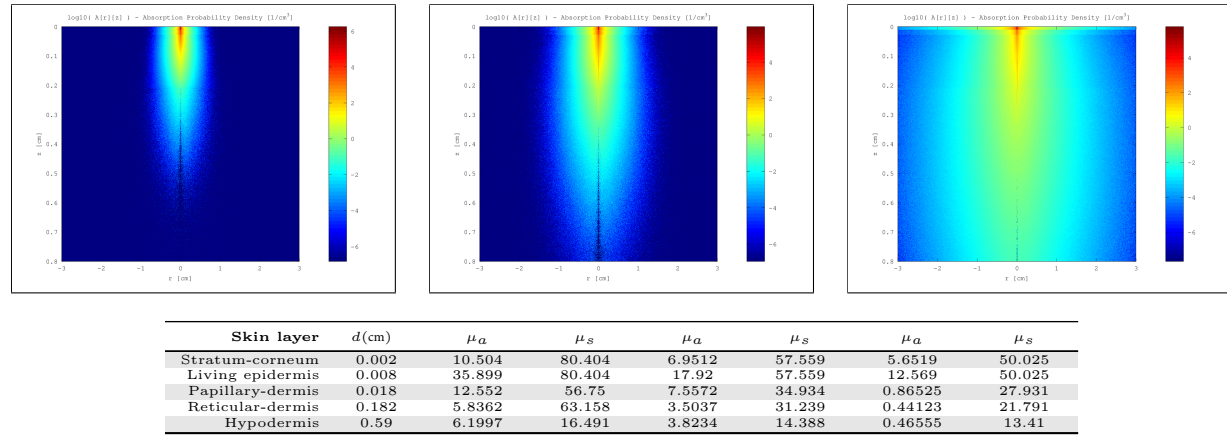


Figure 92: Top row: MonteCarlo simulations for 450nm, 550nm and 610nm. Bottom row: Resultant optical parameters (d , μ_a , μ'_s) applying our skin aging model.

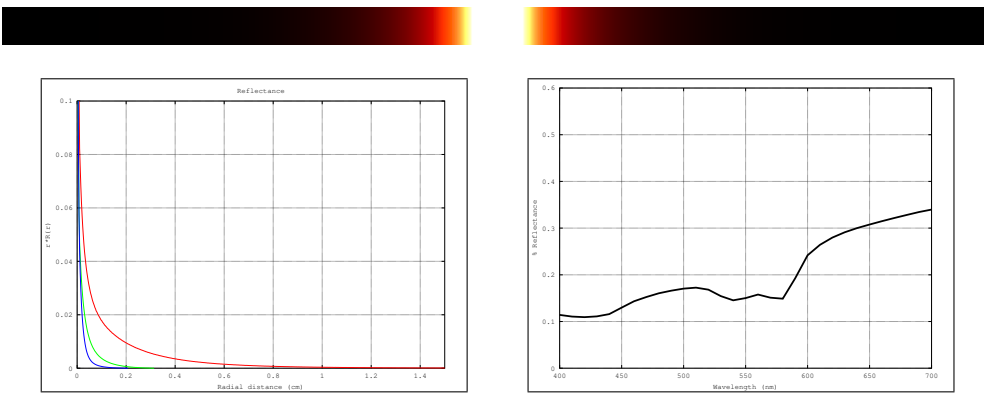


Figure 93: Top row: Diffusion profile response for a pencil light-beam. Middle-row: RGB-profiles and reflectance-per-wavelength. Bottom row: Result of fitting the RGB-profile with 6 weighted Gaussians.

Female Age 55 $\xi = 0$ v_m 2 v_{Hb} 5

Gender	Age	ξ	v_m	v_{Hb}	c_{bil}	c_{car}	Skin roughness
Female	55	0	2	5	0.05	2.1e-4	0.12802

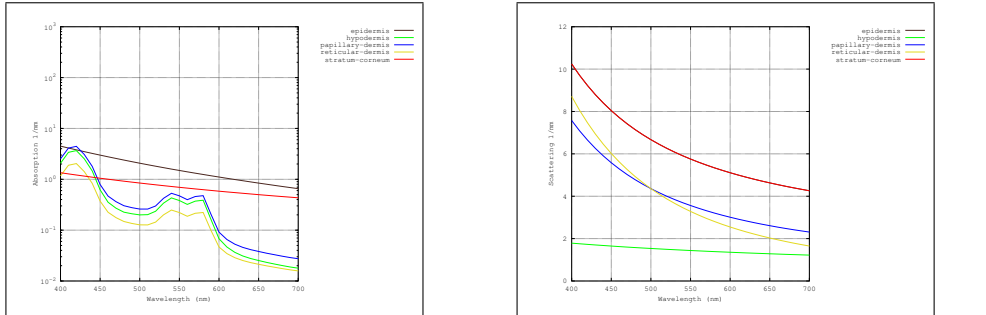


Figure 94: Top row: Full skin phantom description and skin closeup image. Bottom row, from left to right: Absorption and scattering coefficients per-wavelength for each skin layer, and result on a human cheek.

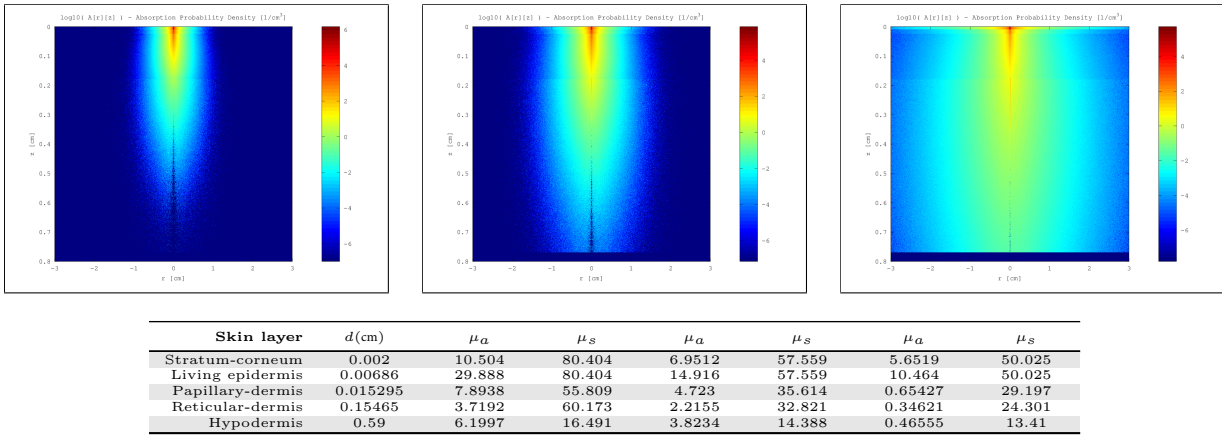
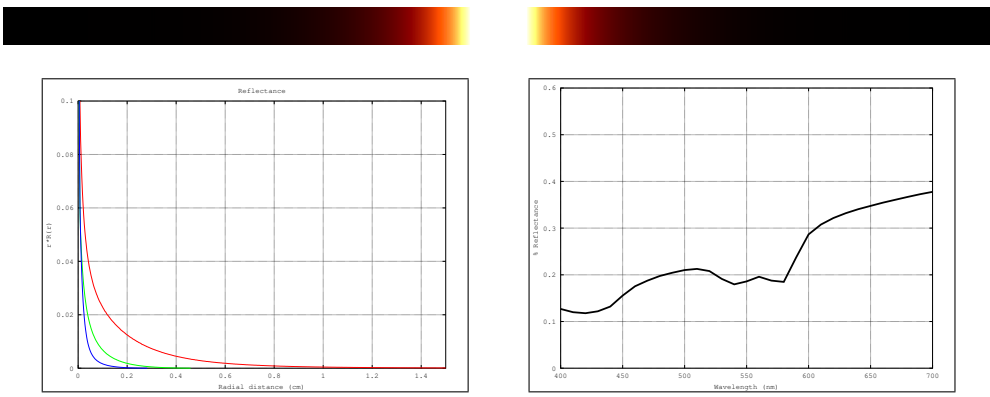


Figure 95: Top row: MonteCarlo simulations for 450nm, 550nm and 610nm. Bottom row: Resultant optical parameters (d , μ_a , μ_s') applying our skin aging model.



Fitting	R	G	B
w_i v_i RMS,AMAX	(658.060, 66.698, 7.286, 1.493, 0.299, 0.044) (0.529, 2.611, 23.272, 172.257, 1385.909, 10275.716) 1.35e-11, 1e-03f	(395.712, 48.244, 5.415, 1.516, 0.355, 0.057) (0.472, 2.097, 13.730, 67.677, 342.245, 1862.011) 3.57e-12, 3e-04f	(469.634, 49.592, 7.519, 2.201, 0.409, 0.046) (0.459, 1.935, 9.111, 34.263, 139.393, 739.537) 1.01e-12, 2e-04f

Figure 96: Top row: Diffusion profile response for a pencil light-beam. Middle-row: RGB-profiles and reflectance-per-wavelength. Bottom row: Result of fitting the RGB-profile with 6 weighted Gaussians.

Female Age 80 $\xi = 0$ v_m 2 v_{Hb} 5

Gender	Age	ξ	v_m	v_{Hb}	c_{bil}	c_{car}	Skin roughness
Female	80	0	2	5	0.05	2.1e-4	0.18059

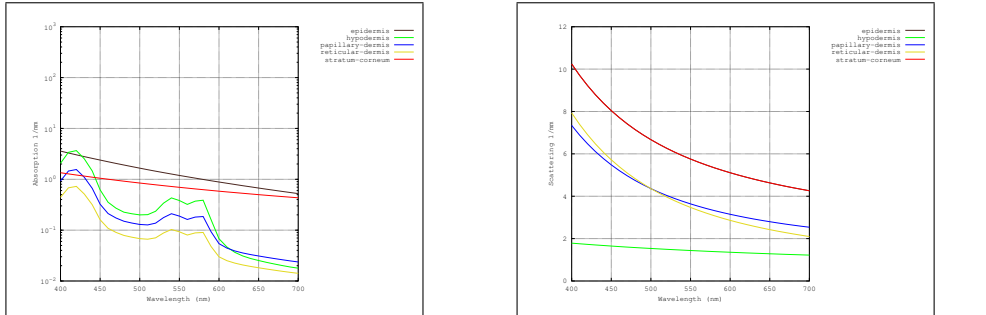


Figure 97: Top row: Full skin phantom description and skin closeup image. Bottom row, from left to right: Absorption and scattering coefficients per-wavelength for each skin layer, and result on a human cheek.

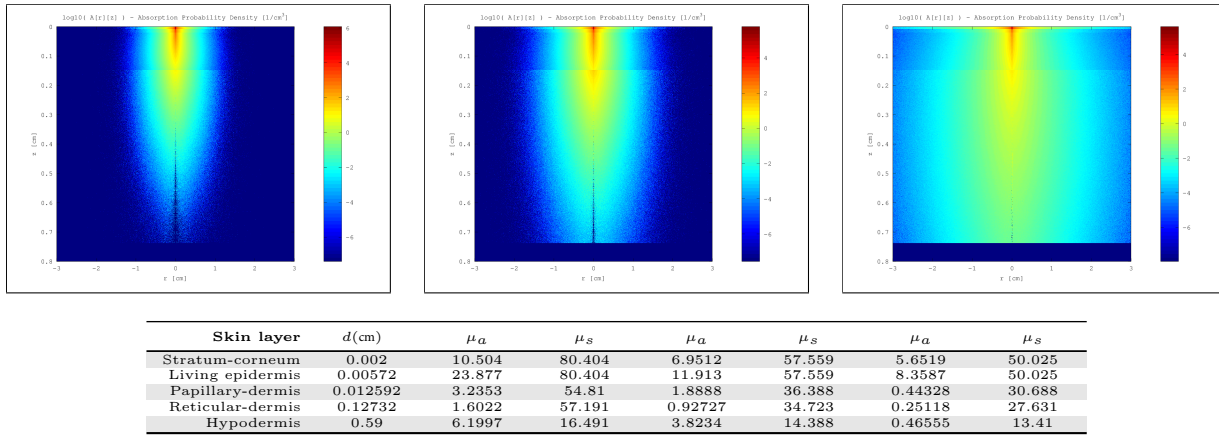
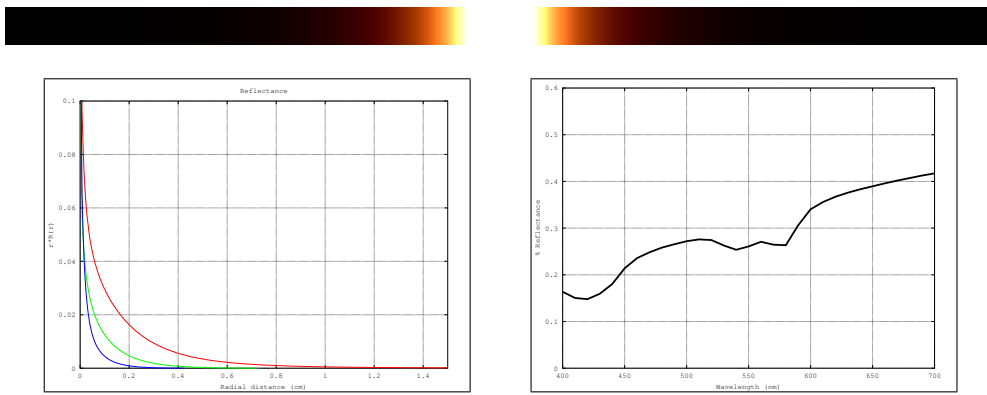


Figure 98: Top row: MonteCarlo simulations for 450nm, 550nm and 610nm. Bottom row: Resultant optical parameters (d , μ_a , μ'_s) applying our skin aging model.



Fitting	R	G	B
w_i v_i RMS,AMAX	(637.605, 42.171, 6.658, 1.464, 0.350, 0.053) (0.587, 3.154, 26.792, 205.230, 1541.957, 10403.274) 9.05e-11, 3e-03f	(373.291, 32.284, 5.035, 1.327, 0.336, 0.059) (0.541, 2.415, 16.901, 99.866, 588.289, 3318.335) 1.36e-11, 7e-04f	(449.440, 40.767, 7.557, 2.085, 0.427, 0.060) (0.500, 2.073, 10.764, 47.624, 230.837, 1258.333) 6.07e-12, 5e-04f

Figure 99: Top row: Diffusion profile response for a pencil light-beam. Middle-row: RGB-profiles and reflectance-per-wavelength. Bottom row: Result of fitting the RGB-profile with 6 weighted Gaussians.

Female Age 30 $\xi = 1$ $v_m = 2$ $v_{Hb} = 5$

Gender	Age	ξ	v_m	v_{Hb}	c_{bil}	c_{car}	Skin roughness
Female	30	1	2	5	0.05	2.1e-4	0.069549

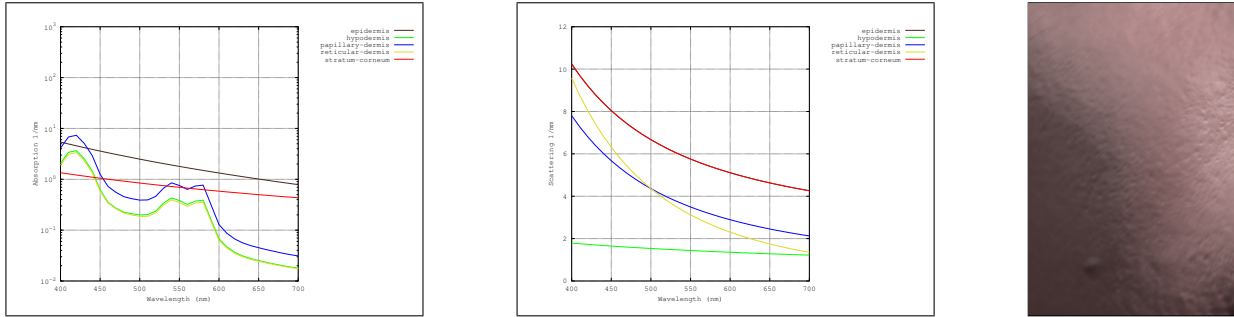


Figure 100: Top row: Full skin phantom description and skin closeup image. Bottom row, from left to right: Absorption and scattering coefficients per-wavelength for each skin layer, and result on a human cheek.

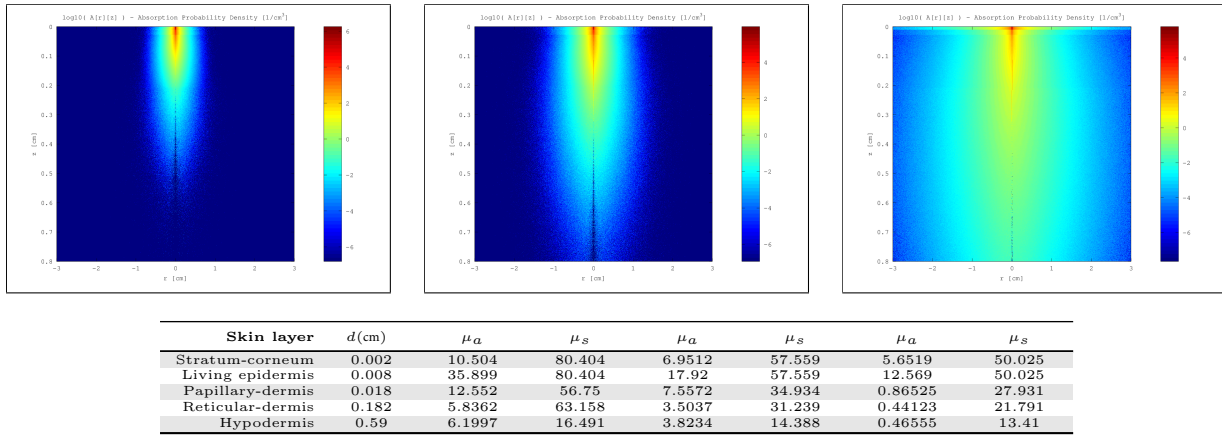
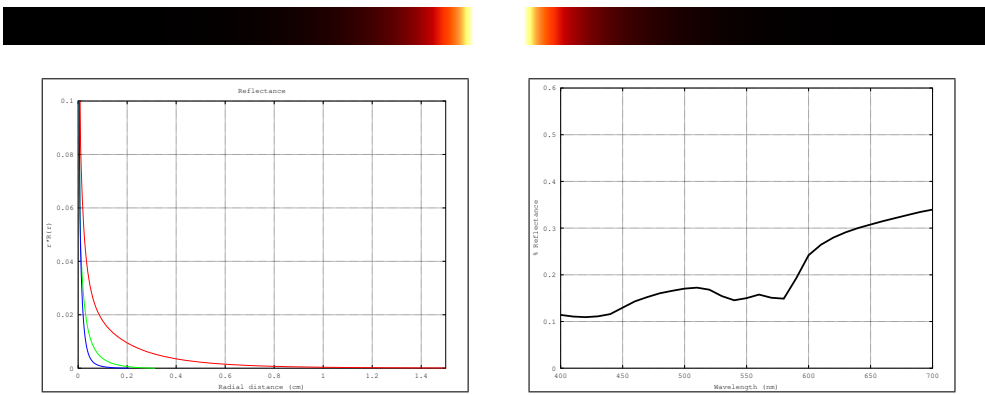


Figure 101: Top row: MonteCarlo simulations for 450nm, 550nm and 610nm. Bottom row: Resultant optical parameters (d , μ_a , μ'_s) applying our skin aging model.



Fitting	R	G	B
w_i v_i RMS,AMAX	(655.361, 66.021, 6.764, 1.366, 0.238, 0.033) (0.536, 2.892, 24.488, 167.168, 1351.068, 10627.503) 3.11e-12, 6e-04f	(383.579, 40.978, 4.818, 1.484, 0.354, 0.054) (0.505, 2.455, 13.649, 55.505, 231.363, 1130.986) 3.22e-15, 1e-05f	(454.860, 39.998, 6.417, 2.033, 0.397, 0.037) (0.489, 2.238, 9.112, 29.601, 102.071, 485.609) 3.82e-15, 1e-05f

Figure 102: Top row: Diffusion profile response for a pencil light-beam. Middle-row: RGB-profiles and reflectance-per-wavelength. Bottom row: Result of fitting the RGB-profile with 6 weighted Gaussians.

Female Age 55 $\xi = 1$ $v_m = 2$ $v_{Hb} = 5$

Gender	Age	ξ	v_m	v_{Hb}	c_{bil}	c_{car}	Skin roughness
Female	55	1	2	5	0.05	2.1e-4	0.099683

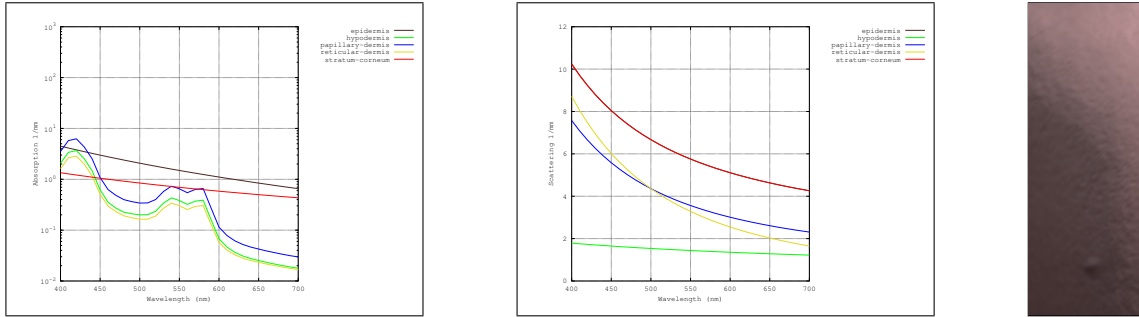


Figure 103: Top row: Full skin phantom description and skin closeup image. Bottom row, from left to right: Absorption and scattering coefficients per-wavelength for each skin layer, and result on a human cheek.

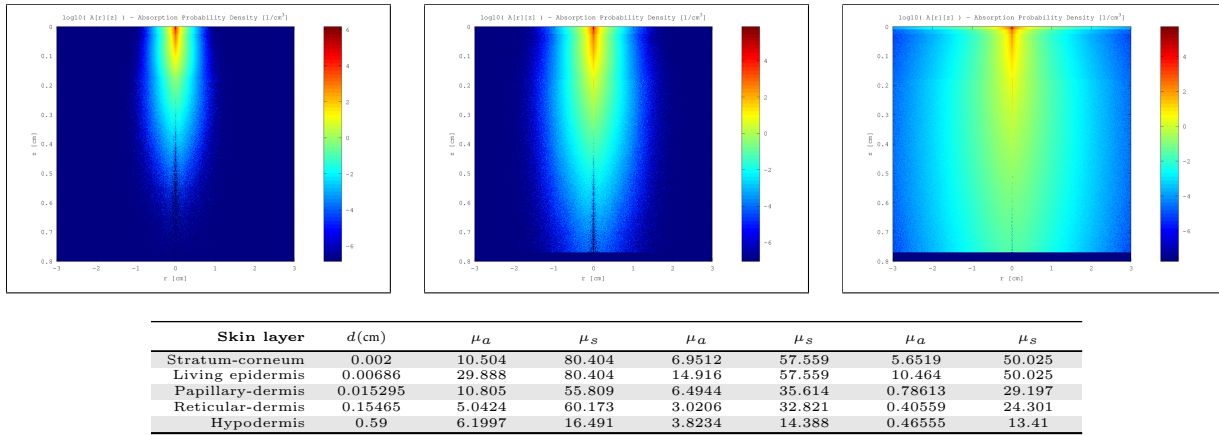
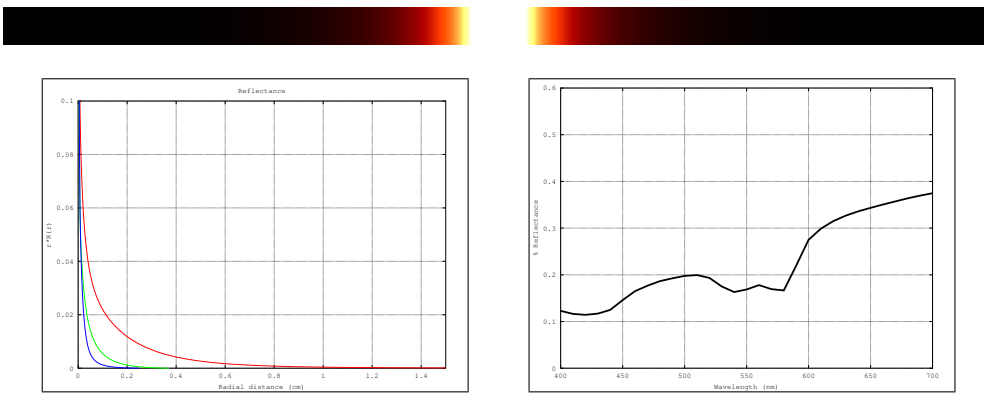


Figure 104: Top row: MonteCarlo simulations for 450nm, 550nm and 610nm. Bottom row: Resultant optical parameters (d , μ_a , μ'_s) applying our skin aging model.



Fitting	R	G	B
w_i v_i RMS,AMAX	(659.813, 68.411, 7.390, 1.521, 0.300, 0.044) (0.525, 2.558, 22.528, 165.086, 1320.646, 9875.285) 1.39e-11, 1e-03f	(377.513, 36.996, 6.161, 4.633, 0.997, 0.131) (0.527, 2.573, 0.008, 20.004, 127.433, 929.682) 1.12e-11, 6e-04f	(469.625, 49.799, 7.566, 2.288, 0.433, 0.046) (0.458, 1.912, 8.661, 31.368, 121.128, 626.595) 6.01e-13, 2e-04f

Figure 105: Top row: Diffusion profile response for a pencil light-beam. Middle-row: RGB-profiles and reflectance-per-wavelength. Bottom row: Result of fitting the RGB-profile with 6 weighted Gaussians.

Female Age 80 $\xi = 1$ $v_m = 2$ $v_{Hb} = 5$

Gender	Age	ξ	v_m	v_{Hb}	c_{bil}	c_{car}	Skin roughness
Female	80	1	2	5	0.05	2.1e-4	0.14797

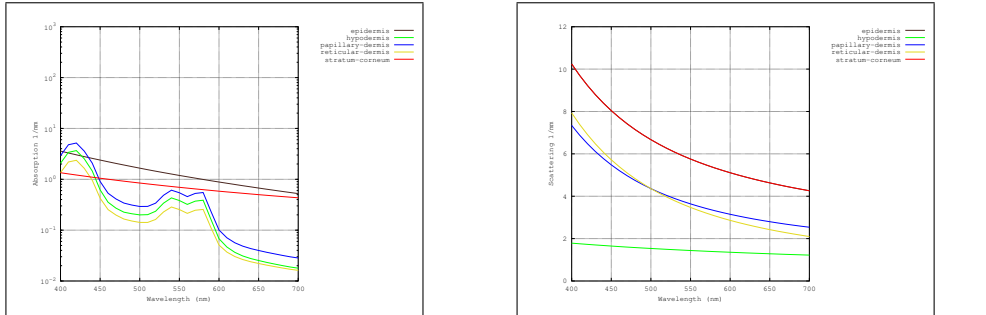


Figure 106: Top row: Full skin phantom description and skin closeup image. Bottom row, from left to right: Absorption and scattering coefficients per-wavelength for each skin layer, and result on a human cheek.

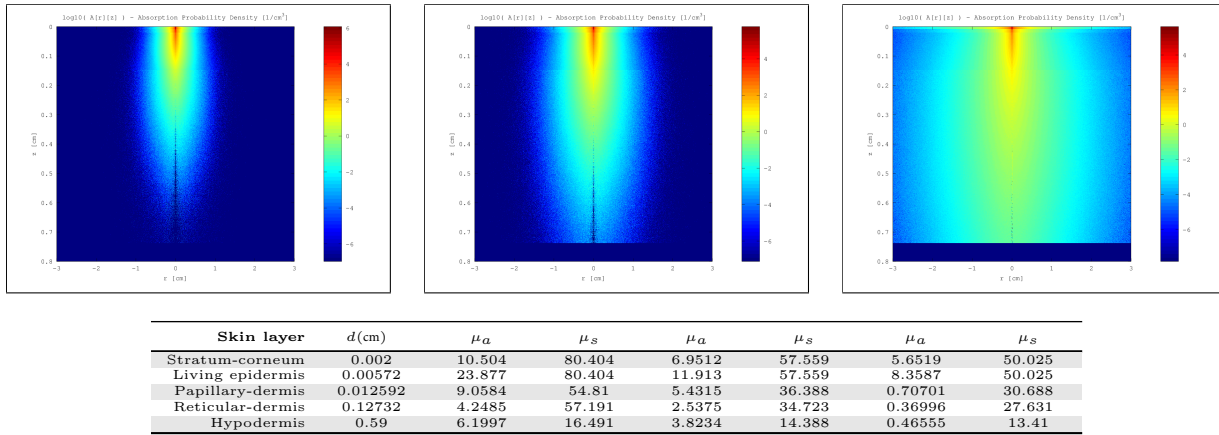
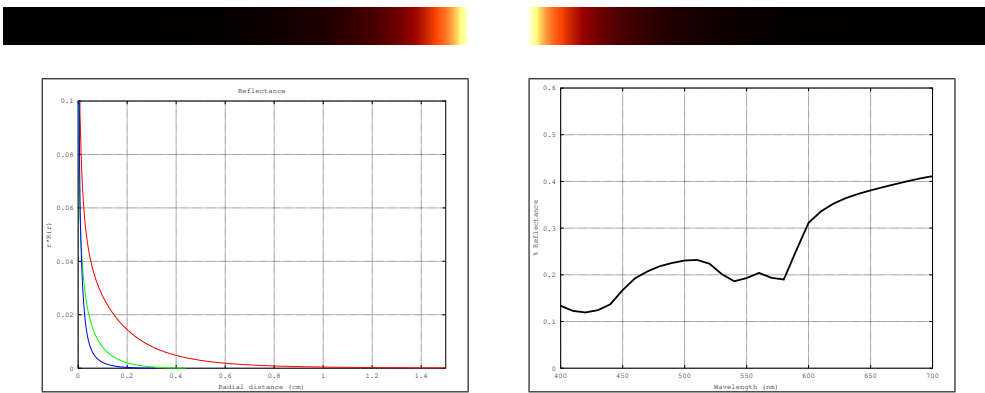


Figure 107: Top row: MonteCarlo simulations for 450nm, 550nm and 610nm. Bottom row: Resultant optical parameters (d , μ_a , μ'_s) applying our skin aging model.



Fitting	R	G	B
w_i v_i RMS,AMAX	(640.414, 45.262, 6.884, 1.505, 0.347, 0.051) (0.577, 2.961, 24.699, 186.005, 1404.126, 9659.555) 4.95e-11, 2e-03f	(383.281, 43.436, 5.619, 1.620, 0.417, 0.070) (0.495, 1.971, 12.899, 65.445, 331.497, 1754.050) 5.51e-11, 1e-03f	(460.250, 49.238, 7.982, 2.339, 0.452, 0.053) (0.470, 1.817, 8.928, 35.386, 151.489, 822.531) 2.28e-12, 3e-04f

Figure 108: Top row: Diffusion profile response for a pencil light-beam. Middle-row: RGB-profiles and reflectance-per-wavelength. Bottom row: Result of fitting the RGB-profile with 6 weighted Gaussians.

Gender	Age	ξ	v_m	v_{Hb}	c_{bil}	c_{car}	Skin roughness
Female	30	0	30	5	0.05	2.1e-4	0.081579

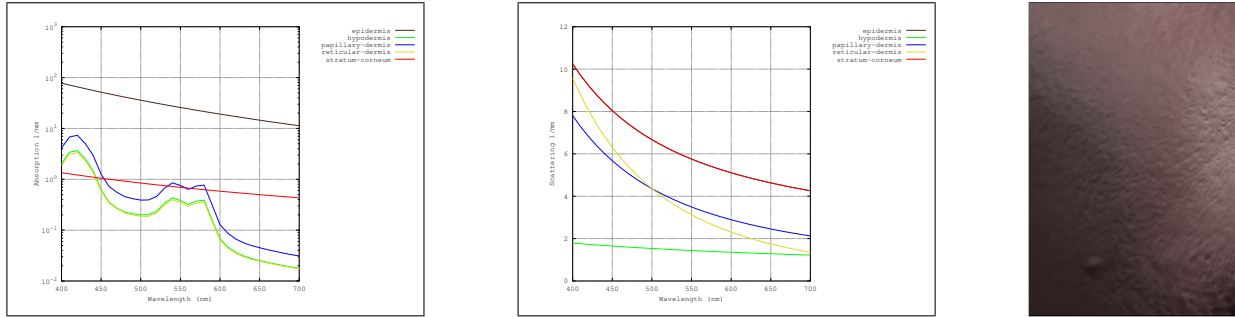


Figure 109: Top row: Full skin phantom description and skin closeup image. Bottom row, from left to right: Absorption and scattering coefficients per-wavelength for each skin layer, and result on a human cheek.

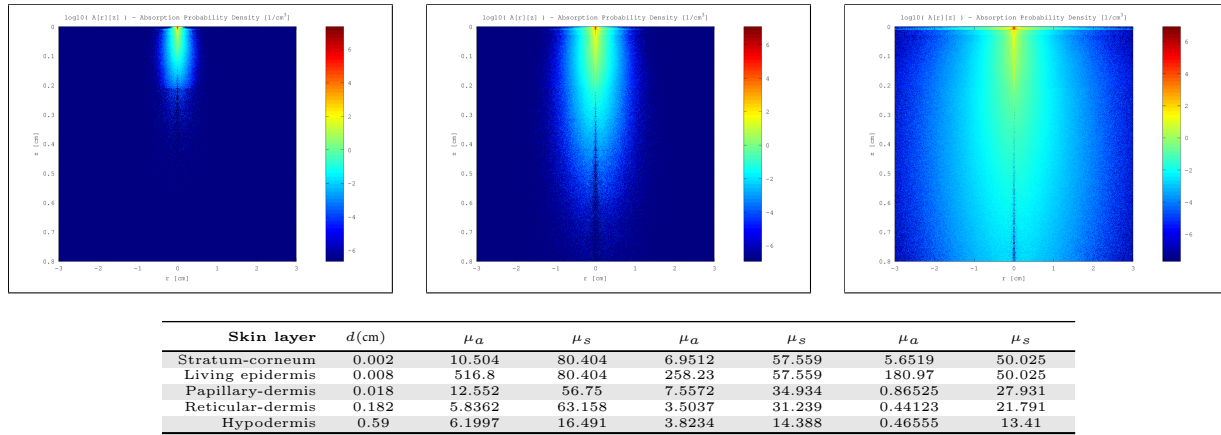
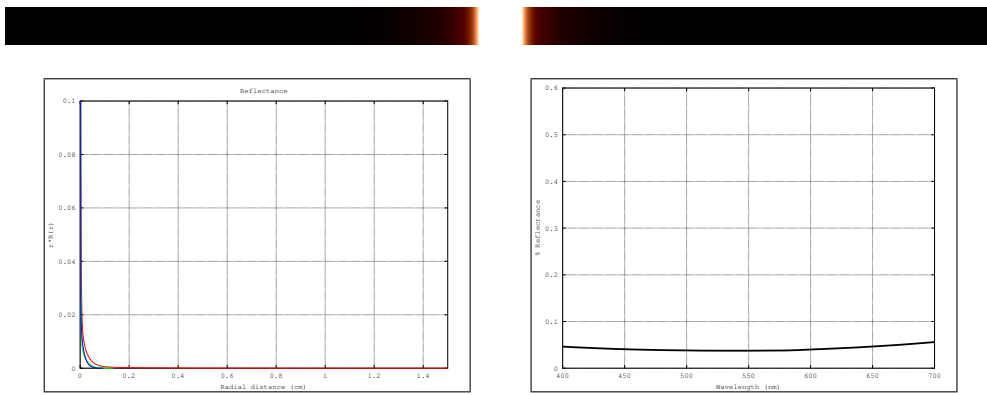


Figure 110: Top row: MonteCarlo simulations for 450nm, 550nm and 610nm. Bottom row: Resultant optical parameters (d , μ_a , μ'_s) applying our skin aging model.



Fitting	R	G	B
w_i v_i RMS,AMAX	(811.209, 54.633, 6.704, 1.138, 0.223, 0.007) (0.355, 1.131, 3.858, 22.247, 134.216, 1927.654) 3.34e-08, 4e-02f	(322.876, 240.376, 29.632, 2.713, 0.548, 0.116) (0.269, 0.345, 0.920, 3.978, 23.112, 114.380) 4.23e-08, 3e-02f	(353.798, 351.586, 70.910, 3.735, 1.003, 0.207) (0.238, 0.270, 0.525, 3.376, 16.326, 65.515) 3.90e-11, 8e-04f

Figure 111: Top row: Diffusion profile response for a pencil light-beam. Middle-row: RGB-profiles and reflectance-per-wavelength. Bottom row: Result of fitting the RGB-profile with 6 weighted Gaussians.

Gender	Age	ξ	v_m	v_{Hb}	c_{bil}	c_{car}	Skin roughness
Female	55	0	30	5	0.05	2.1e-4	0.12802

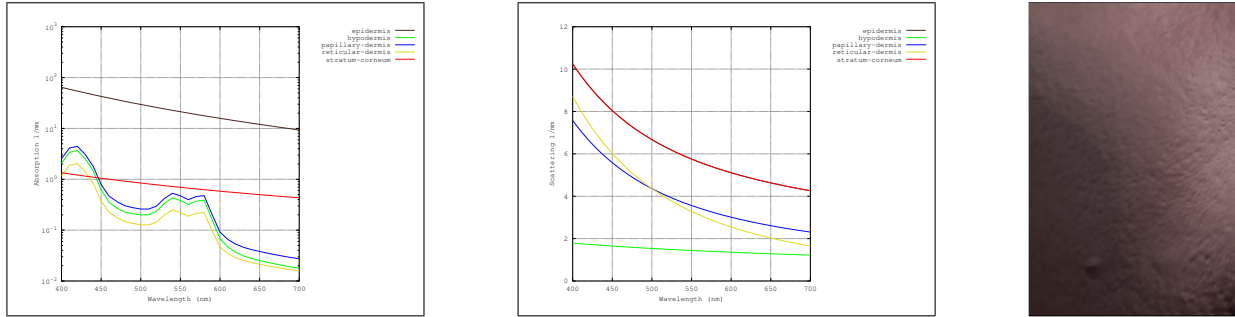


Figure 112: Top row: Full skin phantom description and skin closeup image. Bottom row, from left to right: Absorption and scattering coefficients per-wavelength for each skin layer, and result on a human cheek.

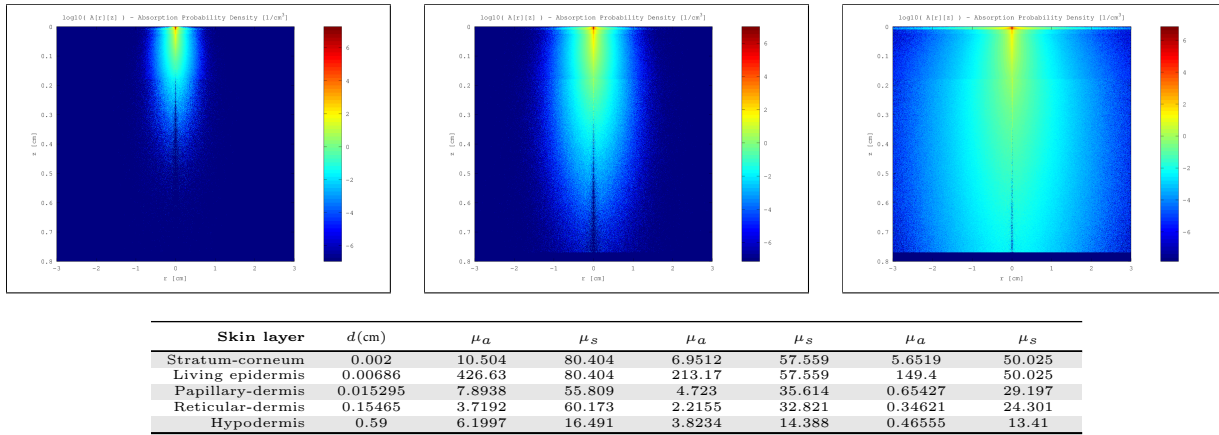


Figure 113: Top row: MonteCarlo simulations for 450nm, 550nm and 610nm. Bottom row: Resultant optical parameters (d , μ_a , μ_s') applying our skin aging model.

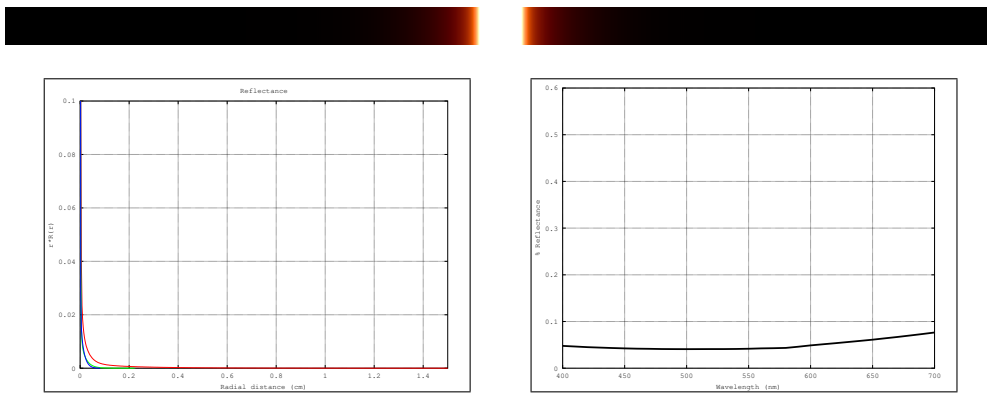


Figure 114: Top row: Diffusion profile response for a pencil light-beam. Middle-row: RGB-profiles and reflectance-per-wavelength. Bottom row: Result of fitting the RGB-profile with 6 weighted Gaussians.

Gender	Age	ξ	v_m	v_{Hb}	c_{bil}	c_{car}	Skin roughness
Female	80	0	30	5	0.05	2.1e-4	0.18059

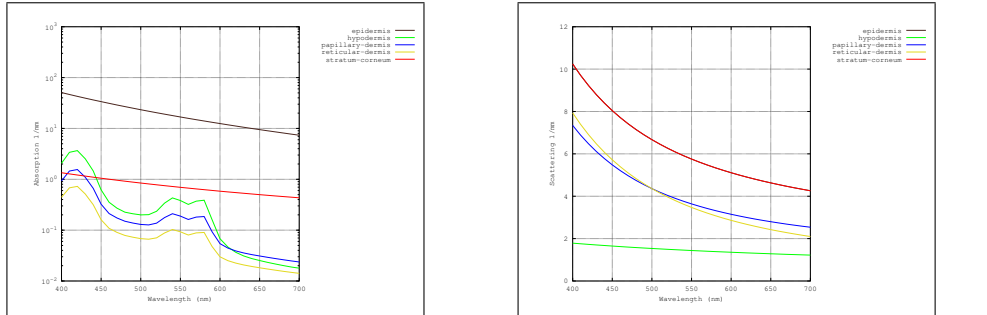


Figure 115: Top row: Full skin phantom description and skin closeup image. Bottom row, from left to right: Absorption and scattering coefficients per-wavelength for each skin layer, and result on a human cheek.

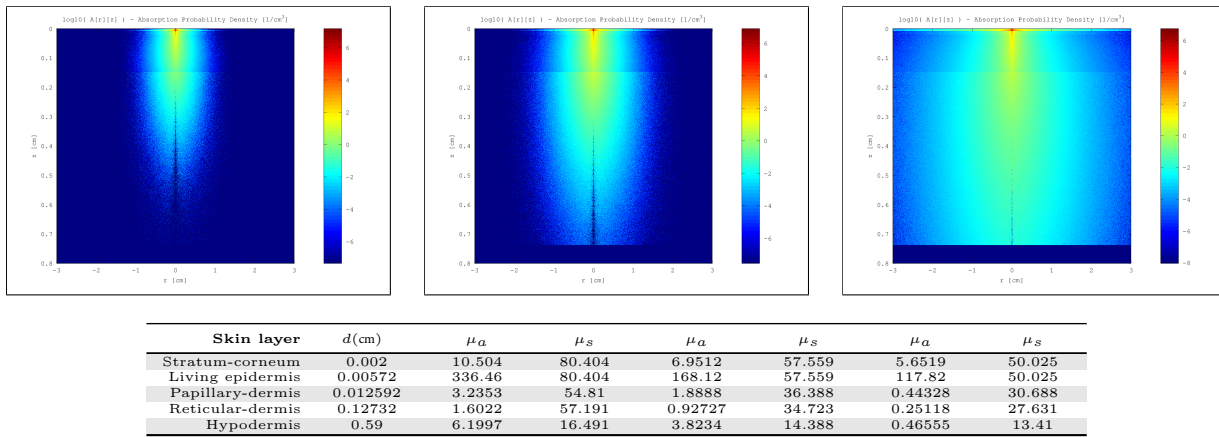
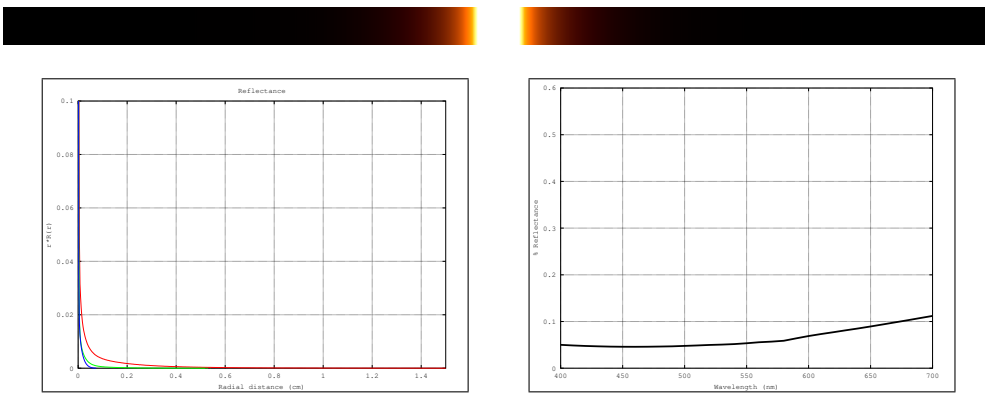


Figure 116: Top row: MonteCarlo simulations for 450nm, 550nm and 610nm. Bottom row: Resultant optical parameters (d , μ_a , μ'_s) applying our skin aging model.



Fitting	R	G	B
w_i v_i RMS,AMAX	(664.669, 25.513, 3.053, 0.578, 0.080, 0.011) (0.481, 2.278, 15.193, 99.543, 780.606, 6871.338) 1.16e-12, 3e-04f	(470.366, 66.142, 5.864, 0.995, 0.196, 0.011) (0.318, 0.776, 3.168, 18.584, 107.440, 1140.105) 5.86e-08, 3e-02f	(107.131, 98.322, 86.770, 66.430, 66.302, -2.454) (0.388, 0.469, 0.414, 0.715, 0.399, 0.198) 1.17e-05, 5e-01f

Figure 117: Top row: Diffusion profile response for a pencil light-beam. Middle-row: RGB-profiles and reflectance-per-wavelength. Bottom row: Result of fitting the RGB-profile with 6 weighted Gaussians.

Gender	Age	ξ	v_m	v_{Hb}	c_{bil}	c_{car}	Skin roughness
Female	30	1	30	5	0.05	2.1e-4	0.069549

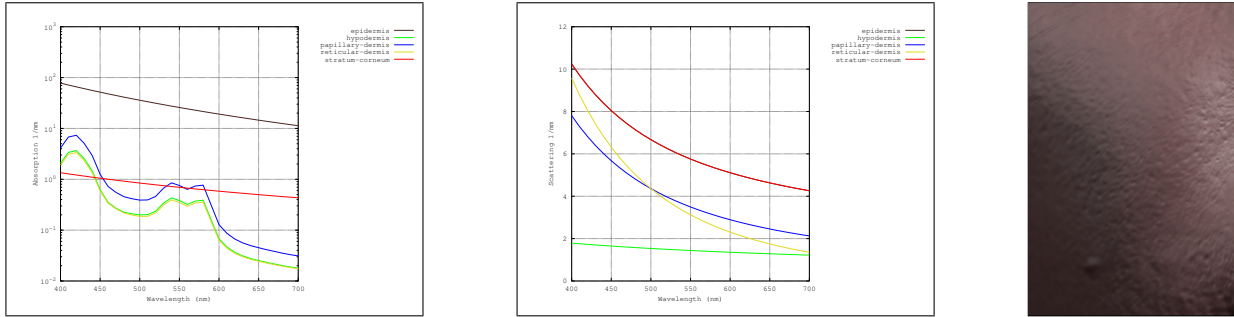


Figure 118: Top row: Full skin phantom description and skin closeup image. Bottom row, from left to right: Absorption and scattering coefficients per-wavelength for each skin layer, and result on a human cheek.

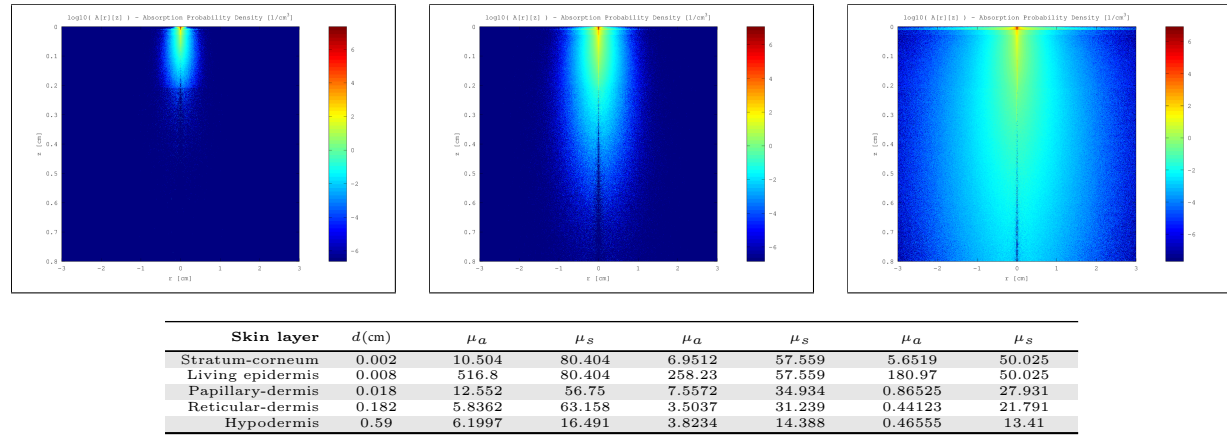
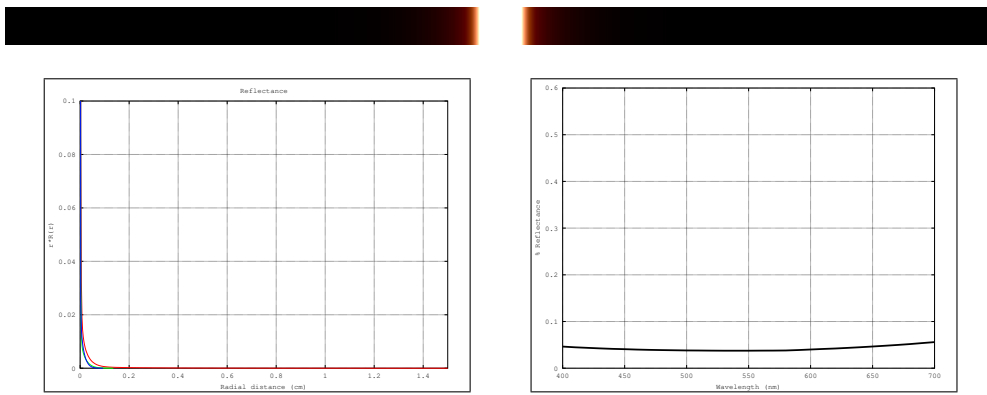


Figure 119: Top row: MonteCarlo simulations for 450nm, 550nm and 610nm. Bottom row: Resultant optical parameters (d , μ_a , μ'_s) applying our skin aging model.



Fitting	R	G	B
w_i v_i RMS,AMAX	(874.760, 252.996, 50.239, 3.285, 0.617, 0.070) (0.255, 0.431, 1.362, 7.499, 48.444, 329.030) 1.60e-07, 1e-01f	(774.644, 73.068, 43.897, 3.155, 0.573, 0.122) (0.222, 0.364, 0.808, 3.645, 22.053, 111.562) 2.67e-08, 2e-02f	(182.843, 81.506, 73.089, 68.004, 55.998, 38.059) (0.256, 0.463, 0.479, 0.487, 0.664, 0.047) 2.91e-07, 7e-02f

Figure 120: Top row: Diffusion profile response for a pencil light-beam. Middle-row: RGB-profiles and reflectance-per-wavelength. Bottom row: Result of fitting the RGB-profile with 6 weighted Gaussians.

Gender	Age	ξ	v_m	v_{Hb}	c_{bil}	c_{car}	Skin roughness
Female	55	1	30	5	0.05	2.1e-4	0.099683

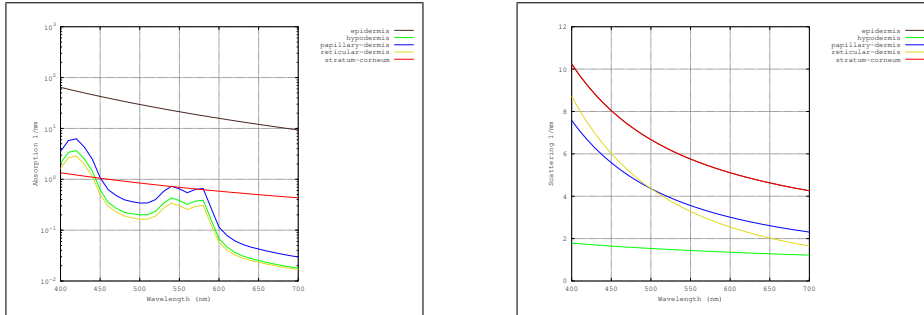


Figure 121: Top row: Full skin phantom description and skin closeup image. Bottom row, from left to right: Absorption and scattering coefficients per-wavelength for each skin layer, and result on a human cheek.

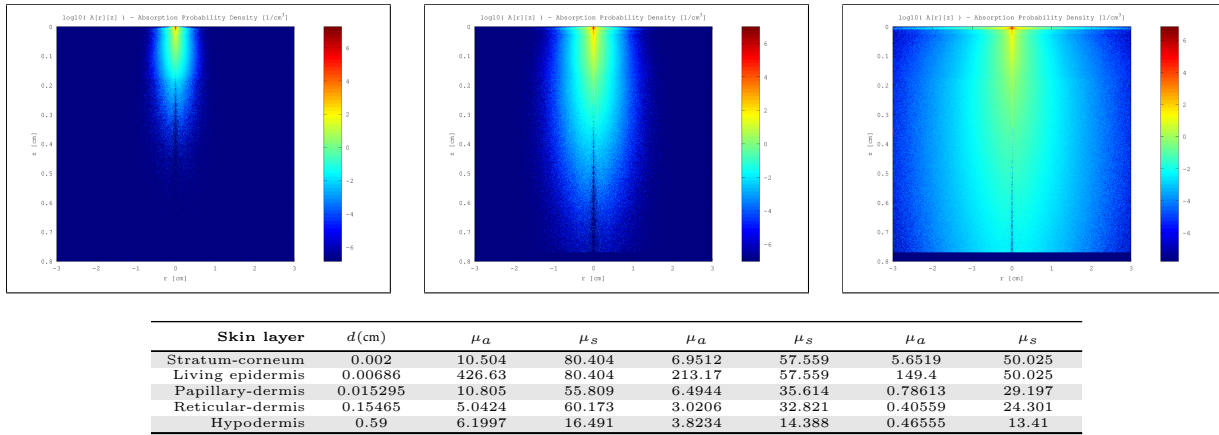


Figure 122: Top row: MonteCarlo simulations for 450nm, 550nm and 610nm. Bottom row: Resultant optical parameters (d , μ_a , μ'_s) applying our skin aging model.

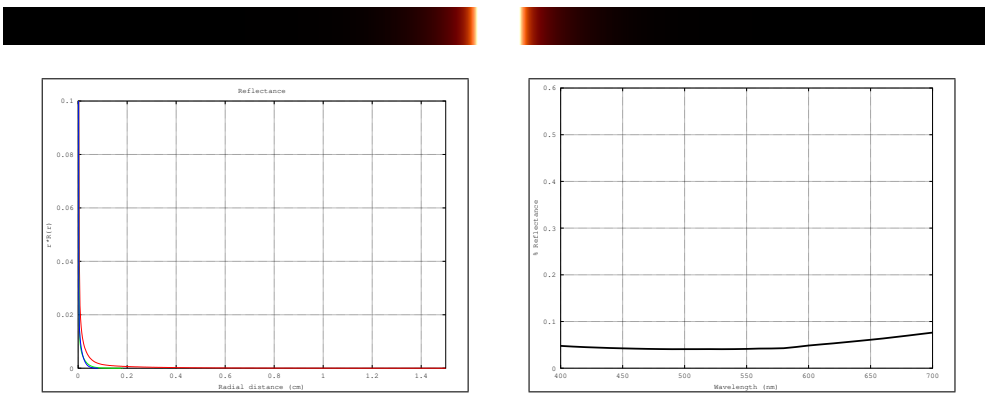


Figure 123: Top row: Diffusion profile response for a pencil light-beam. Middle-row: RGB-profiles and reflectance-per-wavelength. Bottom row: Result of fitting the RGB-profile with 6 weighted Gaussians.

Gender	Age	ξ	v_m	v_{Hb}	c_{bil}	c_{car}	Skin roughness
Female	80	1	30	5	0.05	2.1e-4	0.14797

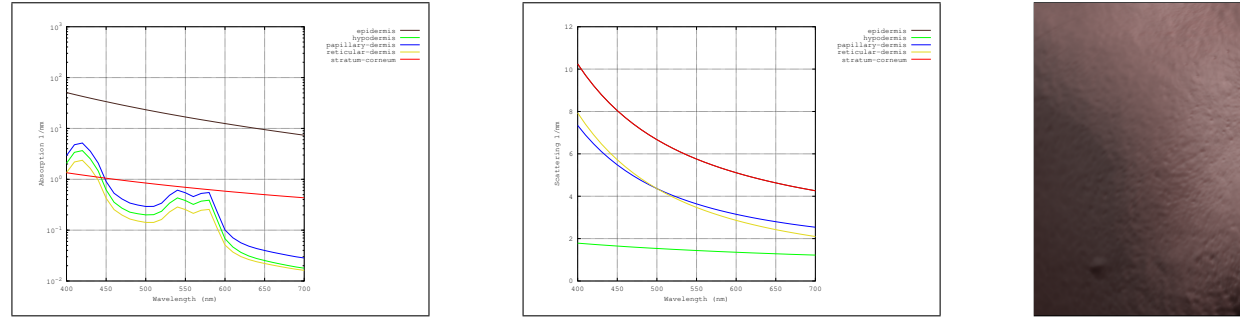


Figure 124: Top row: Full skin phantom description and skin closeup image. Bottom row, from left to right: Absorption and scattering coefficients per-wavelength for each skin layer, and result on a human cheek.

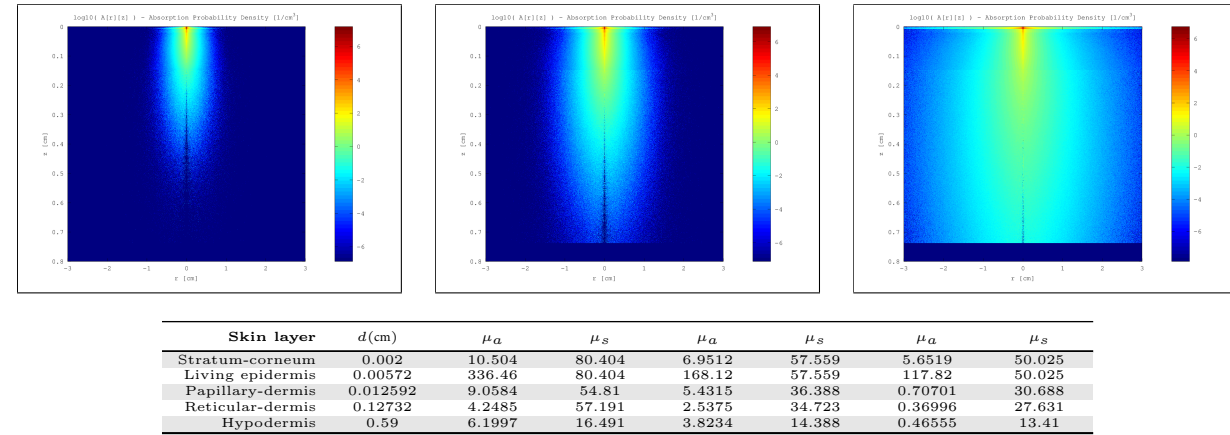


Figure 125: Top row: MonteCarlo simulations for 450nm, 550nm and 610nm. Bottom row: Resultant optical parameters (d , μ_a , μ'_s) applying our skin aging model.

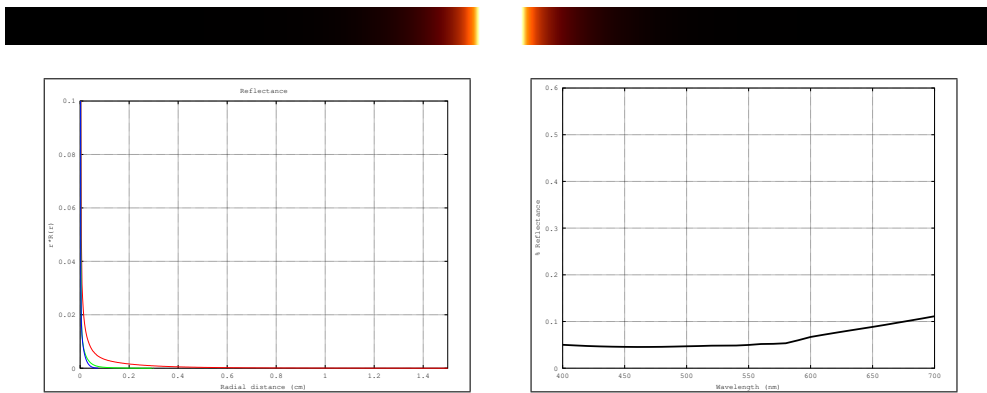


Figure 126: Top row: Diffusion profile response for a pencil light-beam. Middle-row: RGB-profiles and reflectance-per-wavelength. Bottom row: Result of fitting the RGB-profile with 6 weighted Gaussians.

Gender	Age	ξ	v_m	v_{Hb}	c_{bil}	c_{car}	Skin roughness
Female	30	0	35	5	0.05	2.1e-4	0.081579

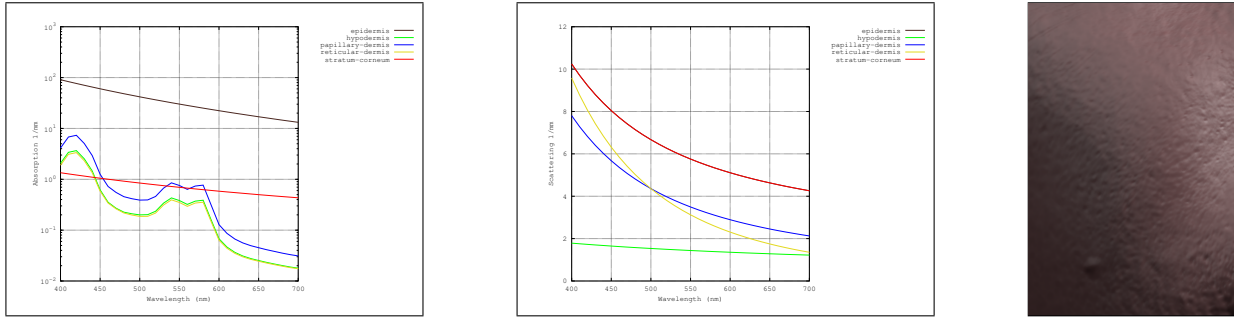


Figure 127: Top row: Full skin phantom description and skin closeup image. Bottom row, from left to right: Absorption and scattering coefficients per-wavelength for each skin layer, and result on a human cheek.

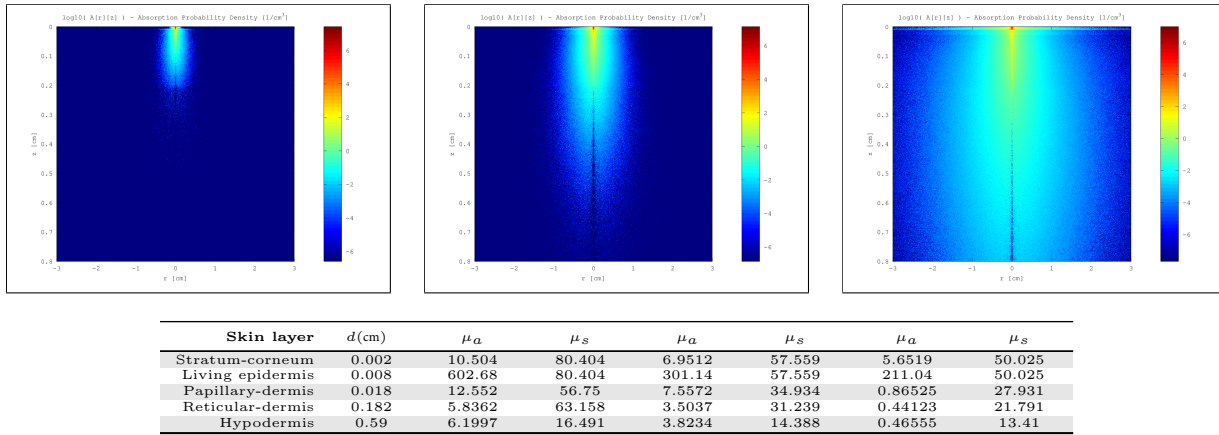
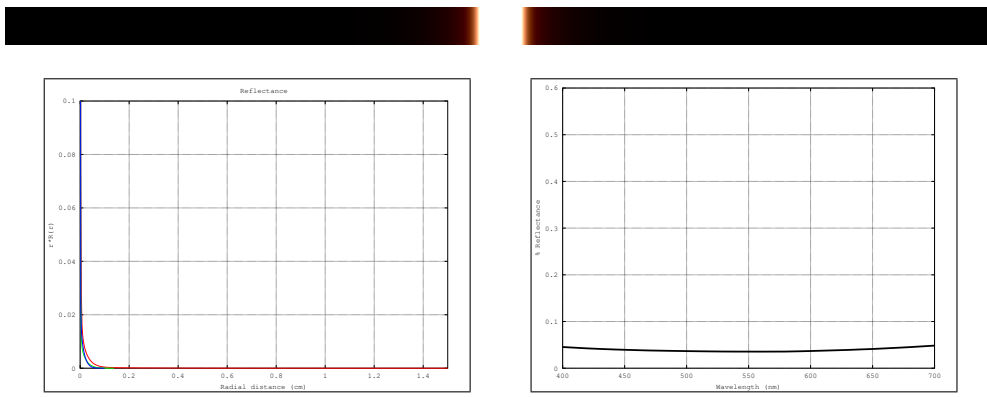


Figure 128: Top row: MonteCarlo simulations for 450nm, 550nm and 610nm. Bottom row: Resultant optical parameters (d , μ_a , μ'_s) applying our skin aging model.



Fitting	R	G	B
w_i v_i RMS,AMAX	(614.719, 345.751, 15.243, 1.503, 0.350, 0.031) (0.261, 0.508, 2.282, 13.574, 76.935, 462.291) 1.77e-09, 1e-02f	(101.827, 93.375, 85.125, 76.889, 53.210, 30.620) (0.309, 0.499, 0.444, 0.445, 0.048, 0.752) 1.30e-08, 1e-02f	(82.678, 72.983, 65.308, 63.844, 56.385, -0.359) (0.447, 0.496, 0.474, 0.670, 0.445, 0.229) 1.57e-04, 2e+00f

Figure 129: Top row: Diffusion profile response for a pencil light-beam. Middle-row: RGB-profiles and reflectance-per-wavelength. Bottom row: Result of fitting the RGB-profile with 6 weighted Gaussians.

Gender	Age	ξ	v_m	v_{Hb}	c_{bil}	c_{car}	Skin roughness
Female	55	0	35	5	0.05	2.1e-4	0.12802

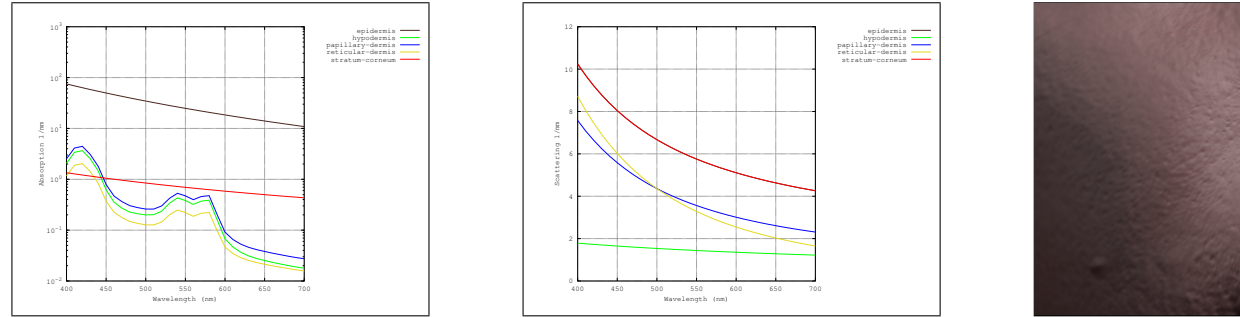


Figure 130: Top row: Full skin phantom description and skin closeup image. Bottom row, from left to right: Absorption and scattering coefficients per-wavelength for each skin layer, and result on a human cheek.

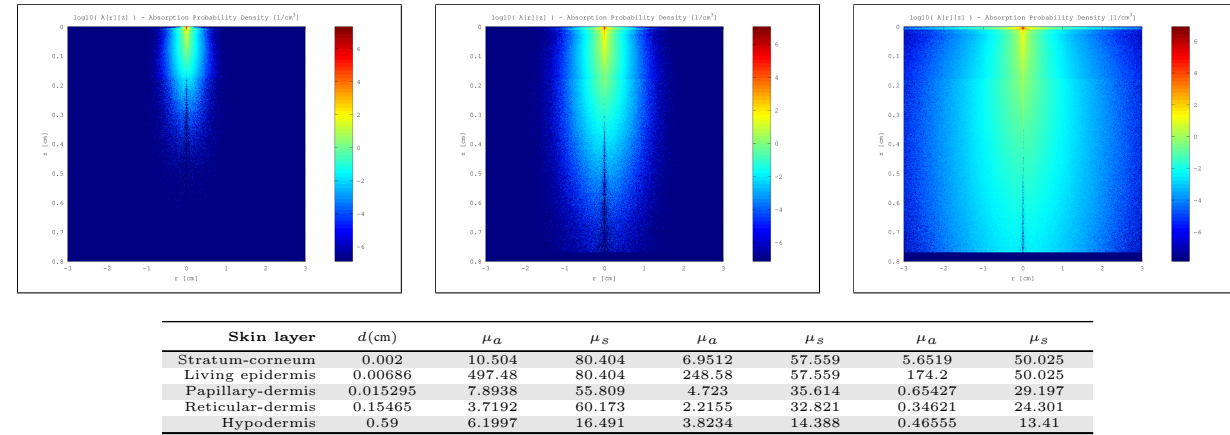
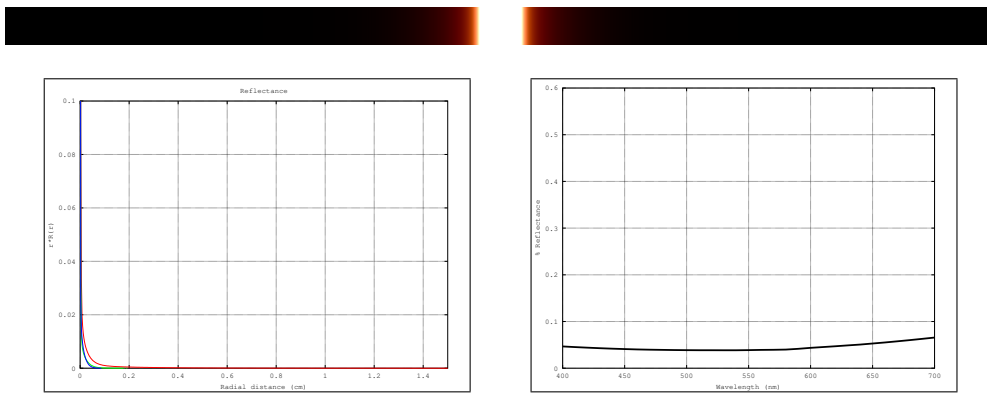


Figure 131: Top row: MonteCarlo simulations for 450nm, 550nm and 610nm. Bottom row: Resultant optical parameters (d , μ_a , μ'_s) applying our skin aging model.



Fitting	R	G	B
w_i v_i RMS,AMAX	(807.714, 84.077, 10.601, 1.387, 0.232, 0.009) (0.338, 0.881, 3.169, 22.017, 153.221, 2718.983) 2.67e-07, 1e-01f	(100.335, 80.075, 65.886, 60.457, 50.634, -7.482) (0.497, 0.612, 0.380, 0.495, 0.510, 0.526) 1.17e-07, 4e-02f	(380.393, 264.588, 4.019, 3.973, 1.085, 0.239) (0.249, 0.398, 0.006, 3.117, 14.656, 61.029) 9.22e-10, 4e-03f

Figure 132: Top row: Diffusion profile response for a pencil light-beam. Middle-row: RGB-profiles and reflectance-per-wavelength. Bottom row: Result of fitting the RGB-profile with 6 weighted Gaussians.

Gender	Age	ξ	v_m	v_{Hb}	c_{bil}	c_{car}	Skin roughness
Female	80	0	35	5	0.05	2.1e-4	0.18059

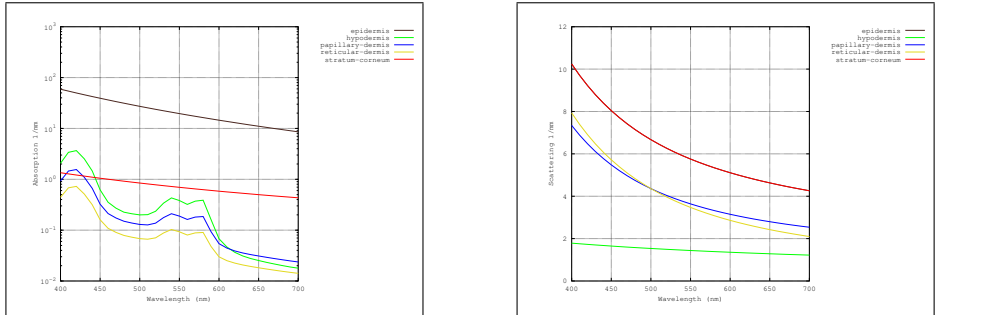


Figure 133: Top row: Full skin phantom description and skin closeup image. Bottom row, from left to right: Absorption and scattering coefficients per-wavelength for each skin layer, and result on a human cheek.

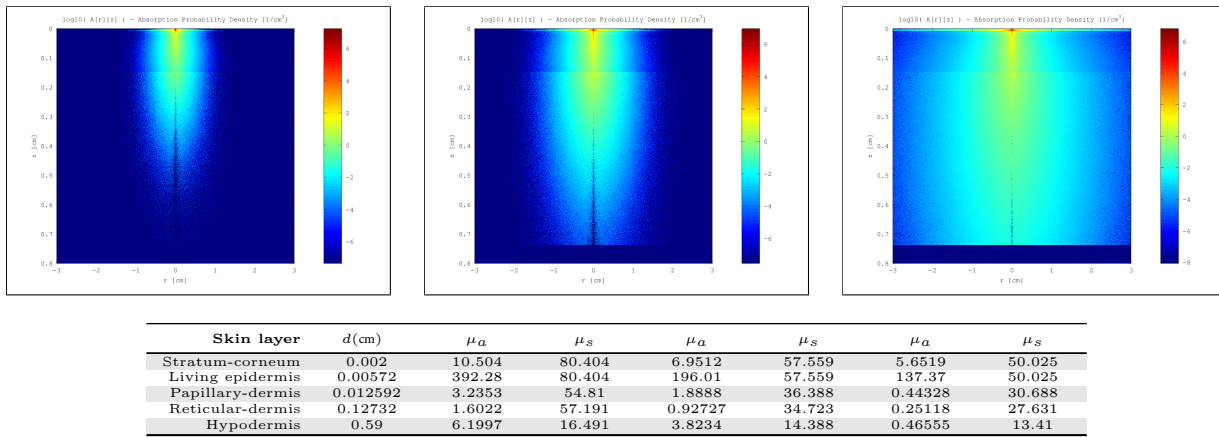
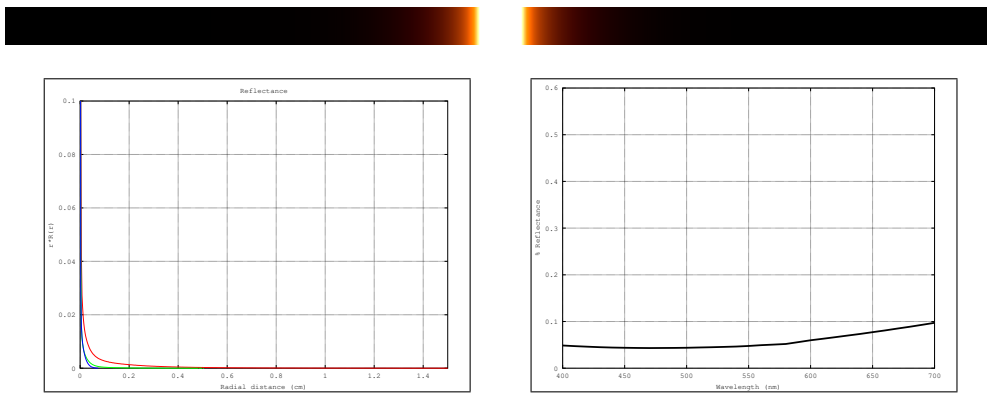


Figure 134: Top row: MonteCarlo simulations for 450nm, 550nm and 610nm. Bottom row: Resultant optical parameters (d , μ_a , μ_s') applying our skin aging model.



Fitting	R	G	B
w_i v_i RMS,AMAX	(670.833, 22.313, 2.698, 0.530, 0.069, 0.009) (0.471, 2.256, 14.452, 92.012, 687.622, 6427.064) 9.44e-13, 2e-04f	(386.294, 140.576, 7.033, 1.065, 0.233, 0.013) (0.292, 0.562, 2.501, 14.440, 83.394, 759.873) 1.36e-08, 2e-02f	(294.064, 247.846, 117.874, 4.666, 1.120, 0.253) (0.280, 0.274, 0.494, 2.997, 14.355, 58.710) 2.06e-12, 2e-04f

Figure 135: Top row: Diffusion profile response for a pencil light-beam. Middle-row: RGB-profiles and reflectance-per-wavelength. Bottom row: Result of fitting the RGB-profile with 6 weighted Gaussians.

Gender	Age	ξ	v_m	v_{Hb}	c_{bil}	c_{car}	Skin roughness
Female	30	1	35	5	0.05	2.1e-4	0.069549

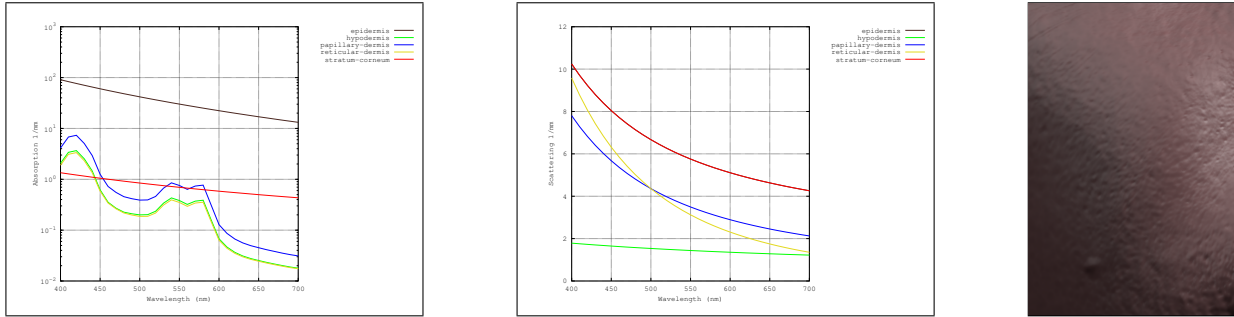


Figure 136: Top row: Full skin phantom description and skin closeup image. Bottom row, from left to right: Absorption and scattering coefficients per-wavelength for each skin layer, and result on a human cheek.

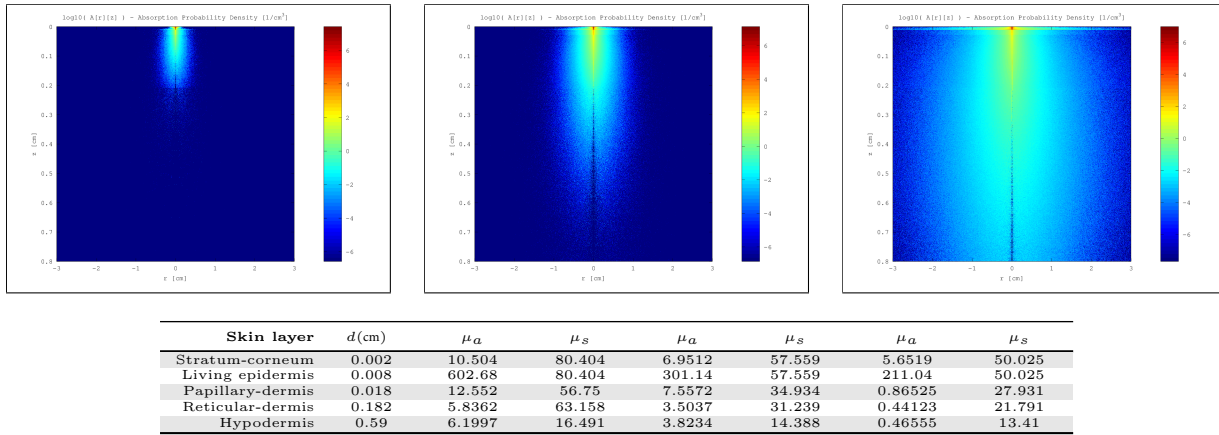
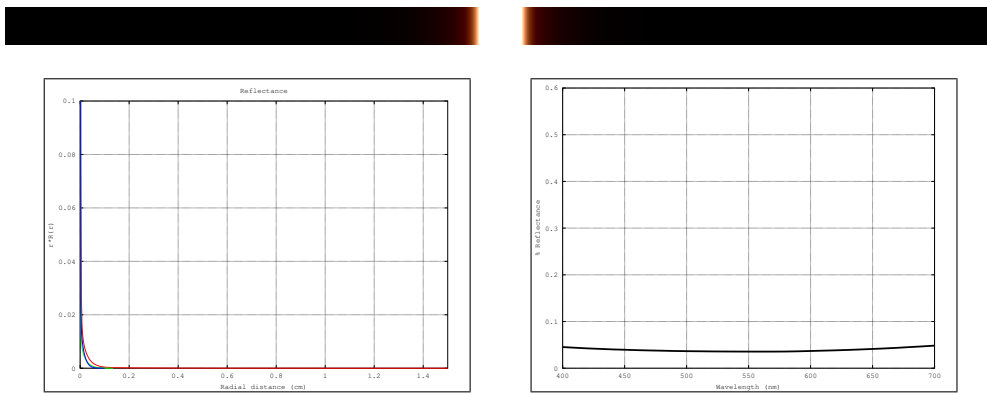


Figure 137: Top row: MonteCarlo simulations for 450nm, 550nm and 610nm. Bottom row: Resultant optical parameters (d , μ_a , μ_s') applying our skin aging model.



Fitting	R	G	B
w_i v_i RMS,AMAX	(693.263, 337.386, 32.737, 2.424, 0.508, 0.061) (0.257, 0.441, 1.504, 8.555, 52.714, 307.189) 3.46e-08, 4e-02f	(258.931, 252.954, 50.848, 3.124, 0.568, 0.123) (0.326, 0.270, 0.660, 3.437, 21.425, 109.764) 2.73e-10, 2e-03f	(108.135, 93.737, 79.516, 78.997, 66.662, 18.696) (0.364, 0.437, 0.419, 0.271, 0.657, 0.013) 1.69e-04, 2e+00f

Figure 138: Top row: Diffusion profile response for a pencil light-beam. Middle-row: RGB-profiles and reflectance-per-wavelength. Bottom row: Result of fitting the RGB-profile with 6 weighted Gaussians.

Gender	Age	ξ	v_m	v_{Hb}	c_{bil}	c_{car}	Skin roughness
Female	55	1	35	5	0.05	2.1e-4	0.099683

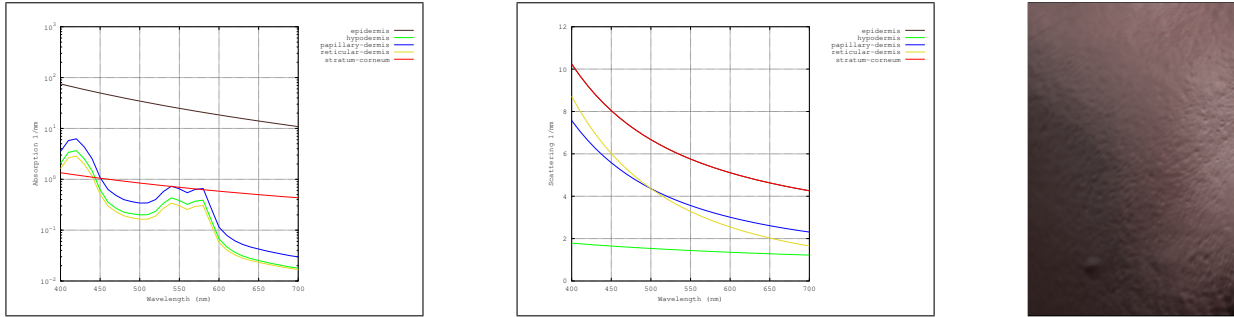


Figure 139: Top row: Full skin phantom description and skin closeup image. Bottom row, from left to right: Absorption and scattering coefficients per-wavelength for each skin layer, and result on a human cheek.

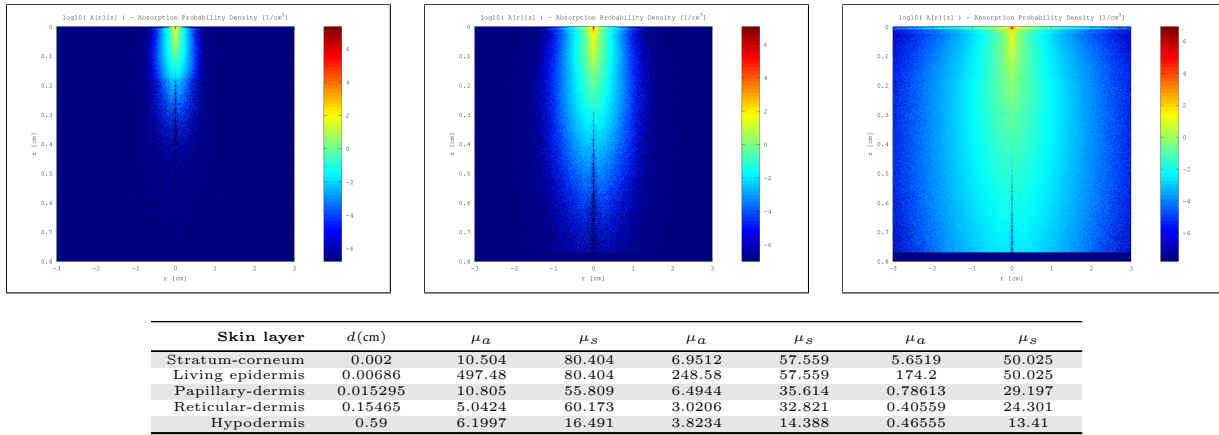
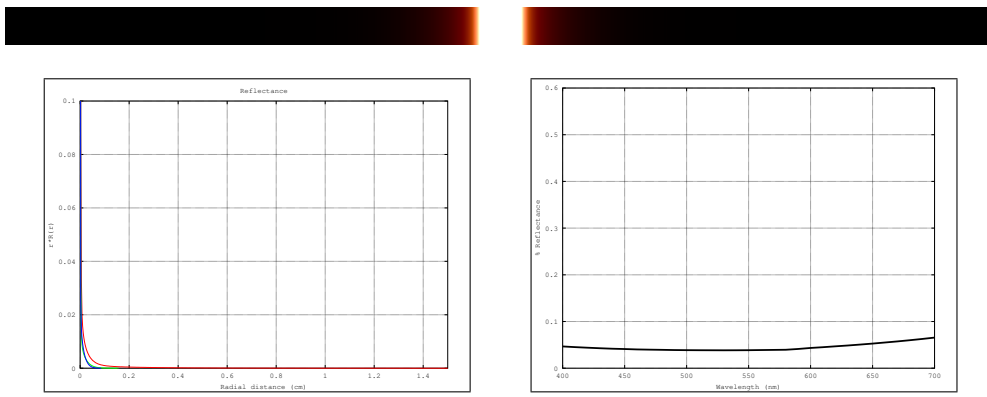


Figure 140: Top row: MonteCarlo simulations for 450nm, 550nm and 610nm. Bottom row: Resultant optical parameters (d , μ_a , μ'_s) applying our skin aging model.



Fitting	R	G	B
w_i v_i RMS,AMAX	(721.430, 29.620, 2.500, 0.547, 0.081, 0.005) (0.417, 1.747, 10.085, 56.041, 311.260, 4649.477) 1.00e-09, 8e-03f	(414.118, 226.524, 34.355, 2.758, 0.559, 0.114) (0.244, 0.339, 0.905, 4.082, 23.726, 119.759) 4.51e-08, 3e-02f	(218.127, 216.193, 102.296, 3.888, -1.791, -62.307) (0.335, 0.339, 0.514, 14.754, 14.746, 0.243) 6.33e-09, 1e-02f

Figure 141: Top row: Diffusion profile response for a pencil light-beam. Middle-row: RGB-profiles and reflectance-per-wavelength. Bottom row: Result of fitting the RGB-profile with 6 weighted Gaussians.

Gender	Age	ξ	v_m	v_{Hb}	c_{bil}	c_{car}	Skin roughness
Female	80	1	35	5	0.05	2.1e-4	0.14797

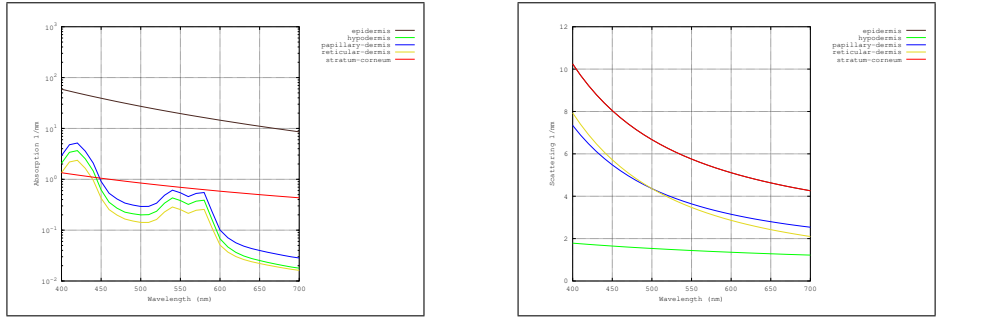


Figure 142: Top row: Full skin phantom description and skin closeup image. Bottom row, from left to right: Absorption and scattering coefficients per-wavelength for each skin layer, and result on a human cheek.

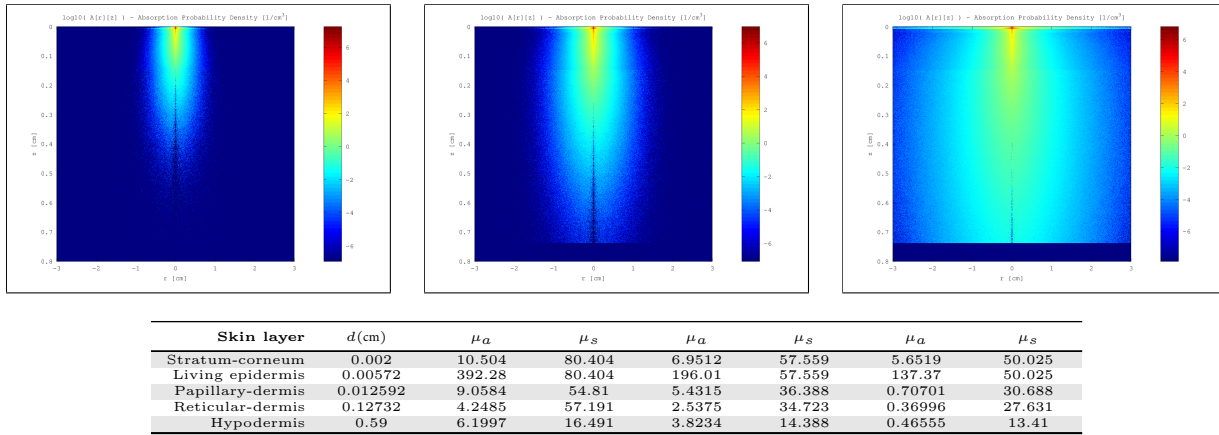


Figure 143: Top row: MonteCarlo simulations for 450nm, 550nm and 610nm. Bottom row: Resultant optical parameters (d , μ_a , μ'_s) applying our skin aging model.

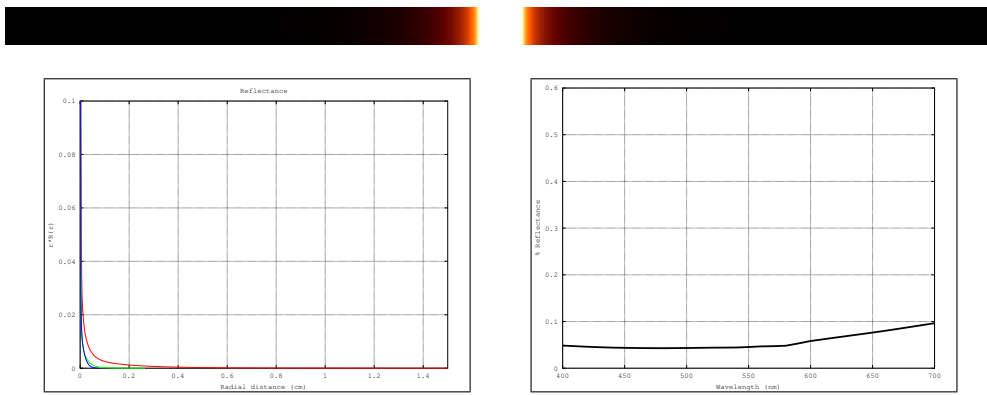


Figure 144: Top row: Diffusion profile response for a pencil light-beam. Middle-row: RGB-profiles and reflectance-per-wavelength. Bottom row: Result of fitting the RGB-profile with 6 weighted Gaussians.

Female Age 30 $\xi = 0$ v_m 3 v_{Hb} 5

Gender	Age	ξ	v_m	v_{Hb}	c_{bil}	c_{car}	Skin roughness
Female	30	0	3	5	0.05	2.1e-4	0.081579

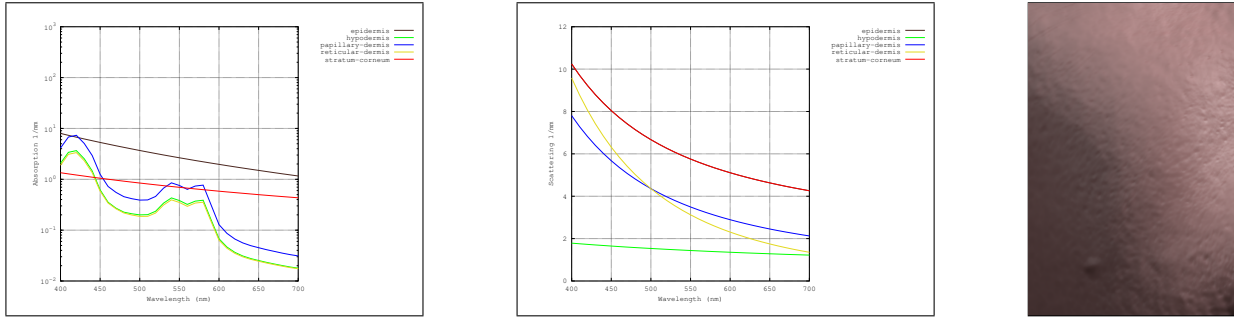


Figure 145: Top row: Full skin phantom description and skin closeup image. Bottom row, from left to right: Absorption and scattering coefficients per-wavelength for each skin layer, and result on a human cheek.

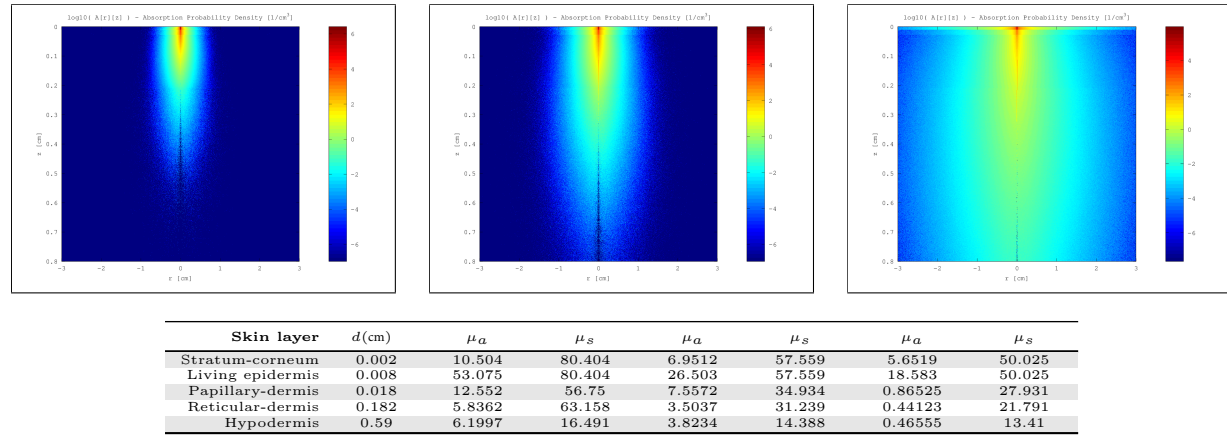
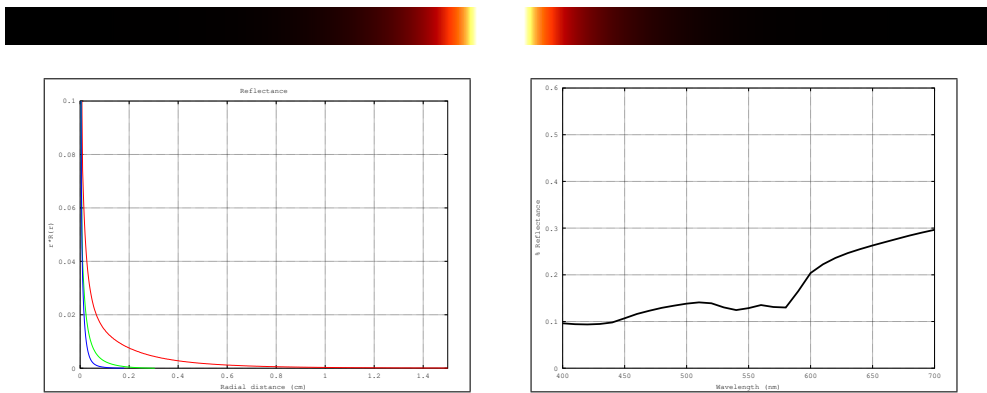


Figure 146: Top row: MonteCarlo simulations for 450nm, 550nm and 610nm. Bottom row: Resultant optical parameters (d , μ_a , μ'_s) applying our skin aging model.



Fitting	R	G	B
w_i	(655.222, 62.771, 6.336, 1.232, 0.203, 0.028)	(386.458, 39.776, 4.479, 1.405, 0.335, 0.047)	(544.681, 60.261, 11.996, 3.673, 0.763, 0.058)
v_i	(0.532, 2.836, 23.206, 156.096, 1269.220, 10224.145)	(0.493, 2.329, 12.035, 45.939, 191.008, 1001.676)	(0.367, 1.336, 3.917, 14.357, 55.113, 287.212)
RMS,AMAX	1.69e-12, 4e-04f	1.58e-09, 7e-03f	2.28e-09, 9e-03f

Figure 147: Top row: Diffusion profile response for a pencil light-beam. Middle-row: RGB-profiles and reflectance-per-wavelength. Bottom row: Result of fitting the RGB-profile with 6 weighted Gaussians.

Female Age 55 $\xi = 0$ v_m 3 v_{Hb} 5

Gender	Age	ξ	v_m	v_{Hb}	c_{bil}	c_{car}	Skin roughness
Female	55	0	3	5	0.05	2.1e-4	0.12802

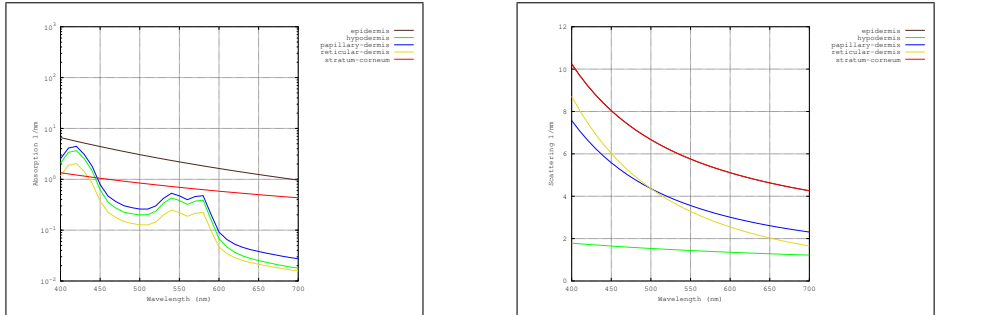


Figure 148: Top row: Full skin phantom description and skin closeup image. Bottom row, from left to right: Absorption and scattering coefficients per-wavelength for each skin layer, and result on a human cheek.

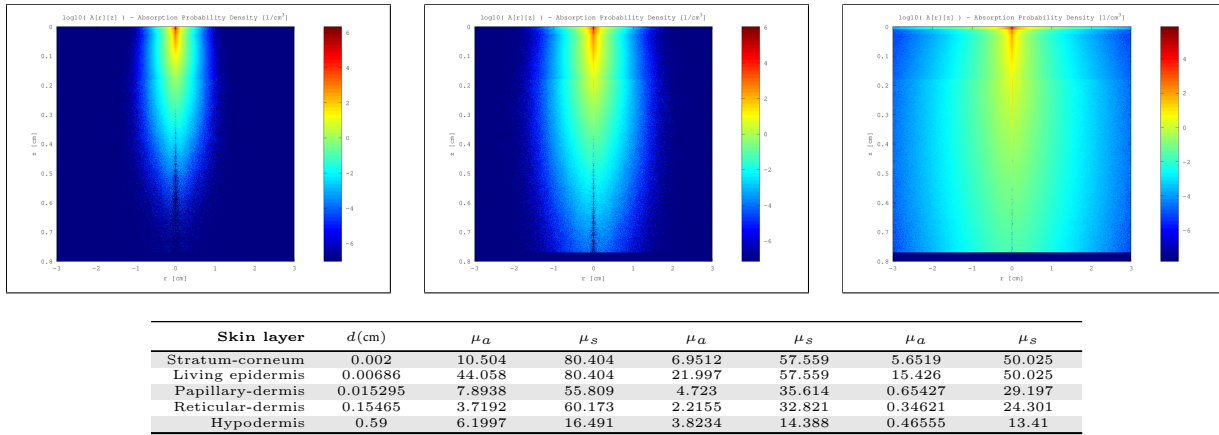
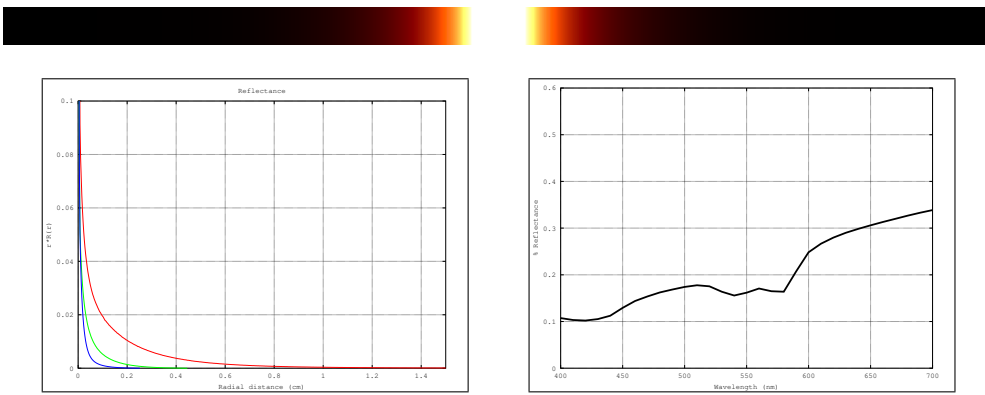


Figure 149: Top row: MonteCarlo simulations for 450nm, 550nm and 610nm. Bottom row: Resultant optical parameters (d , μ_a , μ'_s) applying our skin aging model.



Fitting	R	G	B
w_i v_i RMS,AMAX	(662.019, 60.557, 7.004, 1.416, 0.271, 0.039) (0.519, 2.520, 21.847, 158.468, 1289.309, 9830.835) 1.04e-11, 1e-03f	(400.253, 48.095, 5.129, 1.380, 0.306, 0.047) (0.459, 2.012, 12.836, 62.280, 315.561, 1772.500) 4.21e-12, 4e-04f	(466.676, 43.158, 6.608, 1.868, 0.343, 0.037) (0.459, 1.914, 8.481, 30.783, 120.697, 646.293) 1.10e-12, 2e-04f

Figure 150: Top row: Diffusion profile response for a pencil light-beam. Middle-row: RGB-profiles and reflectance-per-wavelength. Bottom row: Result of fitting the RGB-profile with 6 weighted Gaussians.

Female Age 80 $\xi = 0$ v_m 3 v_{Hb} 5

Gender	Age	ξ	v_m	v_{Hb}	c_{bil}	c_{car}	Skin roughness
Female	80	0	3	5	0.05	2.1e-4	0.18059

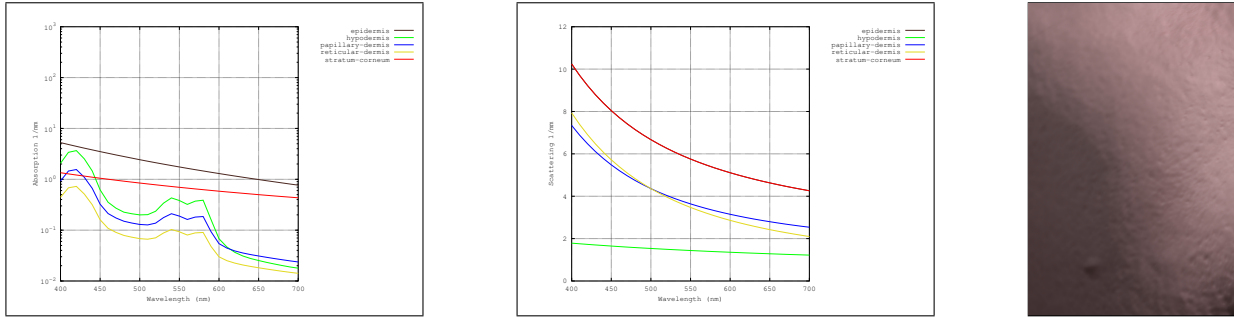


Figure 151: Top row: Full skin phantom description and skin closeup image. Bottom row, from left to right: Absorption and scattering coefficients per-wavelength for each skin layer, and result on a human cheek.

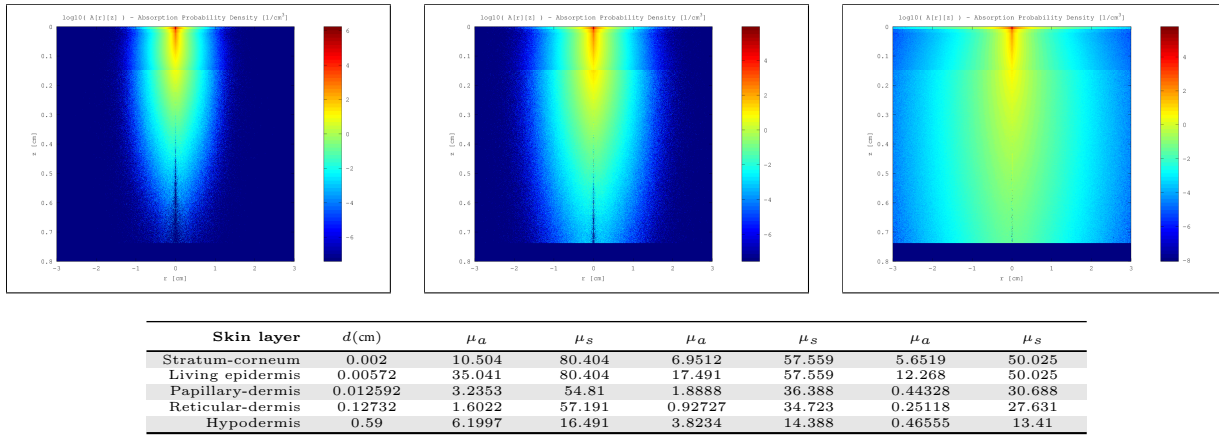
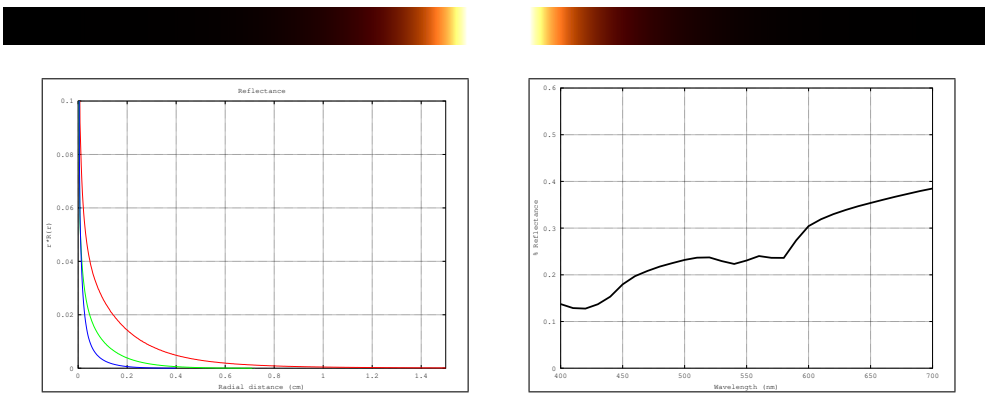


Figure 152: Top row: MonteCarlo simulations for 450nm, 550nm and 610nm. Bottom row: Resultant optical parameters (d , μ_a , μ'_s) applying our skin aging model.



Fitting	R	G	B
w_i v_i RMS,AMAX	(637.621, 42.443, 6.549, 1.420, 0.328, 0.049) (0.579, 3.023, 25.140, 190.131, 1446.649, 9969.370) 6.27e-11, 2e-03f	(2610.510, 82.073, 6.180, 1.534, 0.354, 0.060) (0.159, 1.471, 12.093, 73.984, 470.838, 2933.331) 7.81e-09, 2e-02f	(450.848, 37.227, 6.803, 1.783, 0.346, 0.047) (0.494, 2.049, 10.328, 44.549, 213.339, 1176.079) 2.41e-12, 3e-04f

Figure 153: Top row: Diffusion profile response for a pencil light-beam. Middle-row: RGB-profiles and reflectance-per-wavelength. Bottom row: Result of fitting the RGB-profile with 6 weighted Gaussians.

Female Age 30 $\xi = 1$ v_m 3 v_{Hb} 5

Gender	Age	ξ	v_m	v_{Hb}	c_{bil}	c_{car}	Skin roughness
Female	30	1	3	5	0.05	2.1e-4	0.069549

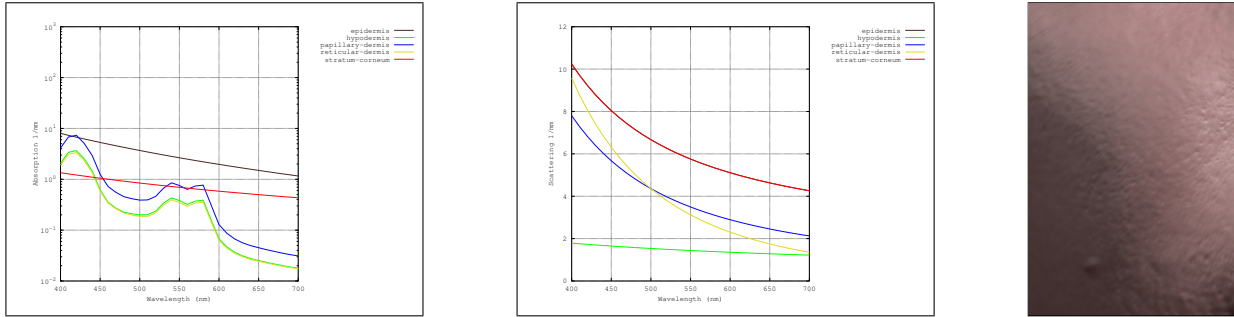


Figure 154: Top row: Full skin phantom description and skin closeup image. Bottom row, from left to right: Absorption and scattering coefficients per-wavelength for each skin layer, and result on a human cheek.

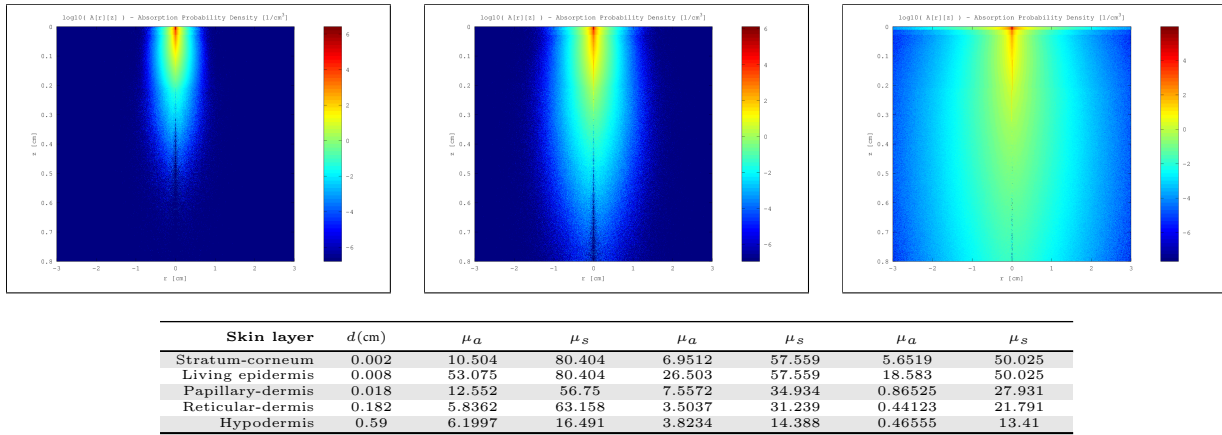
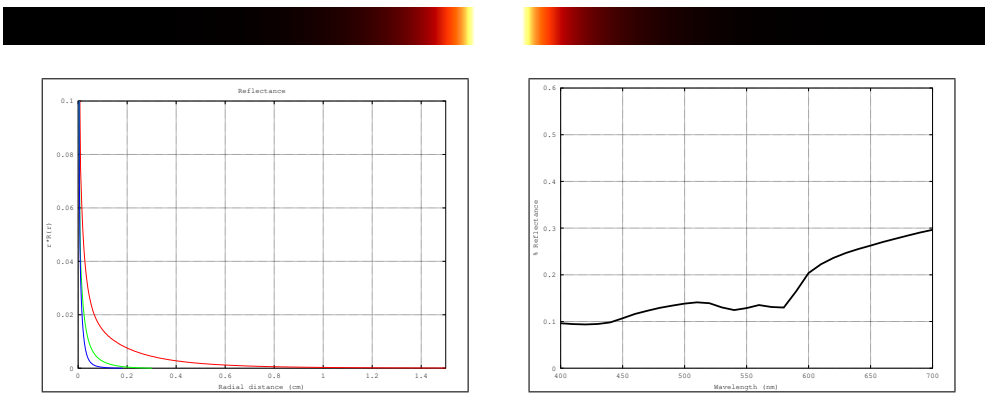


Figure 155: Top row: MonteCarlo simulations for 450nm, 550nm and 610nm. Bottom row: Resultant optical parameters (d , μ_a , μ_s') applying our skin aging model.



Fitting	R	G	B
w_i v_i RMS,AMAX	(659.799, 64.247, 6.410, 1.257, 0.207, 0.029) (0.526, 2.792, 22.860, 152.625, 1243.590, 10085.375) 2.08e-12, 5e-04f	(384.672, 38.730, 4.378, 1.271, 0.284, 0.041) (0.499, 2.391, 13.054, 52.092, 216.764, 1075.516) 2.57e-15, 9e-06f	(475.320, 42.531, 7.405, 2.789, 0.616, 0.049) (0.443, 1.752, 5.488, 17.360, 61.678, 310.624) 4.97e-10, 4e-03f

Figure 156: Top row: Diffusion profile response for a pencil light-beam. Middle-row: RGB-profiles and reflectance-per-wavelength. Bottom row: Result of fitting the RGB-profile with 6 weighted Gaussians.

Female Age 55 $\xi = 1$ v_m 3 v_{Hb} 5

Gender	Age	ξ	v_m	v_{Hb}	c_{bil}	c_{car}	Skin roughness
Female	55	1	3	5	0.05	2.1e-4	0.099683

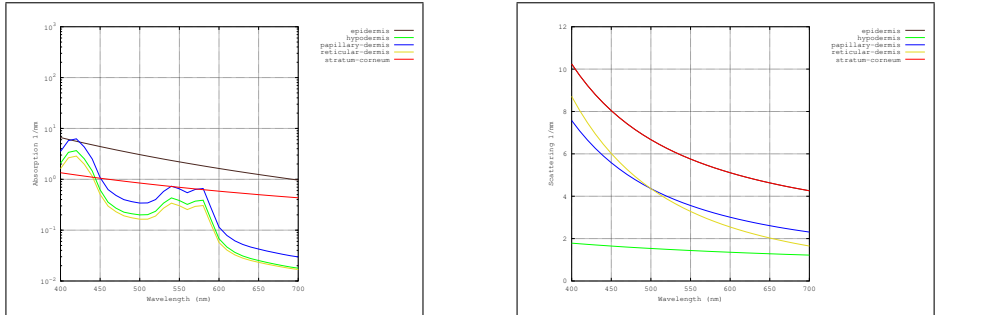


Figure 157: Top row: Full skin phantom description and skin closeup image. Bottom row, from left to right: Absorption and scattering coefficients per-wavelength for each skin layer, and result on a human cheek.

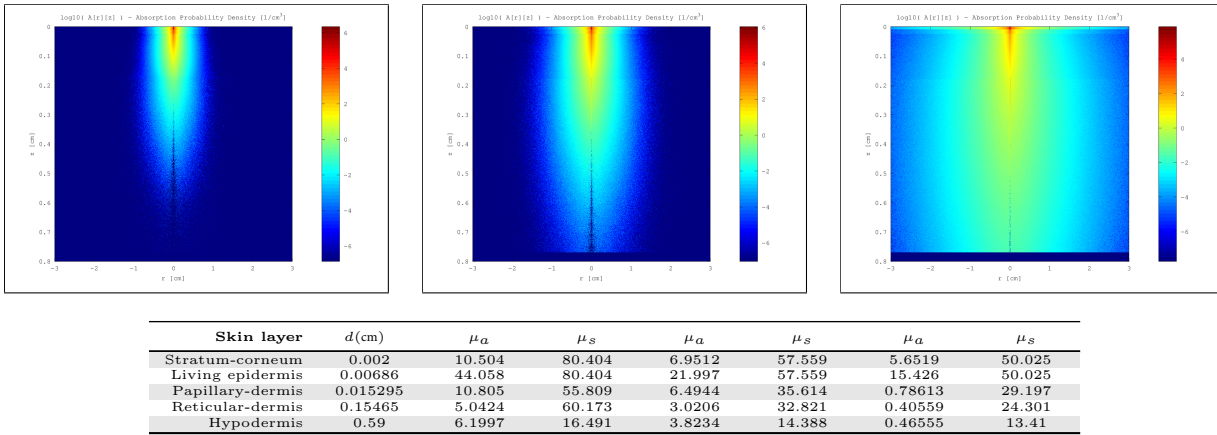


Figure 158: Top row: MonteCarlo simulations for 450nm, 550nm and 610nm. Bottom row: Resultant optical parameters (d , μ_a , μ'_s) applying our skin aging model.

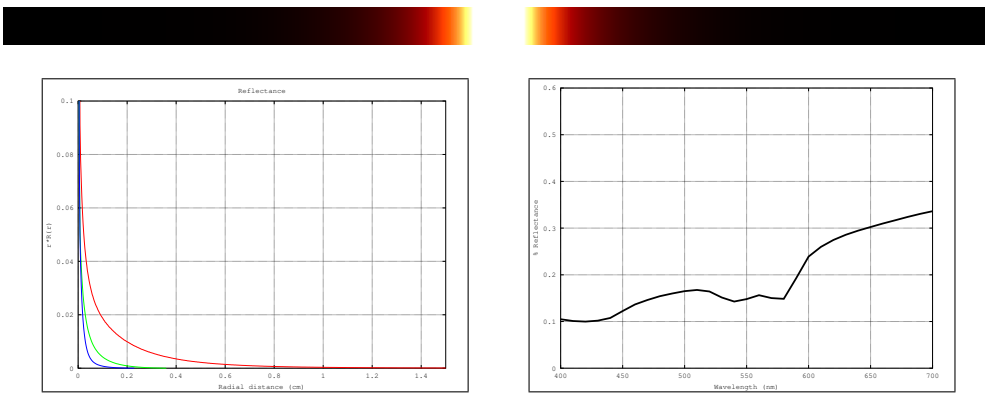


Figure 159: Top row: Diffusion profile response for a pencil light-beam. Middle-row: RGB-profiles and reflectance-per-wavelength. Bottom row: Result of fitting the RGB-profile with 6 weighted Gaussians.

Gender	Age	ξ	v_m	v_{Hb}	c_{bil}	c_{car}	Skin roughness
Female	30	0	40	5	0.05	2.1e-4	0.081579

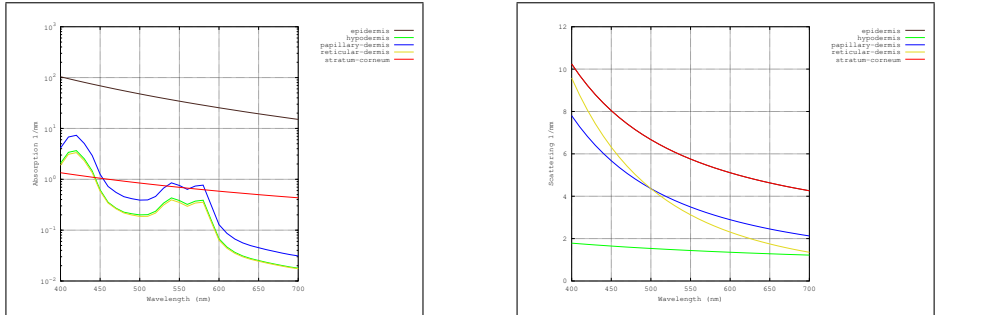


Figure 160: Top row: Full skin phantom description and skin closeup image. Bottom row, from left to right: Absorption and scattering coefficients per-wavelength for each skin layer, and result on a human cheek.

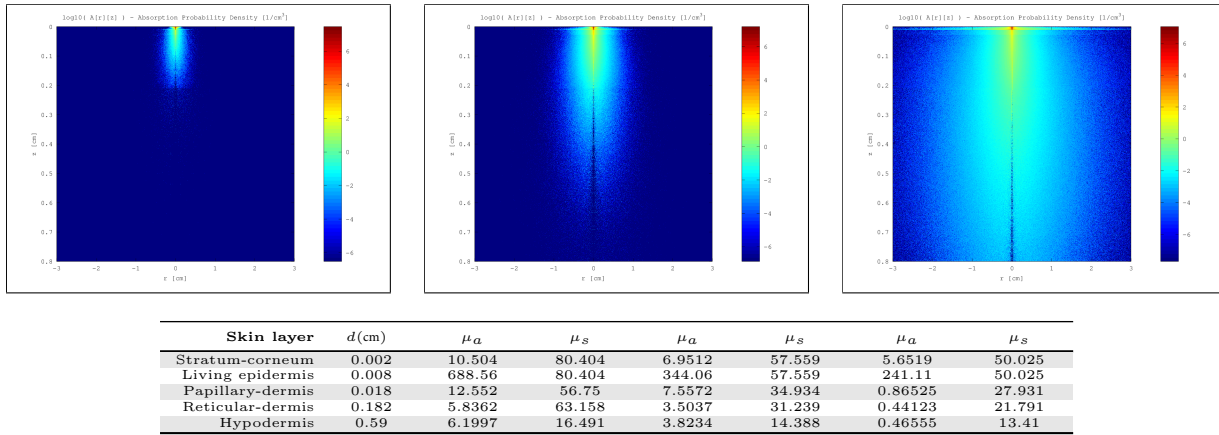
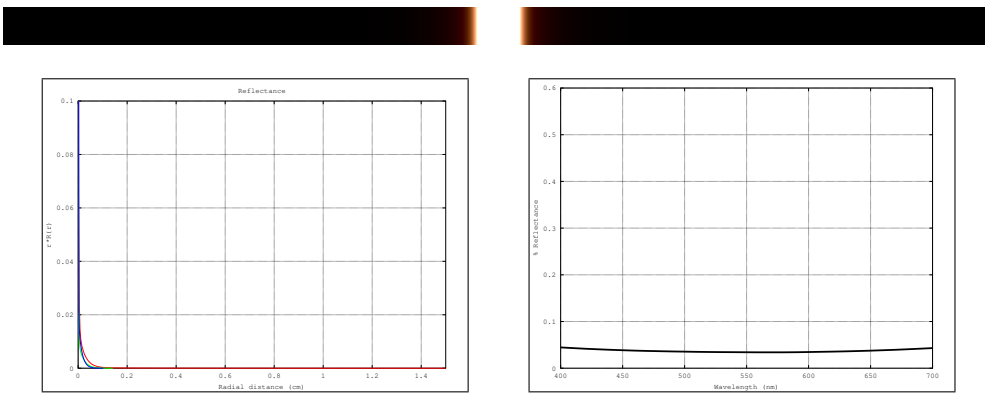


Figure 161: Top row: MonteCarlo simulations for 450nm, 550nm and 610nm. Bottom row: Resultant optical parameters (d , μ_a , μ'_s) applying our skin aging model.



Fitting	R	G	B
w_i v_i RMS,AMAX	(1466.005, 207.022, 49.440, 3.051, 0.632, 0.107) (0.209, 0.395, 1.153, 6.027, 37.077, 203.507) 3.71e-08, 4e-02f	(236.108, 201.975, 95.145, 3.348, 0.613, 0.134) (0.298, 0.290, 0.512, 2.958, 19.420, 103.647) 2.13e-08, 2e-02f	(87.338, 87.004, 77.299, 73.839, 73.559, -1.321) (0.457, 0.354, 0.392, 0.358, 0.623, 0.141) 1.22e-05, 4e-01f

Figure 162: Top row: Diffusion profile response for a pencil light-beam. Middle-row: RGB-profiles and reflectance-per-wavelength. Bottom row: Result of fitting the RGB-profile with 6 weighted Gaussians.

Gender	Age	ξ	v_m	v_{Hb}	c_{bil}	c_{car}	Skin roughness
Female	55	0	40	5	0.05	2.1e-4	0.12802

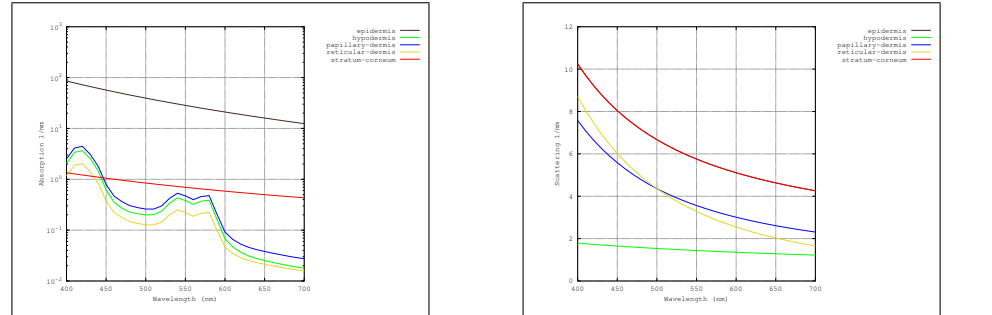


Figure 163: Top row: Full skin phantom description and skin closeup image. Bottom row, from left to right: Absorption and scattering coefficients per-wavelength for each skin layer, and result on a human cheek.

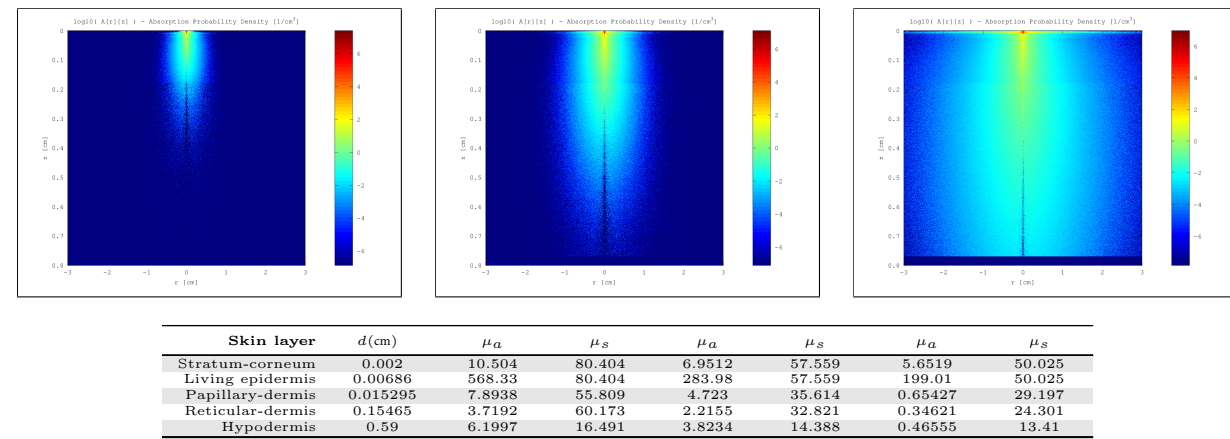
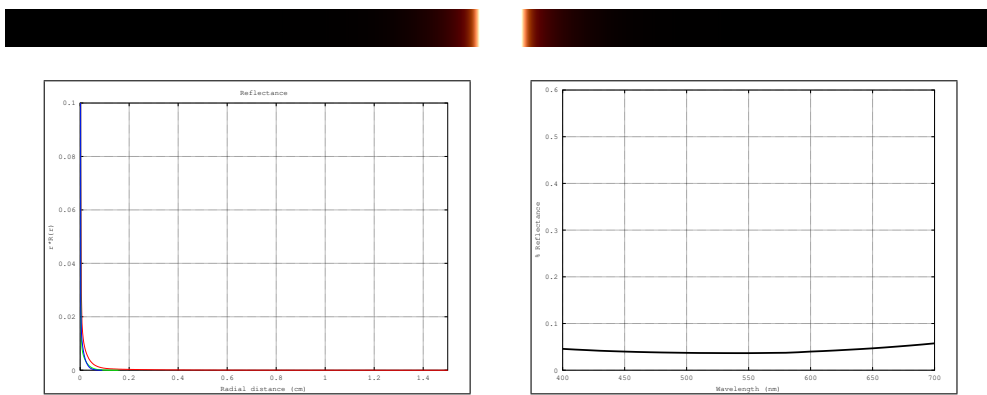


Figure 164: Top row: MonteCarlo simulations for 450nm, 550nm and 610nm. Bottom row: Resultant optical parameters (d , μ_a , μ'_s) applying our skin aging model.



Fitting	R	G	B
w_i v_i RMS,AMAX	(690.022, 239.882, 15.214, 1.562, 0.287, 0.011) (0.290, 0.564, 2.369, 16.771, 115.479, 1632.260) 3.91e-08, 5e-02f	(291.182, 269.823, 87.132, 3.509, 0.593, 0.122) (0.248, 0.277, 0.596, 3.331, 21.531, 112.777) 6.24e-09, 1e-02f	(255.936, 235.073, 168.587, 3.798, 1.051, 0.218) (0.263, 0.261, 0.415, 3.201, 15.428, 63.855) 6.17e-12, 3e-04f

Figure 165: Top row: Diffusion profile response for a pencil light-beam. Middle-row: RGB-profiles and reflectance-per-wavelength. Bottom row: Result of fitting the RGB-profile with 6 weighted Gaussians.

Gender	Age	ξ	v_m	v_{Hb}	c_{bil}	c_{car}	Skin roughness
Female	80	0	40	5	0.05	2.1e-4	0.18059

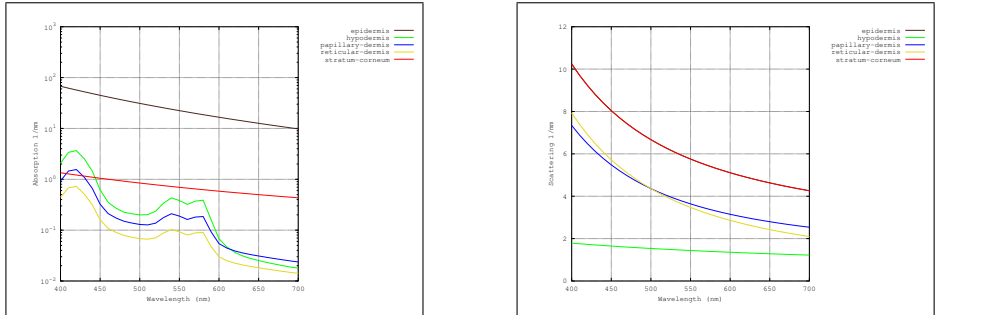


Figure 166: Top row: Full skin phantom description and skin closeup image. Bottom row, from left to right: Absorption and scattering coefficients per-wavelength for each skin layer, and result on a human cheek.

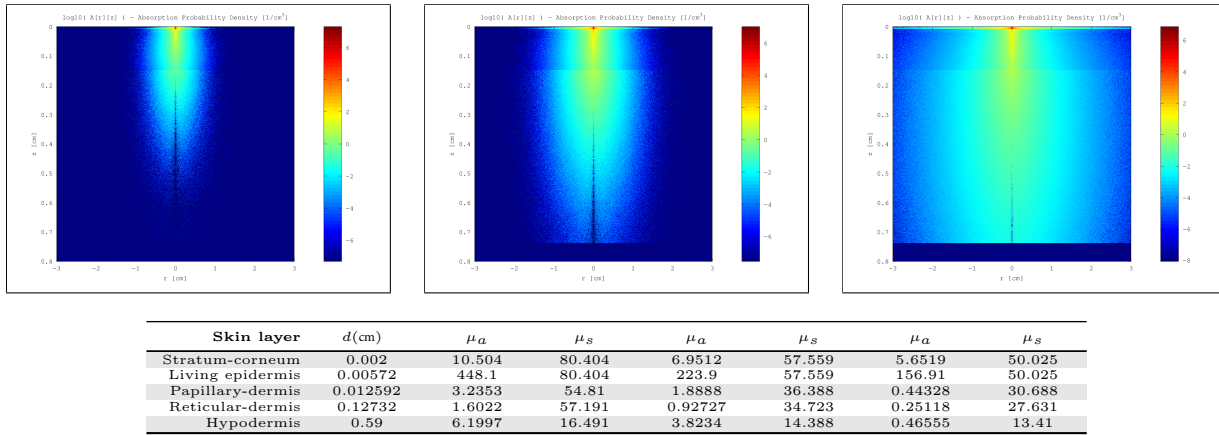
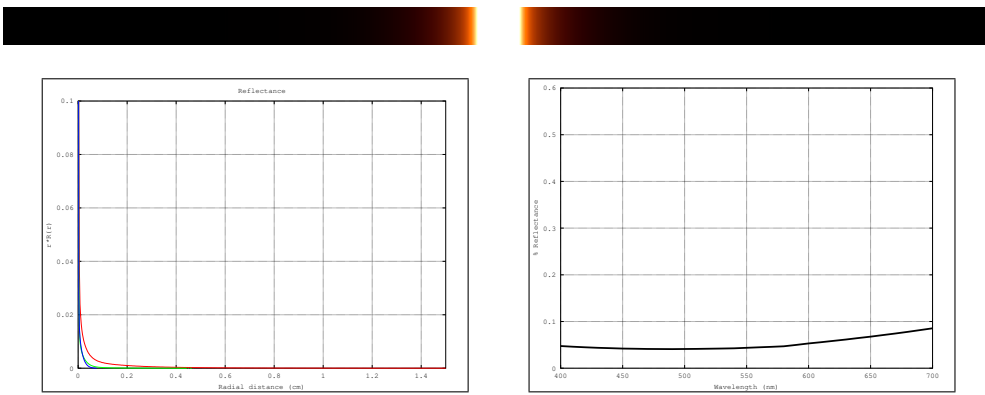


Figure 167: Top row: MonteCarlo simulations for 450nm, 550nm and 610nm. Bottom row: Resultant optical parameters (d , μ_a , μ'_s) applying our skin aging model.



Fitting	R	G	B
w_i v_i RMS,AMAX	(673.694, 18.833, 2.305, 0.478, 0.060, 0.007) (0.464, 2.315, 14.423, 88.086, 624.938, 6130.756) 3.79e-13, 2e-04f	(487.082, 138.105, 20.405, 1.589, 0.349, 0.033) (0.261, 0.431, 1.313, 8.339, 51.064, 317.506) 1.08e-07, 4e-02f	(135.415, 115.737, 73.657, 68.324, 57.710, 7.951) (0.266, 0.437, 0.430, 0.475, 0.712, 0.050) 1.90e-05, 6e-01f

Figure 168: Top row: Diffusion profile response for a pencil light-beam. Middle-row: RGB-profiles and reflectance-per-wavelength. Bottom row: Result of fitting the RGB-profile with 6 weighted Gaussians.

Gender	Age	ξ	v_m	v_{Hb}	c_{bil}	c_{car}	Skin roughness
Female	30	1	40	5	0.05	2.1e-4	0.069549

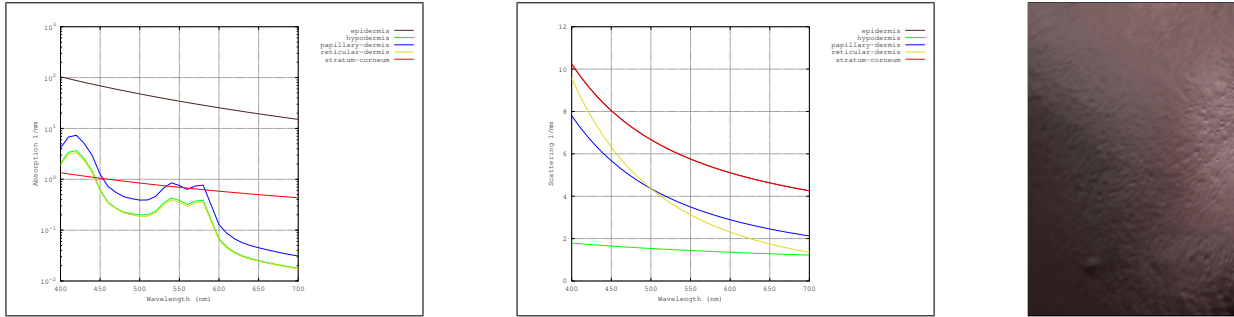


Figure 169: Top row: Full skin phantom description and skin closeup image. Bottom row, from left to right: Absorption and scattering coefficients per-wavelength for each skin layer, and result on a human cheek.

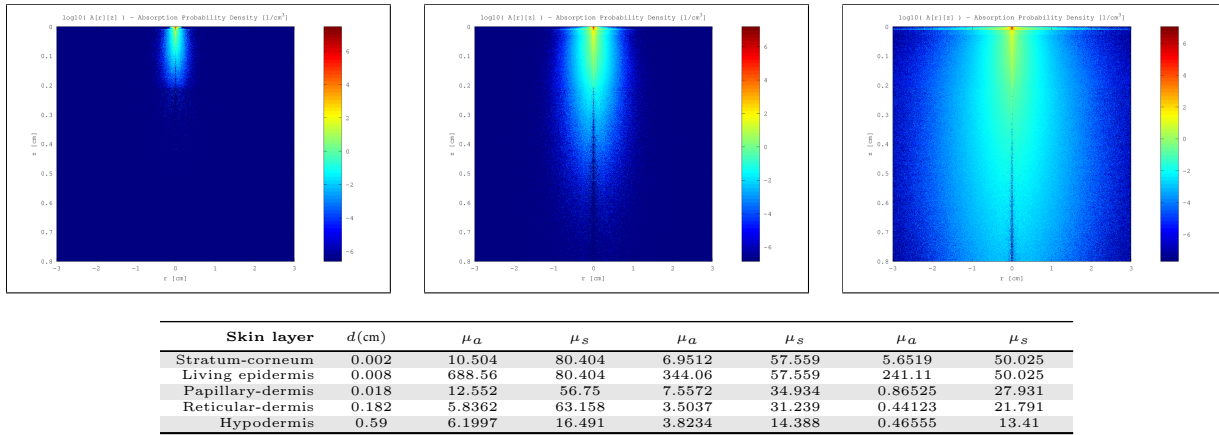
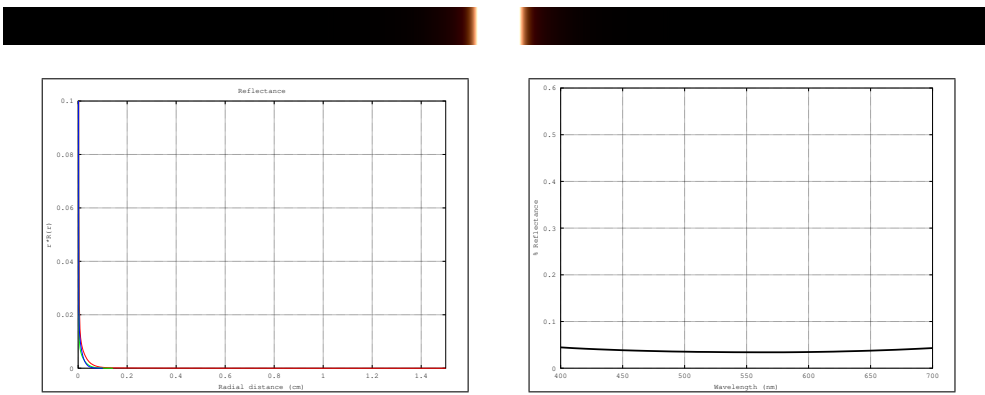


Figure 170: Top row: MonteCarlo simulations for 450nm, 550nm and 610nm. Bottom row: Resultant optical parameters (d , μ_a , μ'_s) applying our skin aging model.



Fitting	R	G	B
w_i v_i RMS,AMAX	(1016.777, 151.330, 20.182, 2.028, 0.484, 0.070) (0.259, 0.564, 1.668, 8.669, 49.926, 257.197) 1.88e-08, 3e-02f	(376.100, 210.838, 72.170, 2.837, 0.546, 0.116) (0.243, 0.292, 0.580, 3.445, 22.265, 112.368) 1.18e-08, 1e-02f	(130.551, 101.399, 70.040, 63.279, 51.776, -5.084) (0.375, 0.382, 0.395, 0.650, 0.410, 0.701) 1.16e-06, 1e-01f

Figure 171: Top row: Diffusion profile response for a pencil light-beam. Middle-row: RGB-profiles and reflectance-per-wavelength. Bottom row: Result of fitting the RGB-profile with 6 weighted Gaussians.

Gender	Age	ξ	v_m	v_{Hb}	c_{bil}	c_{car}	Skin roughness
Female	55	1	40	5	0.05	2.1e-4	0.099683

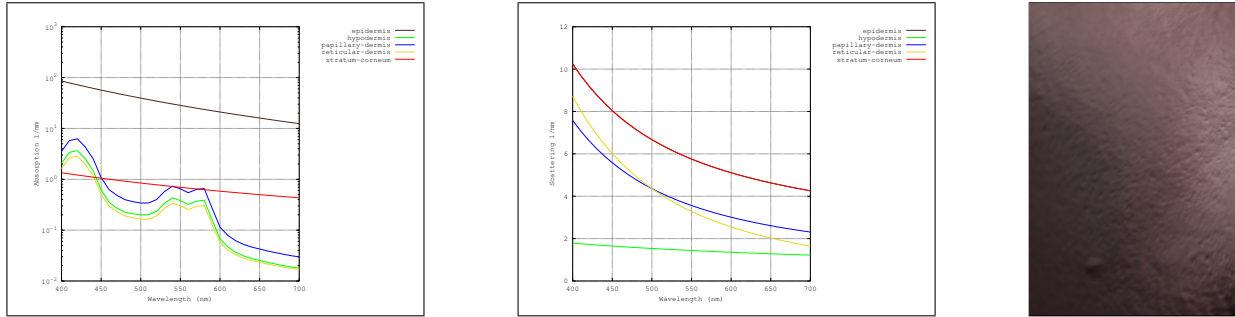


Figure 172: Top row: Full skin phantom description and skin closeup image. Bottom row, from left to right: Absorption and scattering coefficients per-wavelength for each skin layer, and result on a human cheek.

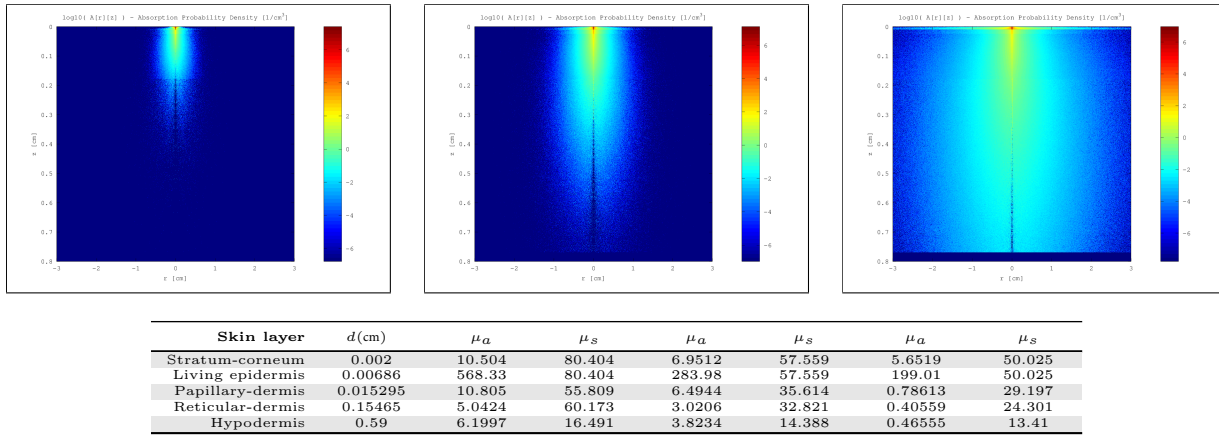


Figure 173: Top row: MonteCarlo simulations for 450nm, 550nm and 610nm. Bottom row: Resultant optical parameters (d , μ_a , μ'_s) applying our skin aging model.

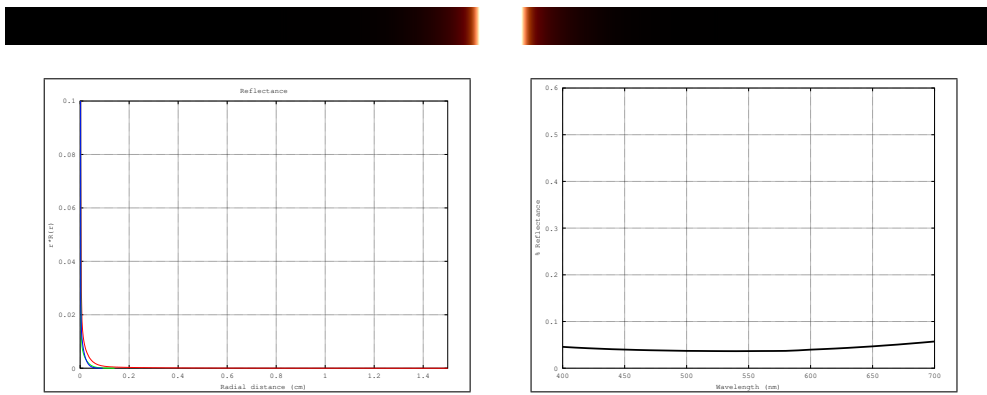


Figure 174: Top row: Diffusion profile response for a pencil light-beam. Middle-row: RGB-profiles and reflectance-per-wavelength. Bottom row: Result of fitting the RGB-profile with 6 weighted Gaussians.

Gender	Age	ξ	v_m	v_{Hb}	c_{bil}	c_{car}	Skin roughness
Female	80	1	40	5	0.05	2.1e-4	0.14797

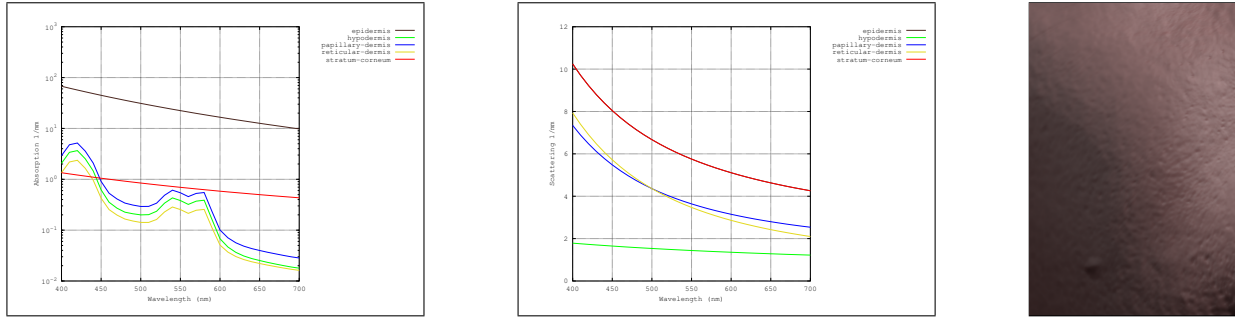


Figure 175: Top row: Full skin phantom description and skin closeup image. Bottom row, from left to right: Absorption and scattering coefficients per-wavelength for each skin layer, and result on a human cheek.

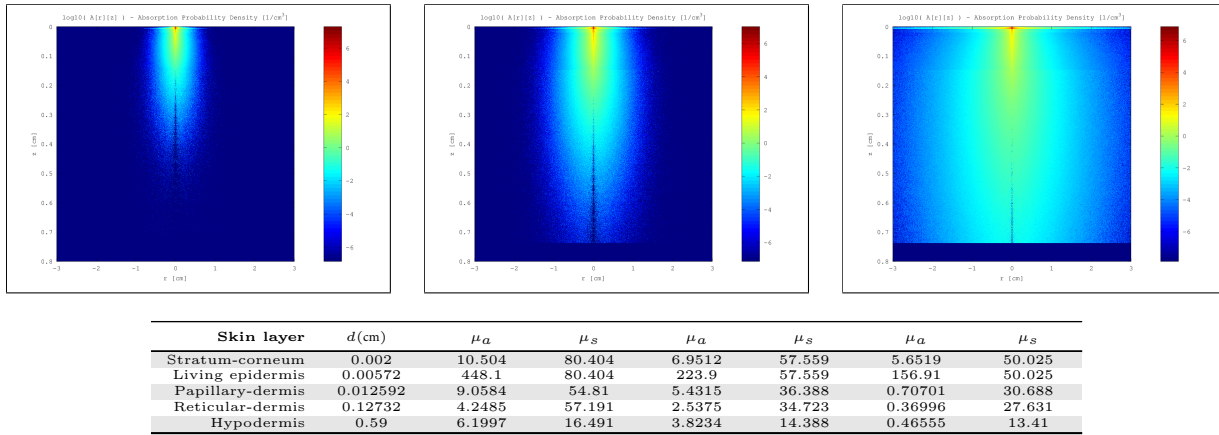
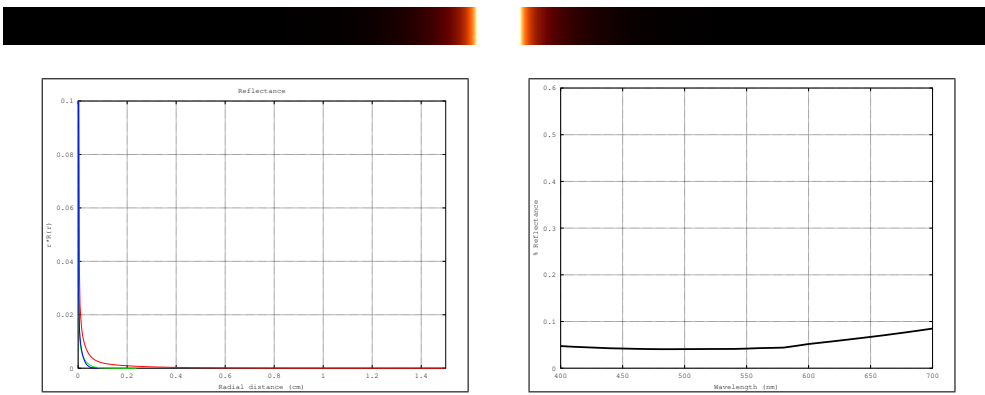


Figure 176: Top row: MonteCarlo simulations for 450nm, 550nm and 610nm. Bottom row: Resultant optical parameters (d , μ_a , μ_s') applying our skin aging model.



Fitting	R	G	B
w_i v_i RMS,AMAX	(672.870, 19.445, 2.381, 0.496, 0.064, 0.007) (0.462, 2.256, 13.768, 83.246, 568.475, 5736.524) 7.81e-13, 2e-04f	(107.720, 97.517, 70.151, 58.281, 53.753, -2.191) (0.396, 0.373, 0.473, 0.514, 0.813, 0.089) 2.21e-05, 6e-01f	(485.069, 186.931, 4.292, 1.052, 0.234, -1.189) (0.257, 0.435, 3.133, 15.199, 60.818, 0.018) 8.13e-11, 1e-03f

Figure 177: Top row: Diffusion profile response for a pencil light-beam. Middle-row: RGB-profiles and reflectance-per-wavelength. Bottom row: Result of fitting the RGB-profile with 6 weighted Gaussians.

Gender	Age	ξ	v_m	v_{Hb}	c_{bil}	c_{car}	Skin roughness
Female	55	0	50	5	0.05	2.1e-4	0.12802

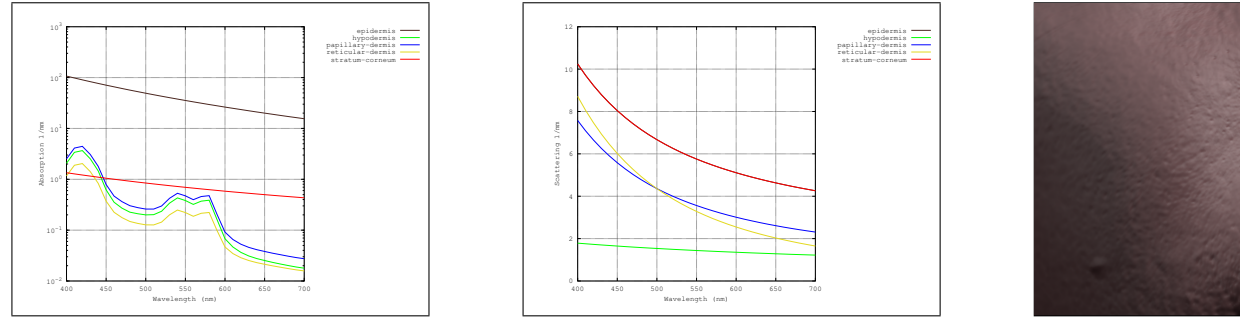


Figure 178: Top row: Full skin phantom description and skin closeup image. Bottom row, from left to right: Absorption and scattering coefficients per-wavelength for each skin layer, and result on a human cheek.

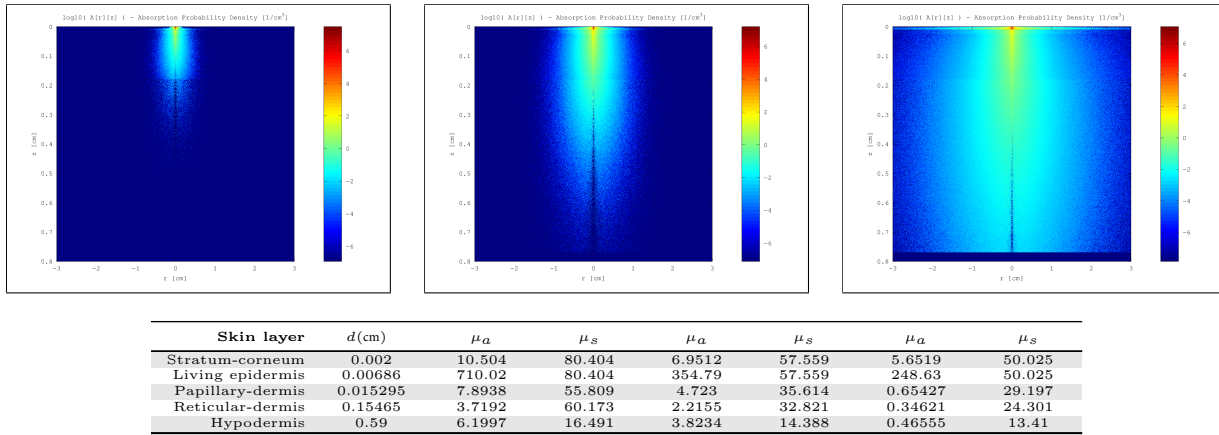
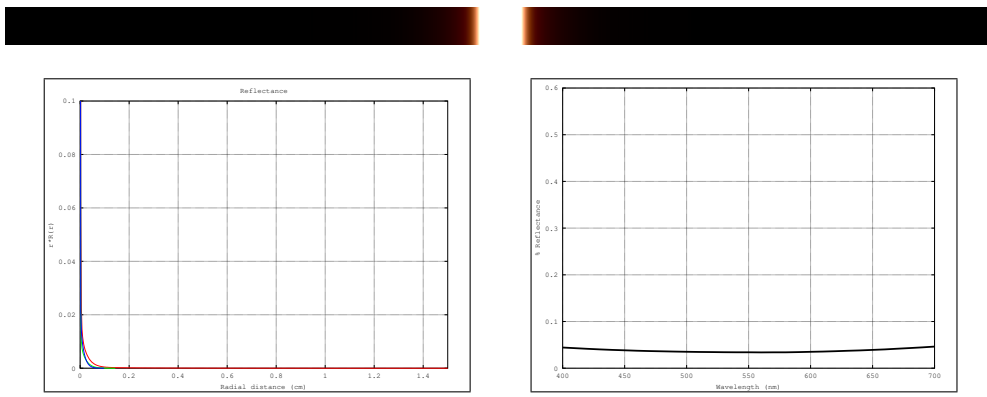


Figure 179: Top row: MonteCarlo simulations for 450nm, 550nm and 610nm. Bottom row: Resultant optical parameters (d , μ_a , μ'_s) applying our skin aging model.



Fitting	R	G	B
w_i v_i RMS,AMAX	(690.252, 363.315, 38.287, 2.444, 0.535, 0.071) (0.257, 0.384, 1.261, 7.654, 48.468, 284.458) 4.31e-08, 5e-02f	(171.625, 145.353, 138.167, 87.433, 2.047, 0.301) (0.478, 0.219, 0.286, 0.309, 6.157, 63.672) 2.80e-09, 6e-03f	(114.417, 93.138, 88.514, 83.406, 48.080, -7.176) (0.397, 0.356, 0.345, 0.437, 0.722, 0.757) 1.70e-11, 5e-04f

Figure 180: Top row: Diffusion profile response for a pencil light-beam. Middle-row: RGB-profiles and reflectance-per-wavelength. Bottom row: Result of fitting the RGB-profile with 6 weighted Gaussians.

Gender	Age	ξ	v_m	v_{Hb}	c_{bil}	c_{car}	Skin roughness
Female	80	0	50	5	0.05	2.1e-4	0.18059

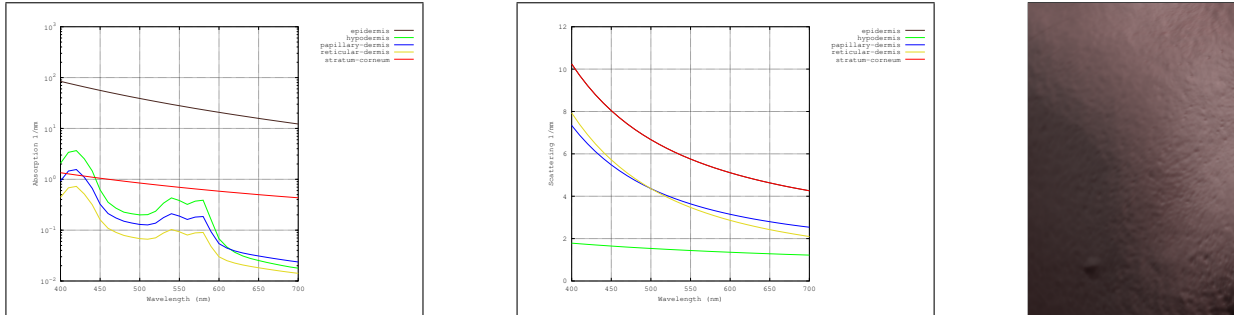


Figure 181: Top row: Full skin phantom description and skin closeup image. Bottom row, from left to right: Absorption and scattering coefficients per-wavelength for each skin layer, and result on a human cheek.

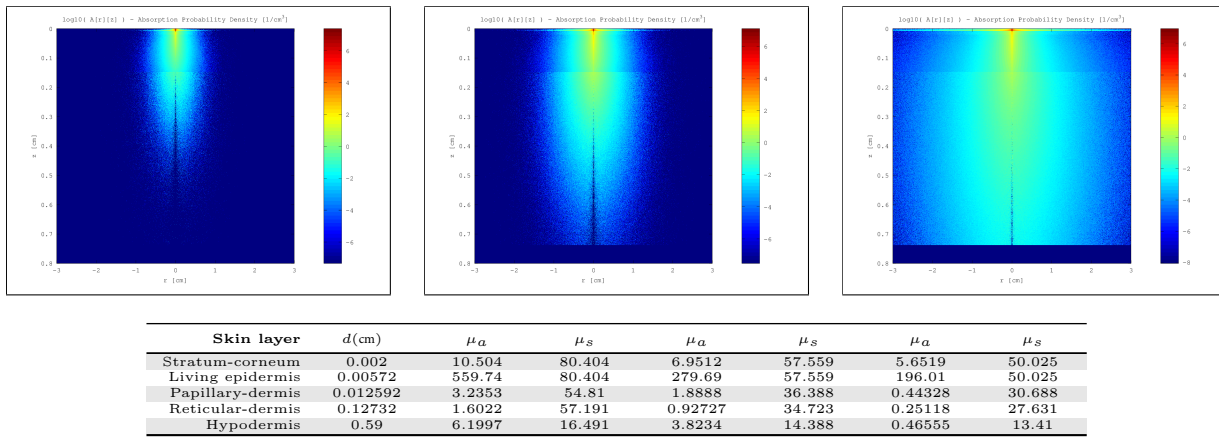


Figure 182: Top row: MonteCarlo simulations for 450nm, 550nm and 610nm. Bottom row: Resultant optical parameters (d , μ_a , μ'_s) applying our skin aging model.

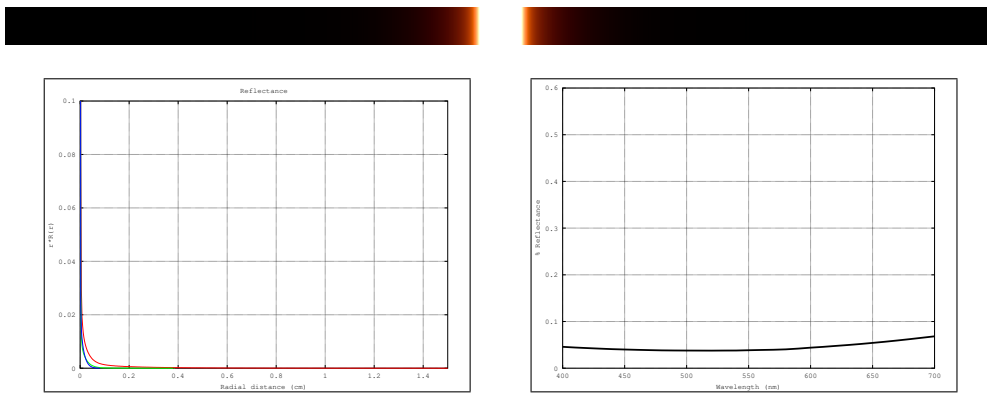


Figure 183: Top row: Diffusion profile response for a pencil light-beam. Middle-row: RGB-profiles and reflectance-per-wavelength. Bottom row: Result of fitting the RGB-profile with 6 weighted Gaussians.

Gender	Age	ξ	v_m	v_{Hb}	c_{bil}	c_{car}	Skin roughness
Female	30	1	50	5	0.05	2.1e-4	0.069549

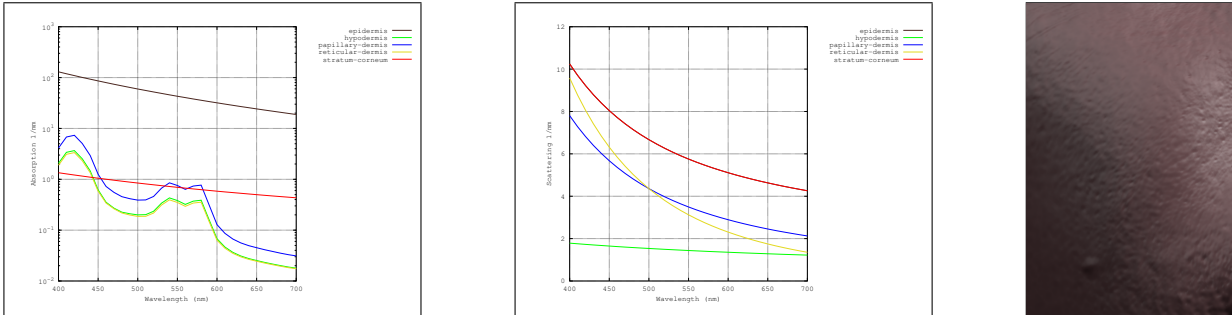


Figure 184: Top row: Full skin phantom description and skin closeup image. Bottom row, from left to right: Absorption and scattering coefficients per-wavelength for each skin layer, and result on a human cheek.

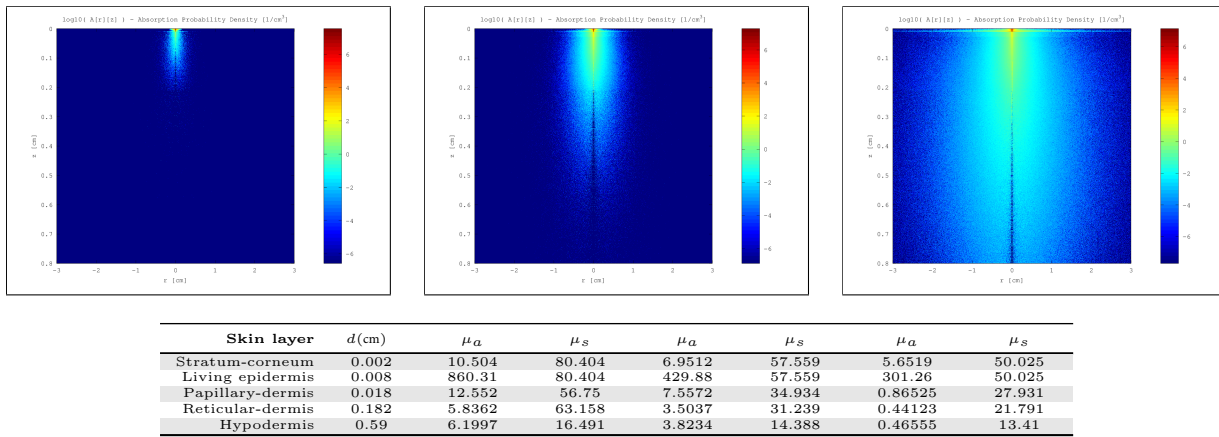
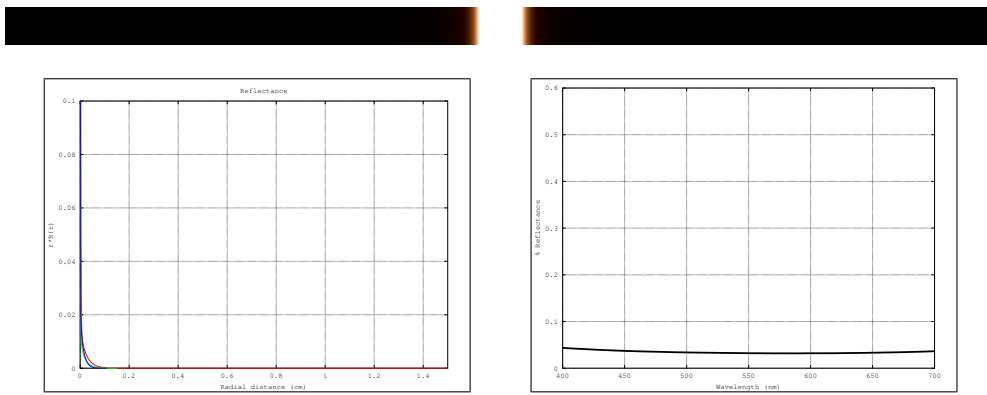


Figure 185: Top row: MonteCarlo simulations for 450nm, 550nm and 610nm. Bottom row: Resultant optical parameters (d , μ_a , μ'_s) applying our skin aging model.



Fitting	R	G	B
w_i v_i RMS,AMAX	(283.933, 141.543, 115.189, 112.049, 58.039, -11.139) (0.394, 0.349, 0.391, 0.755, 0.458, 0.788) 2.59e-06, 4e-01f	(425.401, 172.214, 2.290, 1.370, 0.512, 0.109) (0.248, 0.438, 3.730, 0.005, 23.214, 114.856) 5.51e-10, 3e-03f	(317.038, 235.381, 91.982, 2.849, 0.537, -53.557) (0.259, 0.278, 0.463, 5.734, 40.055, 0.006) 1.09e-08, 1e-02f

Figure 186: Top row: Diffusion profile response for a pencil light-beam. Middle-row: RGB-profiles and reflectance-per-wavelength. Bottom row: Result of fitting the RGB-profile with 6 weighted Gaussians.

Gender	Age	ξ	v_m	v_{Hb}	c_{bil}	c_{car}	Skin roughness
Female	55	1	50	5	0.05	2.1e-4	0.099683

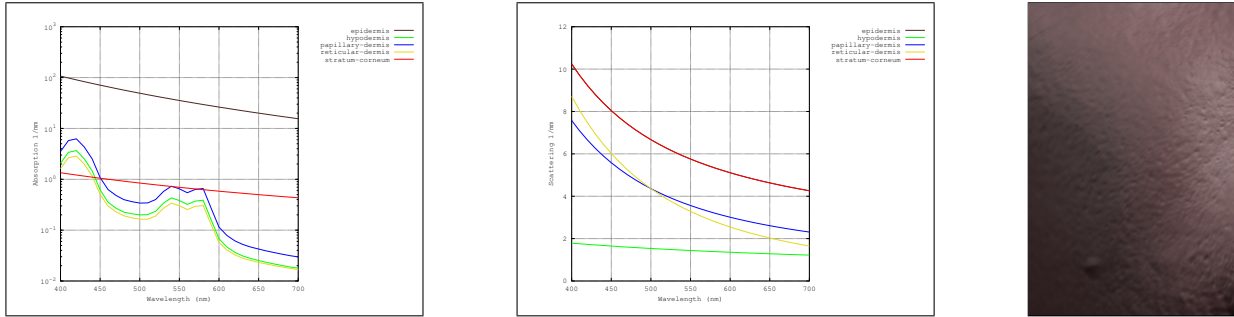


Figure 187: Top row: Full skin phantom description and skin closeup image. Bottom row, from left to right: Absorption and scattering coefficients per-wavelength for each skin layer, and result on a human cheek.

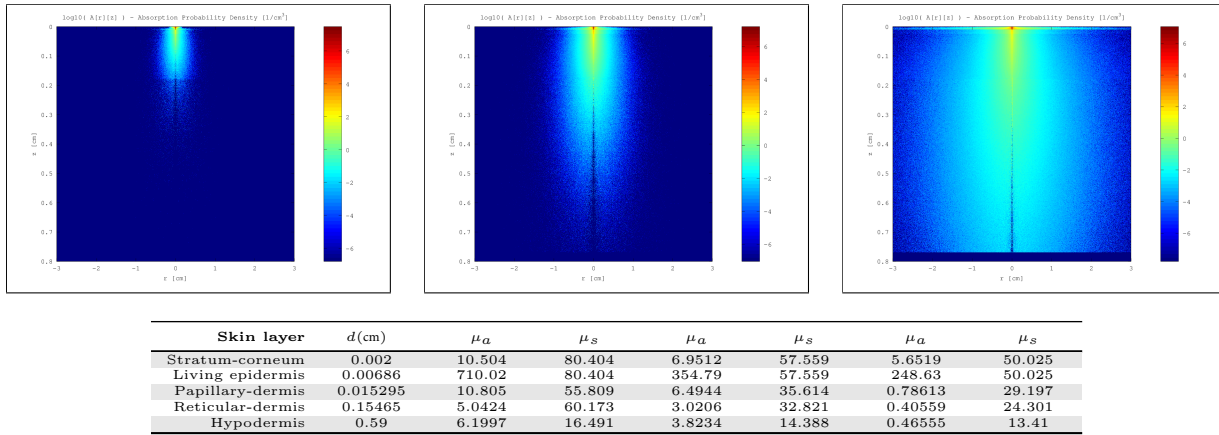


Figure 188: Top row: MonteCarlo simulations for 450nm, 550nm and 610nm. Bottom row: Resultant optical parameters (d , μ_a , μ'_s) applying our skin aging model.

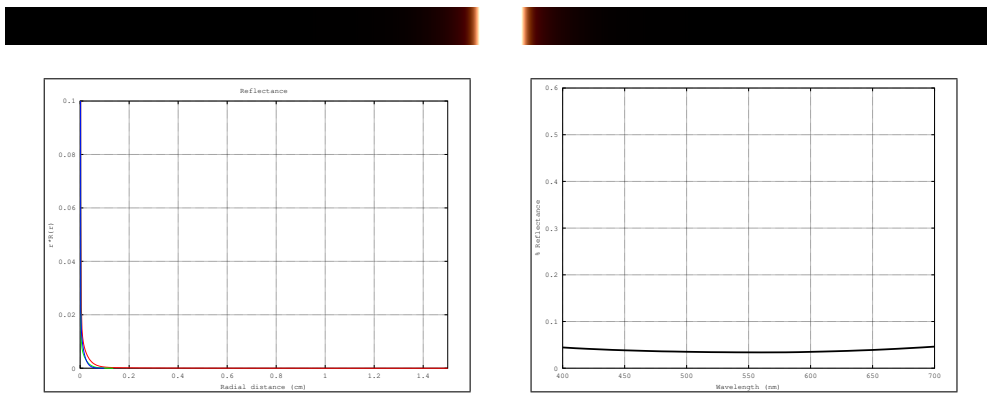


Figure 189: Top row: Diffusion profile response for a pencil light-beam. Middle-row: RGB-profiles and reflectance-per-wavelength. Bottom row: Result of fitting the RGB-profile with 6 weighted Gaussians.

Gender	Age	ξ	v_m	v_{Hb}	c_{bil}	c_{car}	Skin roughness
Female	80	1	50	5	0.05	2.1e-4	0.14797

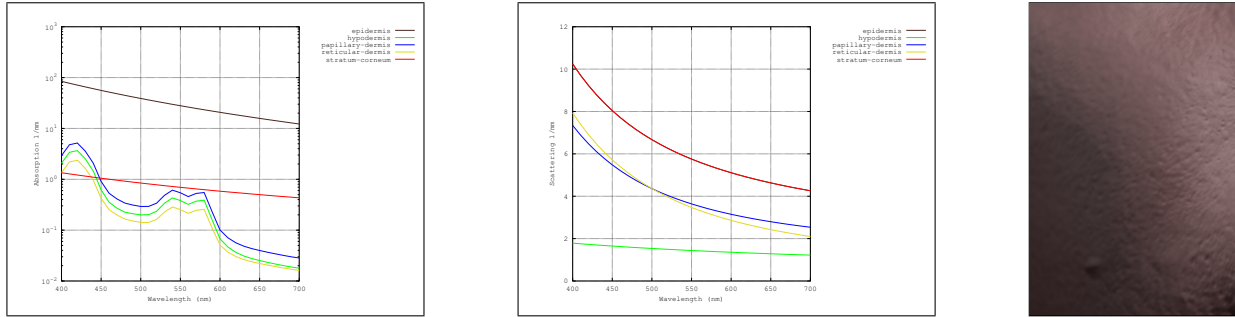


Figure 190: Top row: Full skin phantom description and skin closeup image. Bottom row, from left to right: Absorption and scattering coefficients per-wavelength for each skin layer, and result on a human cheek.

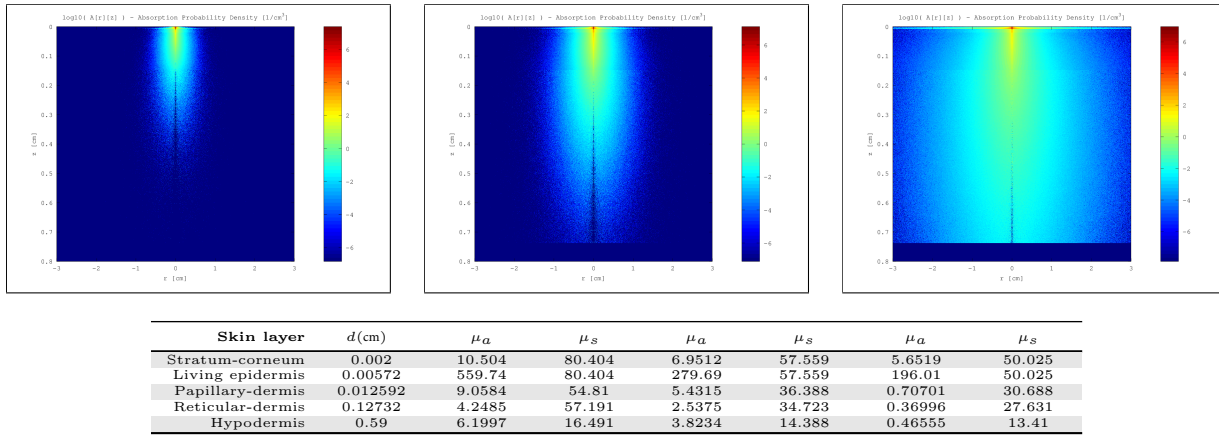
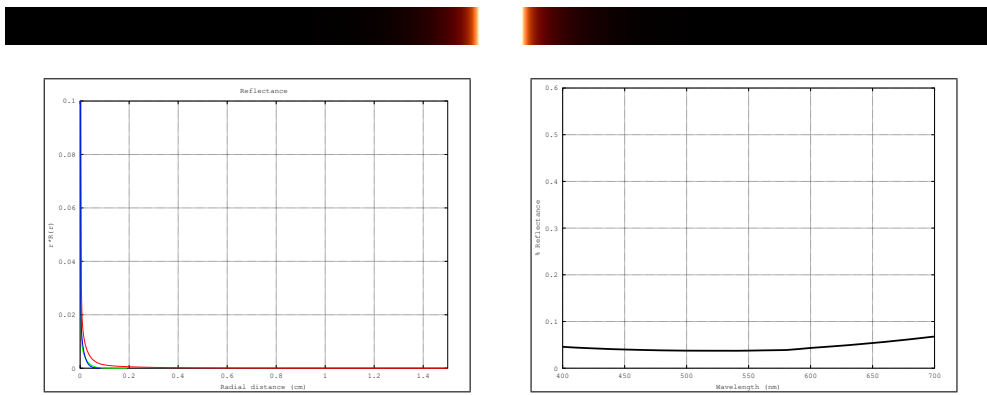


Figure 191: Top row: MonteCarlo simulations for 450nm, 550nm and 610nm. Bottom row: Resultant optical parameters (d , μ_a , μ'_s) applying our skin aging model.



Fitting	R	G	B
w_i v_i RMS,AMAX	(834.328, 70.678, 5.642, 1.063, 0.186, 0.010) (0.336, 0.968, 4.536, 29.047, 189.899, 2957.310) 1.97e-07, 1e-01f	(99.281, 86.808, 67.400, 61.199, 56.793, -4.129) (0.327, 0.590, 0.521, 0.497, 0.437, 0.116) 2.06e-06, 2e-01f	(114.444, 95.860, 80.027, 74.917, 46.655, 1.060) (0.386, 0.385, 0.624, 0.383, 0.422, 0.259) 2.83e-08, 2e-02f

Figure 192: Top row: Diffusion profile response for a pencil light-beam. Middle-row: RGB-profiles and reflectance-per-wavelength. Bottom row: Result of fitting the RGB-profile with 6 weighted Gaussians.

Female Age 30 $\xi = 0$ v_m 5 v_{Hb} 5

Gender	Age	ξ	v_m	v_{Hb}	c_{bil}	c_{car}	Skin roughness
Female	30	0	5	5	0.05	2.1e-4	0.081579

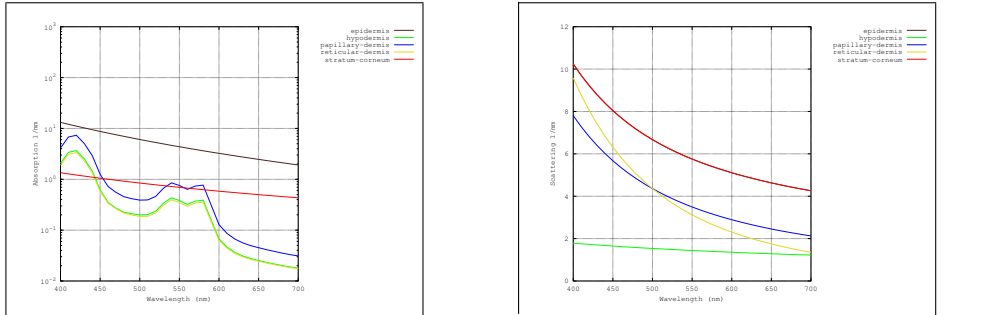


Figure 193: Top row: Full skin phantom description and skin closeup image. Bottom row, from left to right: Absorption and scattering coefficients per-wavelength for each skin layer, and result on a human cheek.

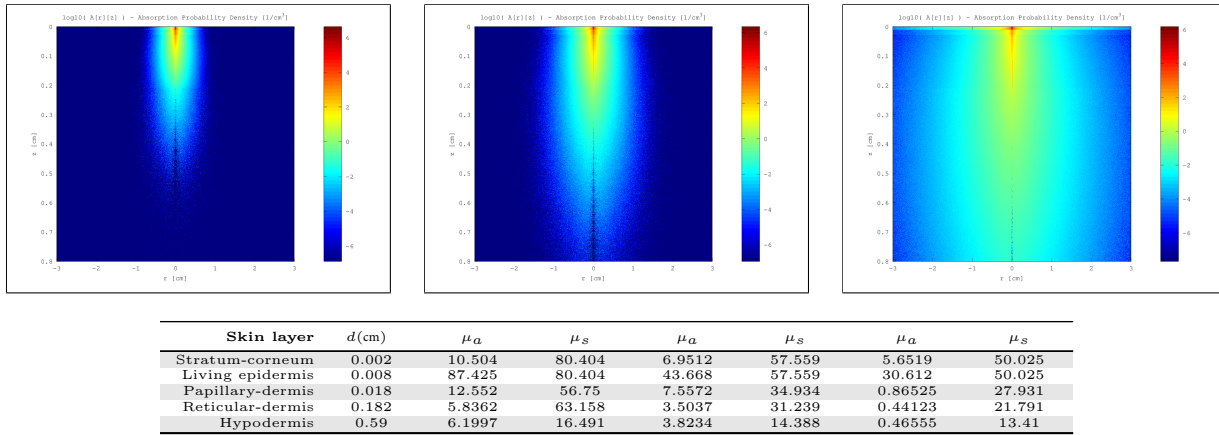
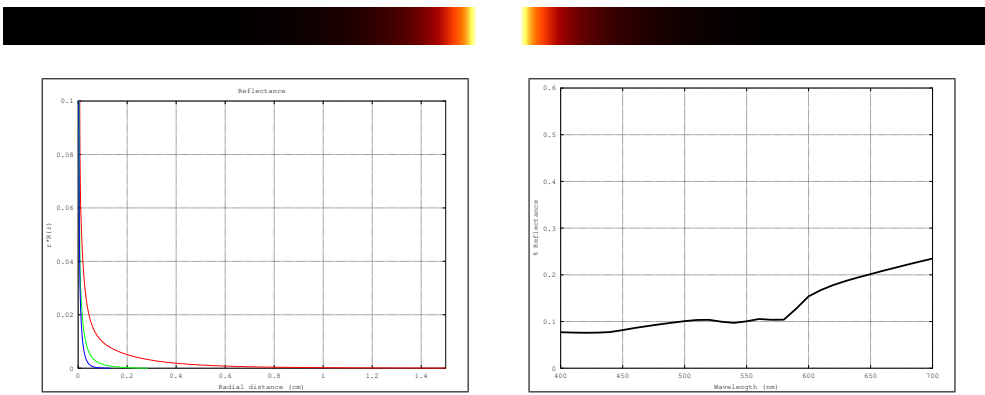


Figure 194: Top row: MonteCarlo simulations for 450nm, 550nm and 610nm. Bottom row: Resultant optical parameters (d , μ_a , μ'_s) applying our skin aging model.



Fitting	R	G	B
w_i v_i RMS,AMAX	(660.773, 58.113, 5.585, 1.032, 0.155, 0.021) (0.519, 2.719, 21.121, 137.566, 1131.494, 9555.068) 6.69e-13, 3e-04f	(393.136, 36.795, 4.944, 2.252, 0.476, 0.051) (0.467, 1.970, 5.862, 21.934, 106.355, 693.779) 1.89e-10, 2e-03f	(147.949, 146.190, 115.119, 3.567, 2.990, -9.228) (0.931, 0.494, 0.529, 19.026, 0.100, 0.922) 4.85e-06, 4e-01f

Figure 195: Top row: Diffusion profile response for a pencil light-beam. Middle-row: RGB-profiles and reflectance-per-wavelength. Bottom row: Result of fitting the RGB-profile with 6 weighted Gaussians.

Female Age 55 $\xi = 0$ v_m 5 v_{Hb} 5

Gender	Age	ξ	v_m	v_{Hb}	c_{bil}	c_{car}	Skin roughness
Female	55	0	5	5	0.05	2.1e-4	0.12802

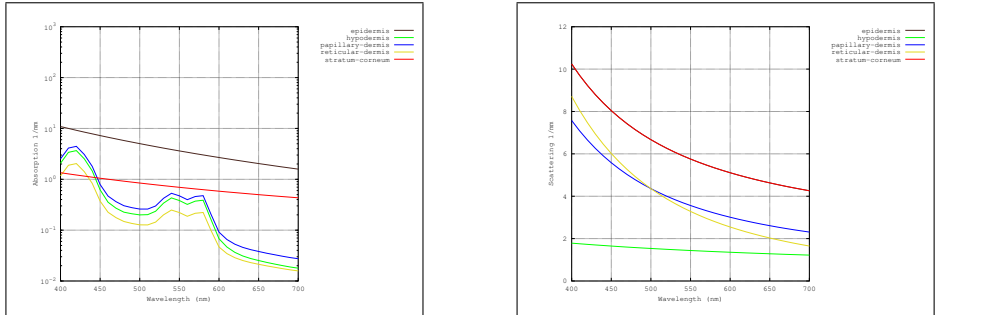


Figure 196: Top row: Full skin phantom description and skin closeup image. Bottom row, from left to right: Absorption and scattering coefficients per-wavelength for each skin layer, and result on a human cheek.

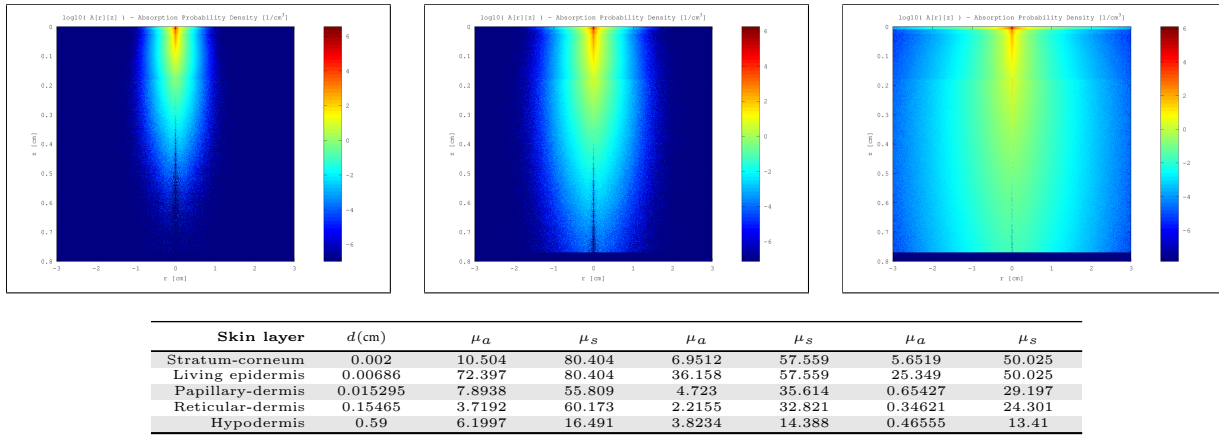
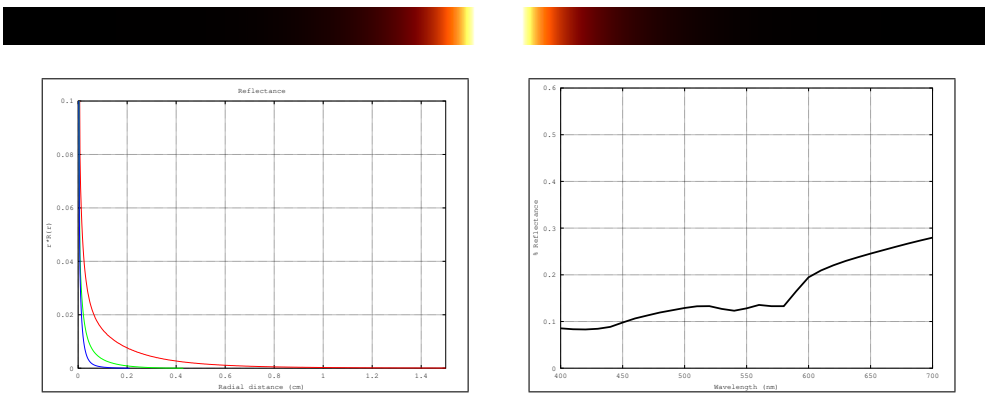


Figure 197: Top row: MonteCarlo simulations for 450nm, 550nm and 610nm. Bottom row: Resultant optical parameters (d , μ_a , μ_s') applying our skin aging model.



Fitting	R	G	B
w_i v_i RMS,AMAX	(664.764, 62.800, 6.345, 1.228, 0.219, 0.031) (0.509, 2.444, 20.390, 143.770, 1176.057, 9270.799) 1.08e-11, 1e-03f	(399.076, 42.315, 4.436, 1.142, 0.233, 0.034) (0.459, 1.979, 11.827, 55.087, 279.908, 1646.881) 4.77e-12, 4e-04f	(515.395, 51.317, 14.298, 3.914, 0.746, 0.057) (0.378, 1.155, 2.851, 11.819, 52.169, 321.691) 1.58e-08, 2e-02f

Figure 198: Top row: Diffusion profile response for a pencil light-beam. Middle-row: RGB-profiles and reflectance-per-wavelength. Bottom row: Result of fitting the RGB-profile with 6 weighted Gaussians.

Female Age 80 $\xi = 0$ v_m 5 v_{Hb} 5

Gender	Age	ξ	v_m	v_{Hb}	c_{bil}	c_{car}	Skin roughness
Female	80	0	5	5	0.05	2.1e-4	0.18059

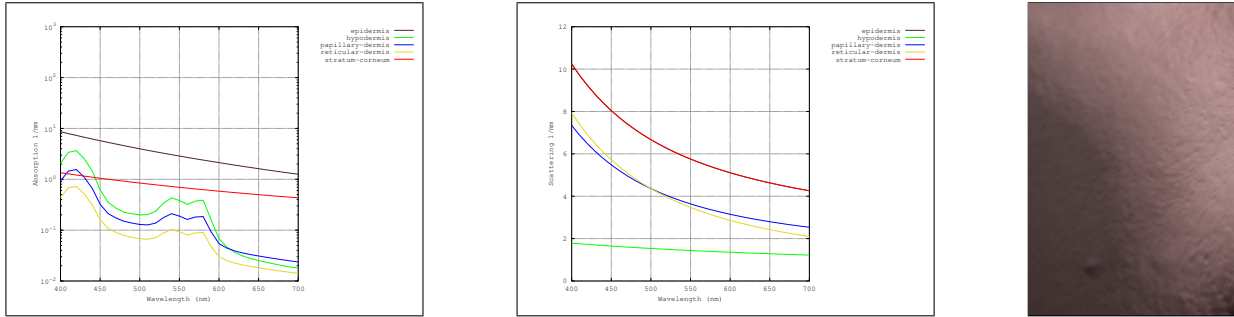


Figure 199: Top row: Full skin phantom description and skin closeup image. Bottom row, from left to right: Absorption and scattering coefficients per-wavelength for each skin layer, and result on a human cheek.

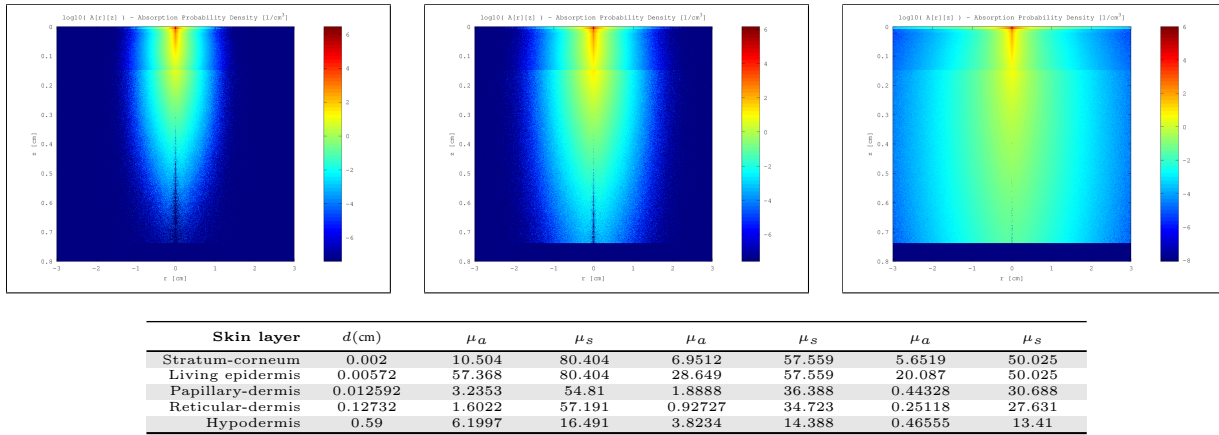
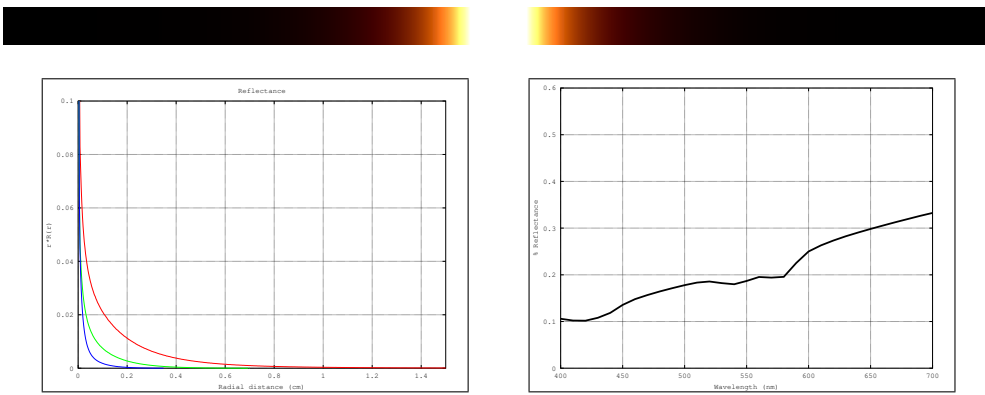


Figure 200: Top row: MonteCarlo simulations for 450nm, 550nm and 610nm. Bottom row: Resultant optical parameters (d , μ_a , μ'_s) applying our skin aging model.



Fitting	R	G	B
w_i v_i RMS,AMAX	(389.583, 308.129, 64.392, 6.142, 0.494, -0.123) (0.547, 0.415, 2.406, 43.132, 1259.277, 30.497) 8.48e-08, 9e-02f	(179.267, 105.218, 77.169, 9.687, 1.965, 0.257) (0.578, 0.530, 0.892, 7.371, 81.596, 0.050) 2.00e-04, 2e+00f	(468.439, 40.623, 6.312, 1.634, 0.297, 0.038) (0.450, 1.716, 8.255, 34.144, 160.071, 949.315) 9.98e-10, 6e-03f

Figure 201: Top row: Diffusion profile response for a pencil light-beam. Middle-row: RGB-profiles and reflectance-per-wavelength. Bottom row: Result of fitting the RGB-profile with 6 weighted Gaussians.

Female Age 30 $\xi = 1$ v_m 5 v_{Hb} 5

Gender	Age	ξ	v_m	v_{Hb}	c_{bil}	c_{car}	Skin roughness
Female	30	1	5	5	0.05	2.1e-4	0.069549

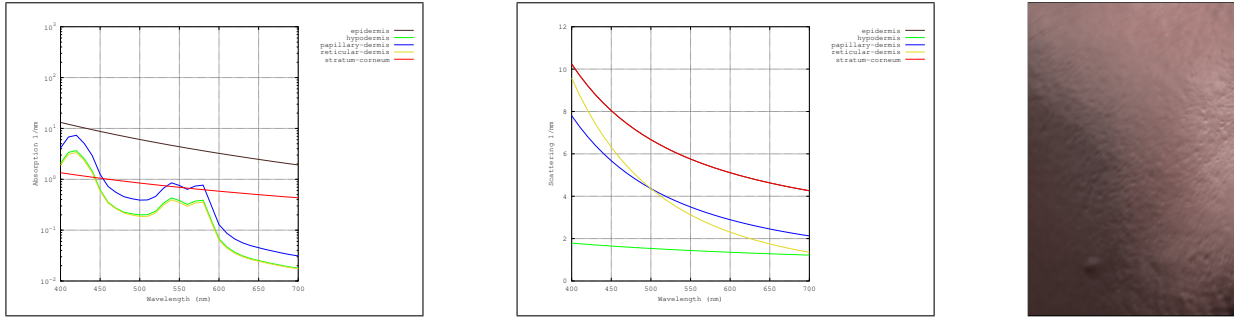


Figure 202: Top row: Full skin phantom description and skin closeup image. Bottom row, from left to right: Absorption and scattering coefficients per-wavelength for each skin layer, and result on a human cheek.

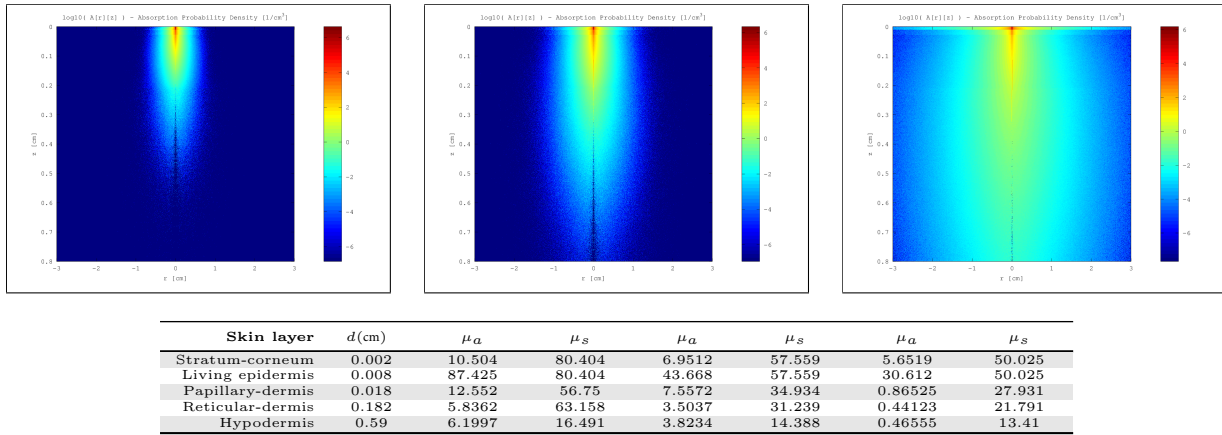
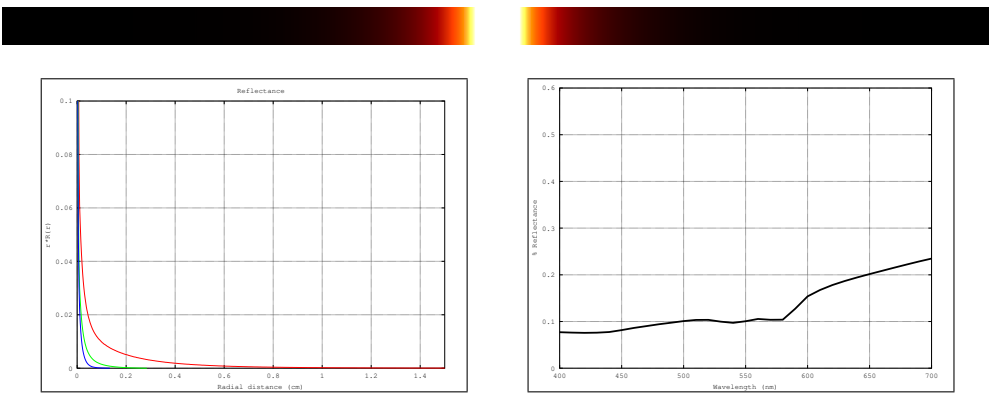


Figure 203: Top row: MonteCarlo simulations for 450nm, 550nm and 610nm. Bottom row: Resultant optical parameters (d , μ_a , μ'_s) applying our skin aging model.



Fitting	R	G	B
w_i v_i RMS,AMAX	(659.468, 58.515, 5.624, 1.043, 0.156, 0.021) (0.519, 2.699, 20.938, 136.197, 1123.901, 9527.442) 8.31e-13, 3e-04f	(386.301, 33.685, 3.684, 1.020, 0.218, 0.028) (0.489, 2.291, 11.551, 44.294, 182.312, 947.270) 9.35e-16, 5e-06f	(177.415, 142.138, 137.747, 4.865, 1.158, -15.222) (0.451, 0.890, 0.463, 15.188, 0.133, 0.925) 6.38e-06, 5e-01f

Figure 204: Top row: Diffusion profile response for a pencil light-beam. Middle-row: RGB-profiles and reflectance-per-wavelength. Bottom row: Result of fitting the RGB-profile with 6 weighted Gaussians.

Female Age 55 $\xi = 1$ v_m 5 v_{Hb} 5

Gender	Age	ξ	v_m	v_{Hb}	c_{bil}	c_{car}	Skin roughness
Female	55	1	5	5	0.05	2.1e-4	0.099683

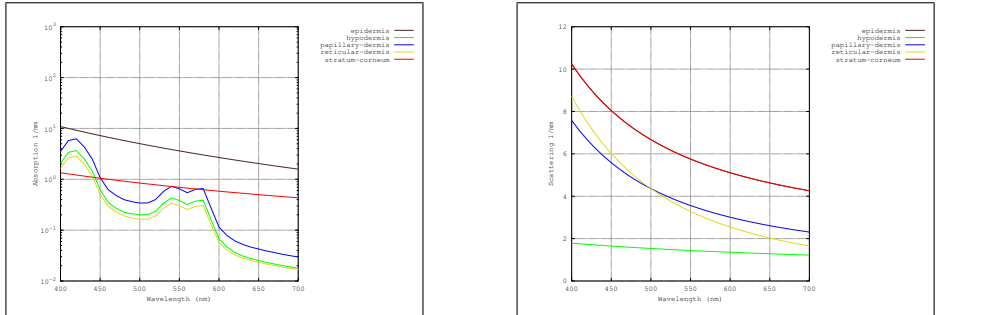


Figure 205: Top row: Full skin phantom description and skin closeup image. Bottom row, from left to right: Absorption and scattering coefficients per-wavelength for each skin layer, and result on a human cheek.

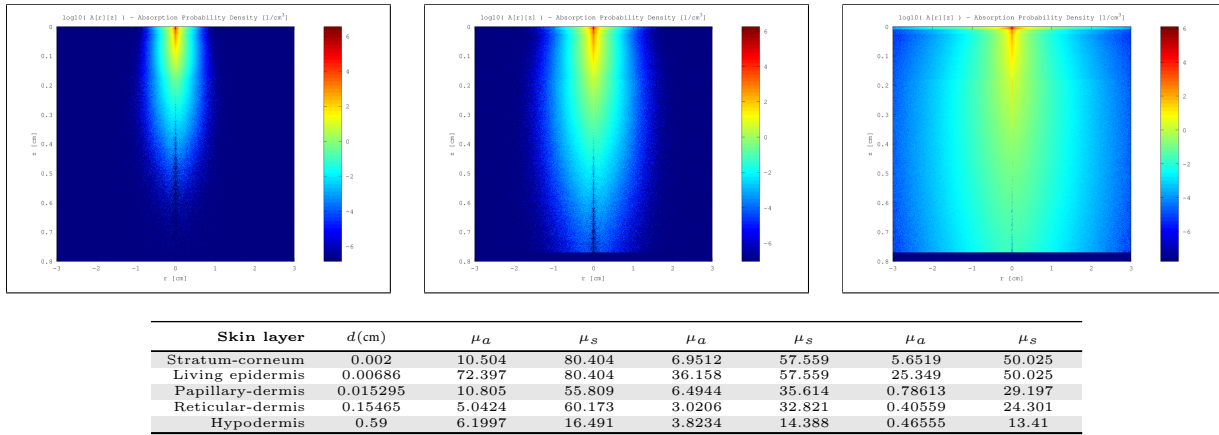
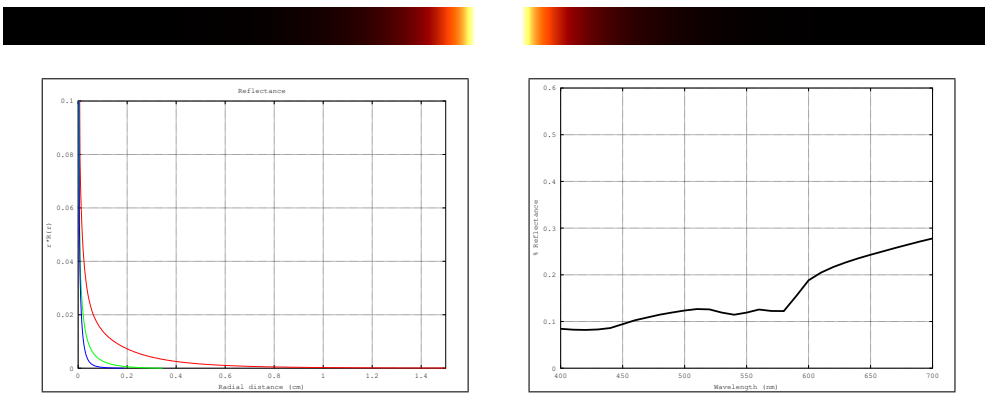


Figure 206: Top row: MonteCarlo simulations for 450nm, 550nm and 610nm. Bottom row: Resultant optical parameters (d , μ_a , μ'_s) applying our skin aging model.



Fitting	R	G	B
w_i v_i RMS,AMAX	(664.384, 63.538, 6.414, 1.250, 0.220, 0.031) (0.508, 2.413, 19.917, 138.547, 1124.270, 8926.604) 6.63e-12, 8e-04f	(408.023, 45.802, 4.620, 1.255, 0.270, 0.038) (0.442, 1.877, 10.718, 46.720, 219.035, 1222.895) 8.18e-12, 5e-04f	(516.944, 74.190, 22.644, 4.320, 0.848, 0.066) (0.348, 0.848, 2.351, 10.562, 45.502, 256.253) 1.78e-08, 3e-02f

Figure 207: Top row: Diffusion profile response for a pencil light-beam. Middle-row: RGB-profiles and reflectance-per-wavelength. Bottom row: Result of fitting the RGB-profile with 6 weighted Gaussians.

Female Age 80 $\xi = 1$ v_m 5 v_{Hb} 5

Gender	Age	ξ	v_m	v_{Hb}	c_{bil}	c_{car}	Skin roughness
Female	80	1	5	5	0.05	2.1e-4	0.14797

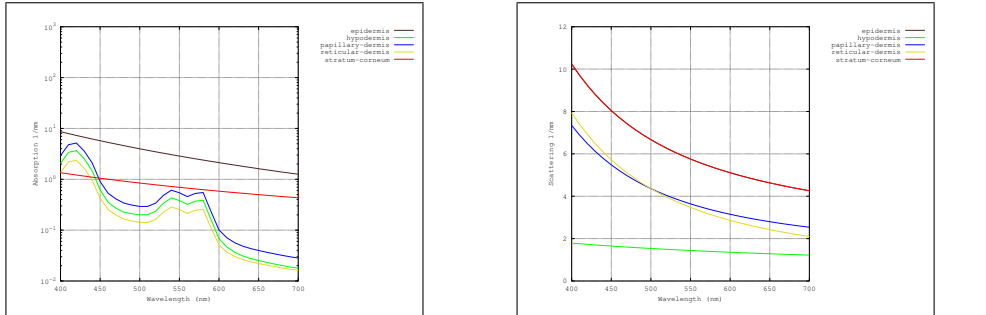


Figure 208: Top row: Full skin phantom description and skin closeup image. Bottom row, from left to right: Absorption and scattering coefficients per-wavelength for each skin layer, and result on a human cheek.

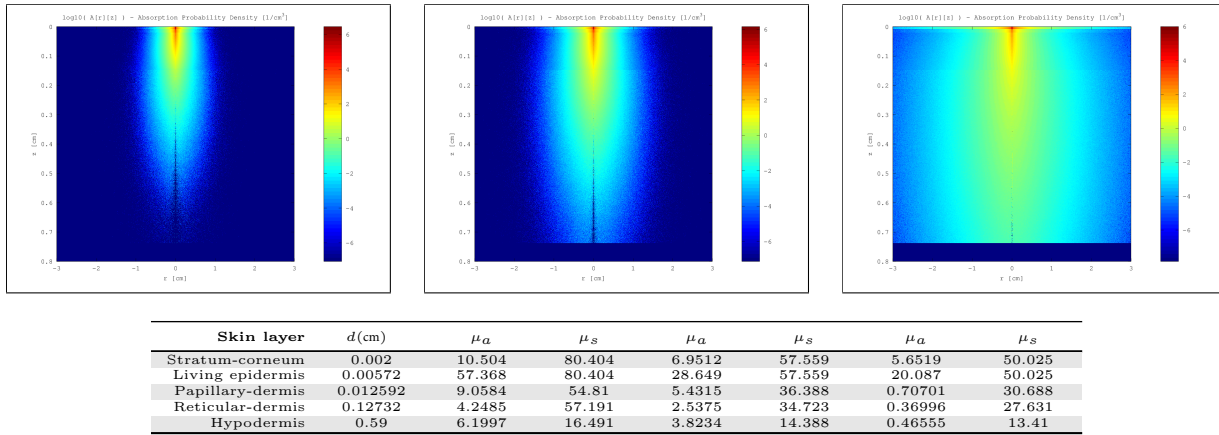
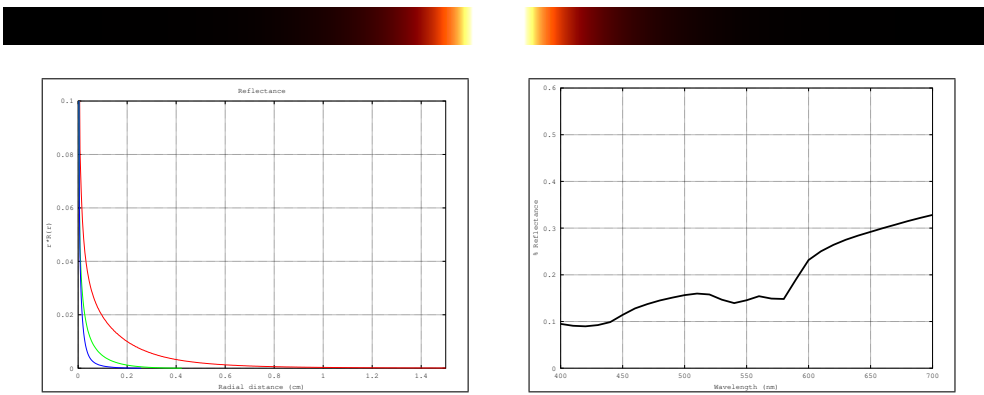


Figure 209: Top row: MonteCarlo simulations for 450nm, 550nm and 610nm. Bottom row: Resultant optical parameters (d , μ_a , μ'_s) applying our skin aging model.



Fitting	R	G	B
w_i v_i RMS,AMAX	(646.224, 45.342, 6.418, 1.332, 0.280, 0.040) (0.555, 2.698, 21.799, 159.938, 1230.653, 8832.370) 1.95e-11, 1e-03f	(383.706, 38.870, 4.954, 1.321, 0.300, 0.047) (0.487, 1.895, 11.563, 56.775, 290.650, 1610.997) 1.32e-11, 6e-04f	(469.001, 40.418, 6.244, 1.696, 0.311, 0.032) (0.449, 1.701, 7.648, 28.561, 115.555, 638.849) 1.20e-10, 2e-03f

Figure 210: Top row: Diffusion profile response for a pencil light-beam. Middle-row: RGB-profiles and reflectance-per-wavelength. Bottom row: Result of fitting the RGB-profile with 6 weighted Gaussians.

Female Age 30 $\xi = 0$ v_m 7 v_{Hb} 5

Gender	Age	ξ	v_m	v_{Hb}	c_{bil}	c_{car}	Skin roughness
Female	30	0	7	5	0.05	2.1e-4	0.081579

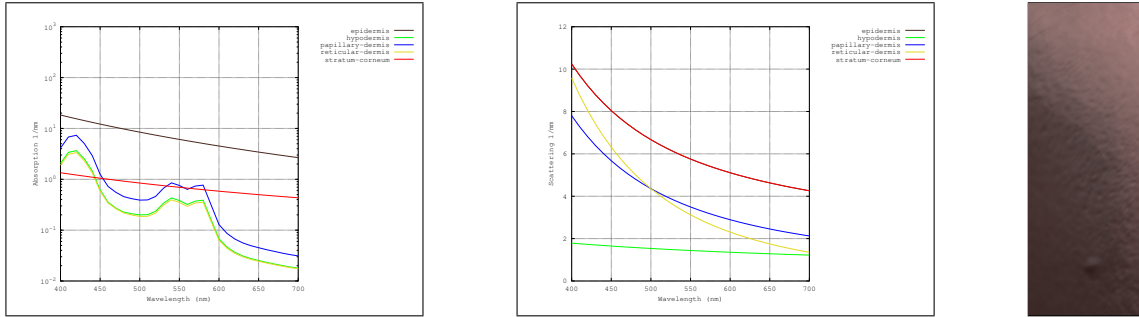


Figure 211: Top row: Full skin phantom description and skin closeup image. Bottom row, from left to right: Absorption and scattering coefficients per-wavelength for each skin layer, and result on a human cheek.

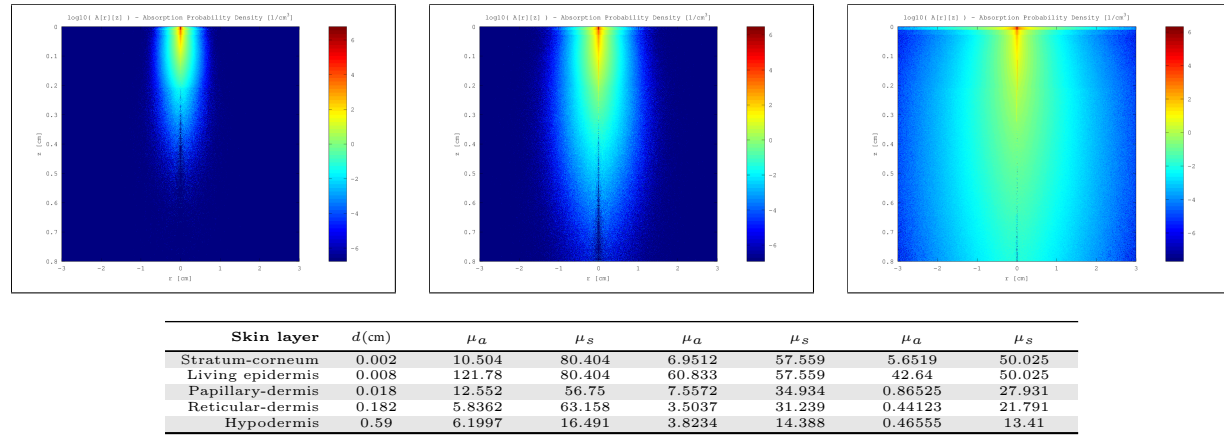
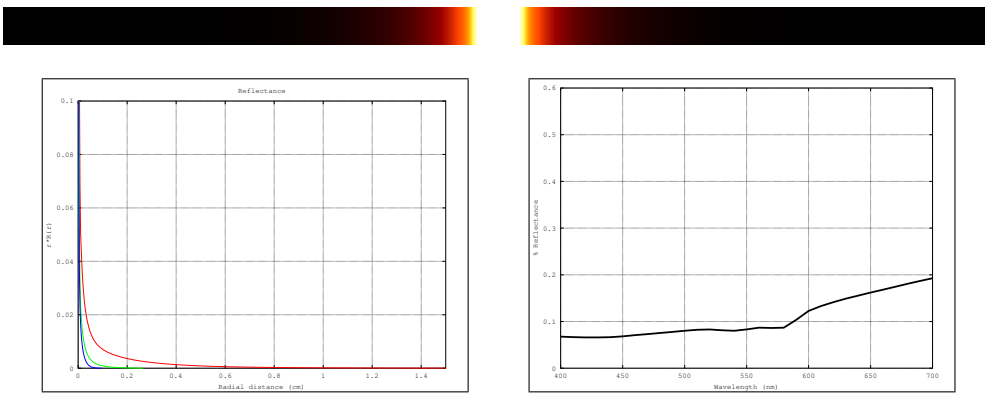


Figure 212: Top row: MonteCarlo simulations for 450nm, 550nm and 610nm. Bottom row: Resultant optical parameters (d , μ_a , μ'_s) applying our skin aging model.



Fitting	R	G	B
w_i v_i RMS,AMAX	(661.509, 52.997, 4.931, 0.870, 0.121, 0.016) (0.511, 2.646, 19.666, 125.983, 1041.692, 9151.829) 3.68e-13, 2e-04f	(390.623, 30.737, 3.308, 1.027, 0.239, 0.026) (0.473, 2.109, 9.090, 31.678, 129.848, 738.863) 5.65e-11, 1e-03f	(484.162, 178.467, 38.546, 5.213, 1.225, 0.194) (0.278, 0.457, 1.378, 5.330, 20.509, 81.665) 3.63e-09, 1e-02f

Figure 213: Top row: Diffusion profile response for a pencil light-beam. Middle-row: RGB-profiles and reflectance-per-wavelength. Bottom row: Result of fitting the RGB-profile with 6 weighted Gaussians.

Female Age 55 $\xi = 0$ v_m 7 v_{Hb} 5

Gender	Age	ξ	v_m	v_{Hb}	c_{bil}	c_{car}	Skin roughness
Female	55	0	7	5	0.05	2.1e-4	0.12802

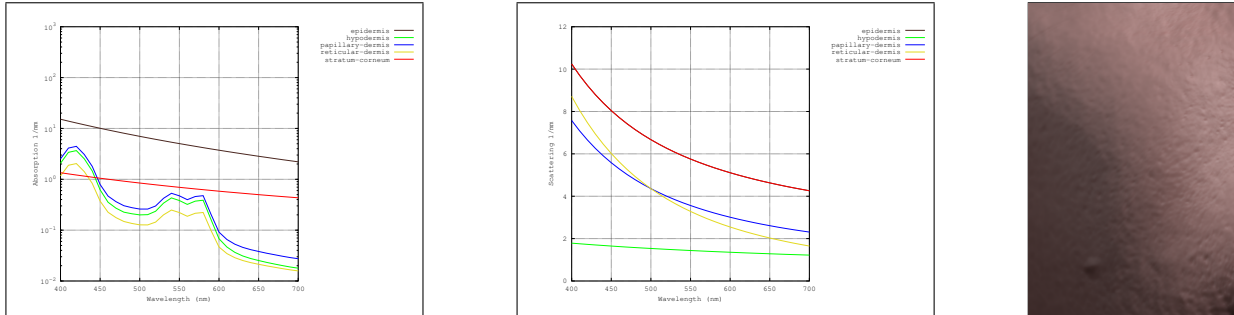


Figure 214: Top row: Full skin phantom description and skin closeup image. Bottom row, from left to right: Absorption and scattering coefficients per-wavelength for each skin layer, and result on a human cheek.

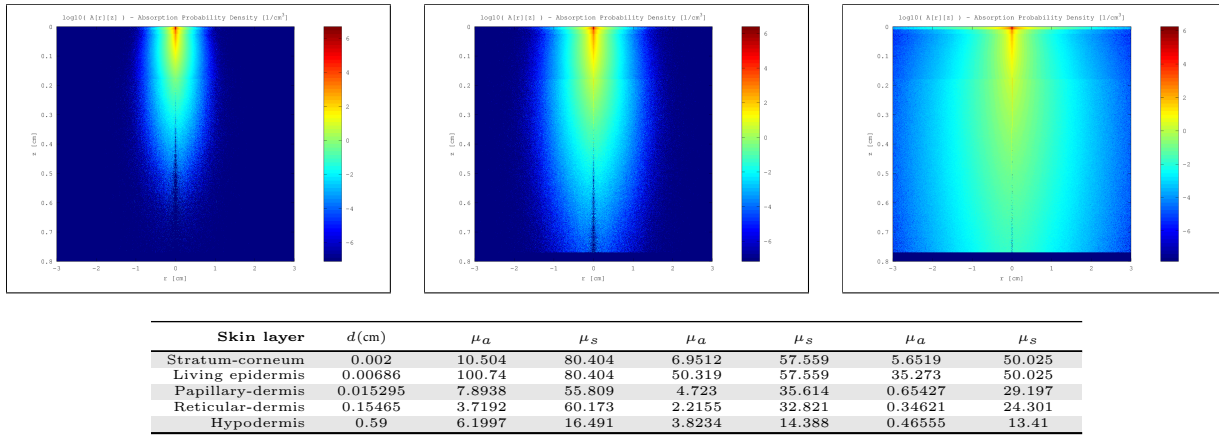
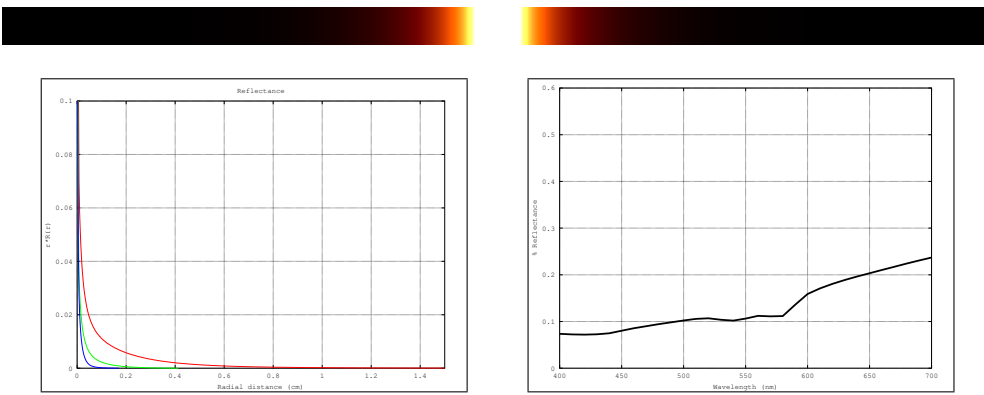


Figure 215: Top row: MonteCarlo simulations for 450nm, 550nm and 610nm. Bottom row: Resultant optical parameters (d , μ_a , μ'_s) applying our skin aging model.



Fitting	R	G	B
w_i v_i RMS,AMAX	(667.268, 59.608, 5.816, 1.085, 0.182, 0.026) (0.501, 2.363, 19.065, 131.607, 1083.020, 8815.819) 4.18e-12, 6e-04f	(399.778, 38.193, 3.895, 0.934, 0.181, 0.025) (0.455, 1.927, 11.182, 51.579, 257.308, 1561.148) 1.58e-12, 2e-04f	(503.526, 99.097, 20.359, 3.560, 0.708, 0.058) (0.327, 0.705, 2.208, 9.759, 41.697, 213.987) 1.93e-09, 8e-03f

Figure 216: Top row: Diffusion profile response for a pencil light-beam. Middle-row: RGB-profiles and reflectance-per-wavelength. Bottom row: Result of fitting the RGB-profile with 6 weighted Gaussians.

Female Age 80 $\xi = 0$ v_m 7 v_{Hb} 5

Gender	Age	ξ	v_m	v_{Hb}	c_{bil}	c_{car}	Skin roughness
Female	80	0	7	5	0.05	2.1e-4	0.18059

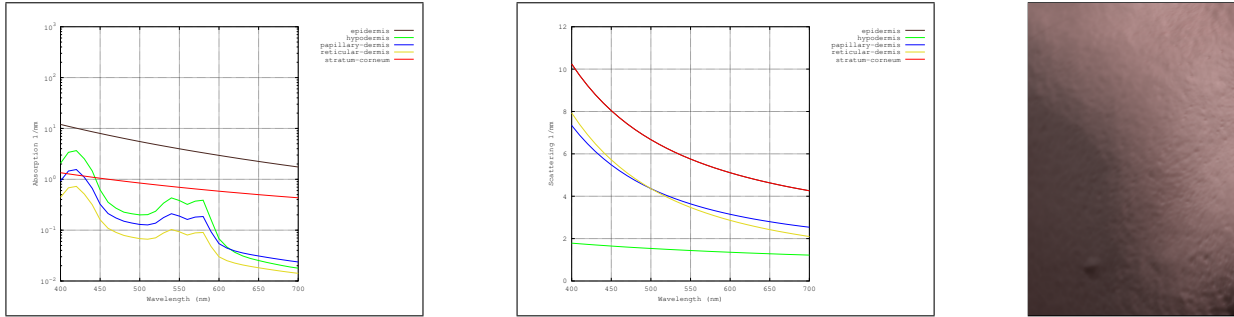


Figure 217: Top row: Full skin phantom description and skin closeup image. Bottom row, from left to right: Absorption and scattering coefficients per-wavelength for each skin layer, and result on a human cheek.

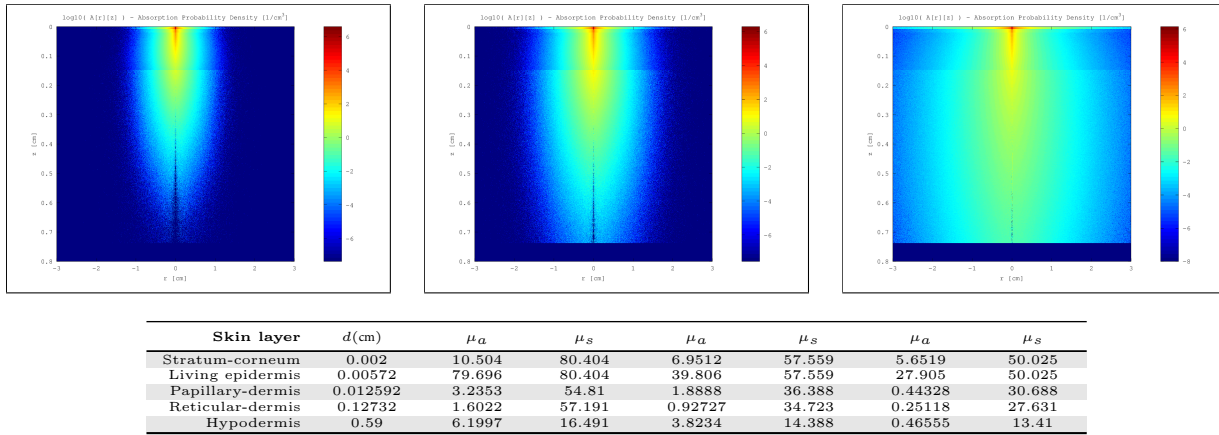
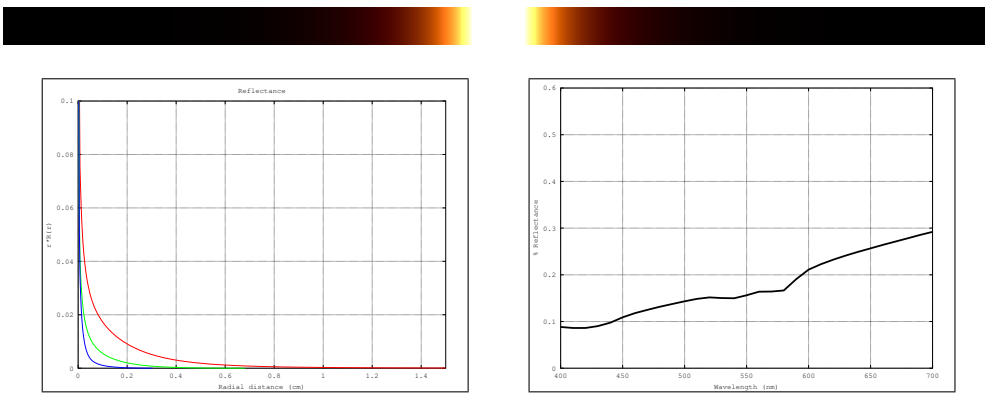


Figure 218: Top row: MonteCarlo simulations for 450nm, 550nm and 610nm. Bottom row: Resultant optical parameters (d , μ_a , μ'_s) applying our skin aging model.



Fitting	R	G	B
w_i v_i RMS,AMAX	(643.456, 41.186, 5.837, 1.192, 0.248, 0.036) (0.553, 2.753, 21.863, 159.747, 1244.379, 9010.152) 1.65e-11, 1e-03f	(377.579, 28.982, 4.026, 0.923, 0.193, 0.031) (0.510, 2.174, 14.060, 78.617, 472.358, 2920.177) 8.52e-12, 5e-04f	(143.992, 102.519, 87.255, 85.045, 5.905, -0.736) (0.575, 0.500, 0.487, 0.896, 14.277, 0.032) 1.34e-05, 7e-01f

Figure 219: Top row: Diffusion profile response for a pencil light-beam. Middle-row: RGB-profiles and reflectance-per-wavelength. Bottom row: Result of fitting the RGB-profile with 6 weighted Gaussians.

Female Age 30 $\xi = 1$ v_m 7 v_{Hb} 5

Gender	Age	ξ	v_m	v_{Hb}	c_{bil}	c_{car}	Skin roughness
Female	30	1	7	5	0.05	2.1e-4	0.069549

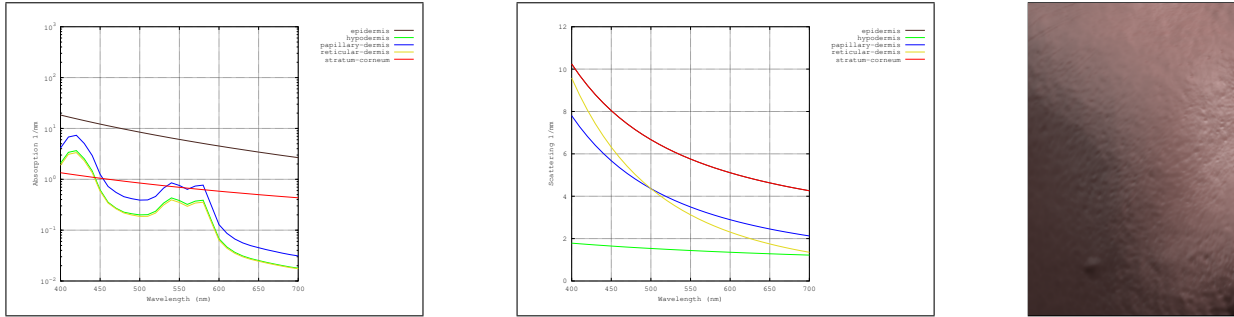


Figure 220: Top row: Full skin phantom description and skin closeup image. Bottom row, from left to right: Absorption and scattering coefficients per-wavelength for each skin layer, and result on a human cheek.

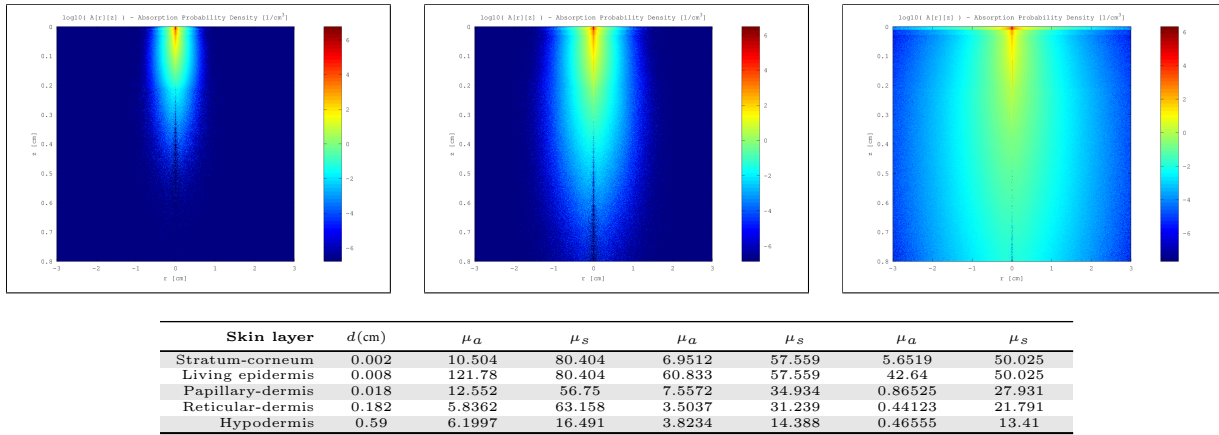
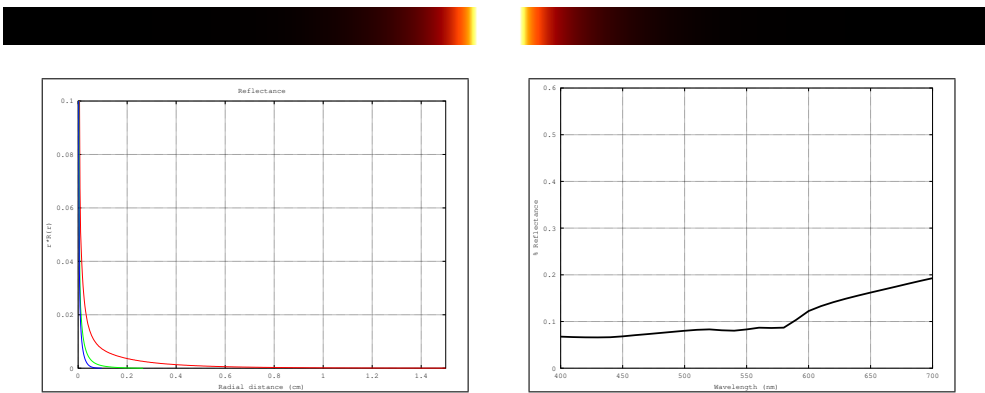


Figure 221: Top row: MonteCarlo simulations for 450nm, 550nm and 610nm. Bottom row: Resultant optical parameters (d , μ_a , μ'_s) applying our skin aging model.



Fitting	R	G	B
w_i v_i RMS,AMAX	(661.854, 53.815, 4.976, 0.880, 0.123, 0.016) (0.509, 2.616, 19.470, 124.426, 1028.764, 9080.293) 3.16e-13, 2e-04f	(391.823, 31.020, 3.249, 0.962, 0.215, 0.024) (0.472, 2.119, 9.546, 34.234, 140.403, 781.266) 1.48e-11, 6e-04f	(496.064, 161.451, 22.043, 3.764, 0.934, 0.150) (0.283, 0.567, 1.858, 6.882, 24.728, 90.343) 1.79e-10, 2e-03f

Figure 222: Top row: Diffusion profile response for a pencil light-beam. Middle-row: RGB-profiles and reflectance-per-wavelength. Bottom row: Result of fitting the RGB-profile with 6 weighted Gaussians.

Female Age 55 $\xi = 1$ v_m 7 v_{Hb} 5

Gender	Age	ξ	v_m	v_{Hb}	c_{bil}	c_{car}	Skin roughness
Female	55	1	7	5	0.05	2.1e-4	0.099683

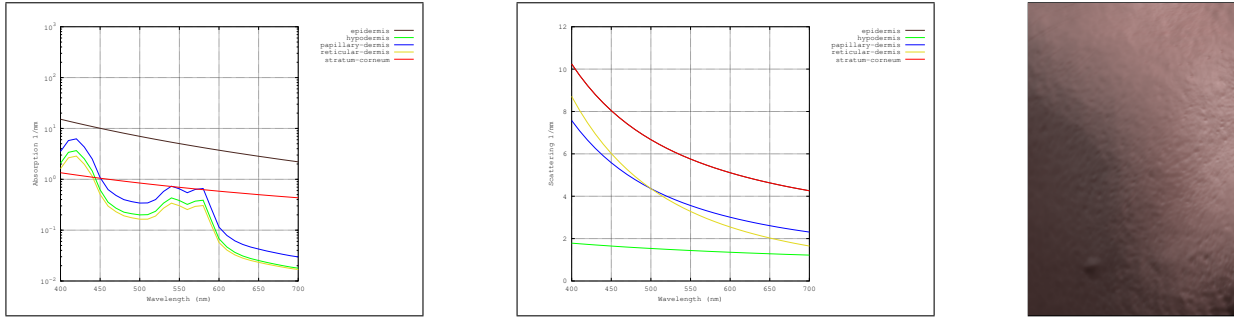


Figure 223: Top row: Full skin phantom description and skin closeup image. Bottom row, from left to right: Absorption and scattering coefficients per-wavelength for each skin layer, and result on a human cheek.

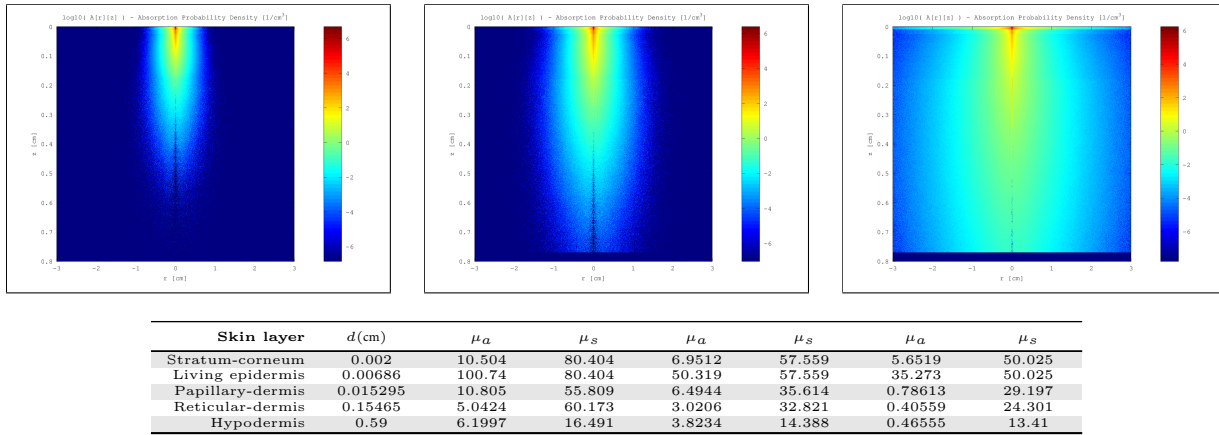


Figure 224: Top row: MonteCarlo simulations for 450nm, 550nm and 610nm. Bottom row: Resultant optical parameters (d , μ_a , μ'_s) applying our skin aging model.

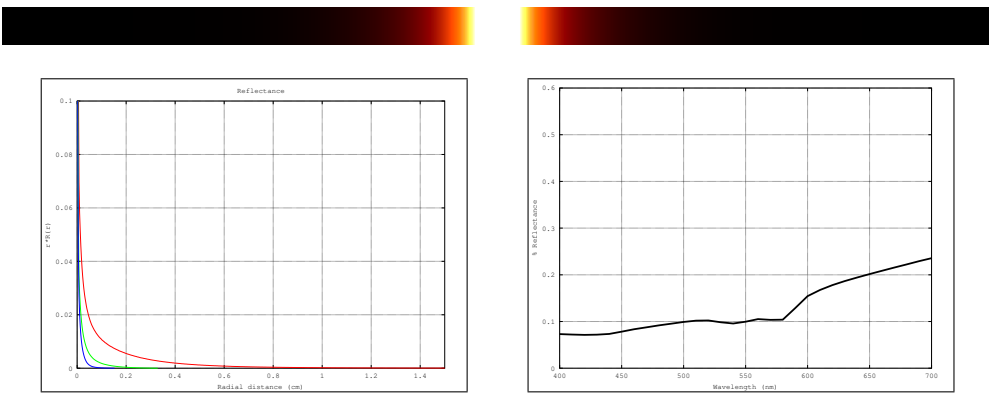


Figure 225: Top row: Diffusion profile response for a pencil light-beam. Middle-row: RGB-profiles and reflectance-per-wavelength. Bottom row: Result of fitting the RGB-profile with 6 weighted Gaussians.

Female Age 80 $\xi = 1$ v_m 7 v_{Hb} 5

Gender	Age	ξ	v_m	v_{Hb}	c_{bil}	c_{car}	Skin roughness
Female	80	1	7	5	0.05	2.1e-4	0.14797

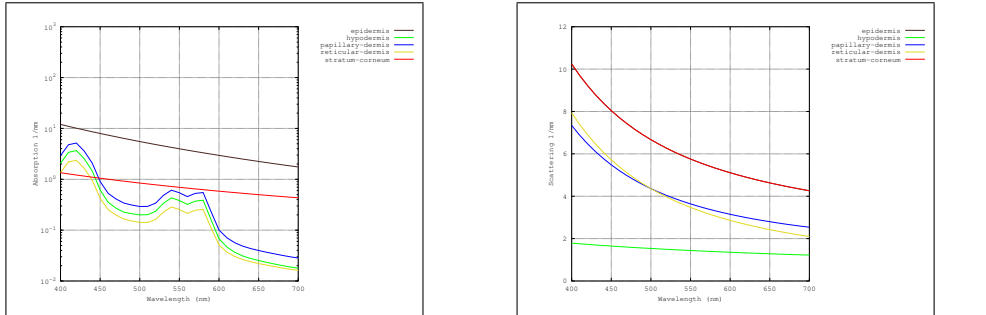


Figure 226: Top row: Full skin phantom description and skin closeup image. Bottom row, from left to right: Absorption and scattering coefficients per-wavelength for each skin layer, and result on a human cheek.

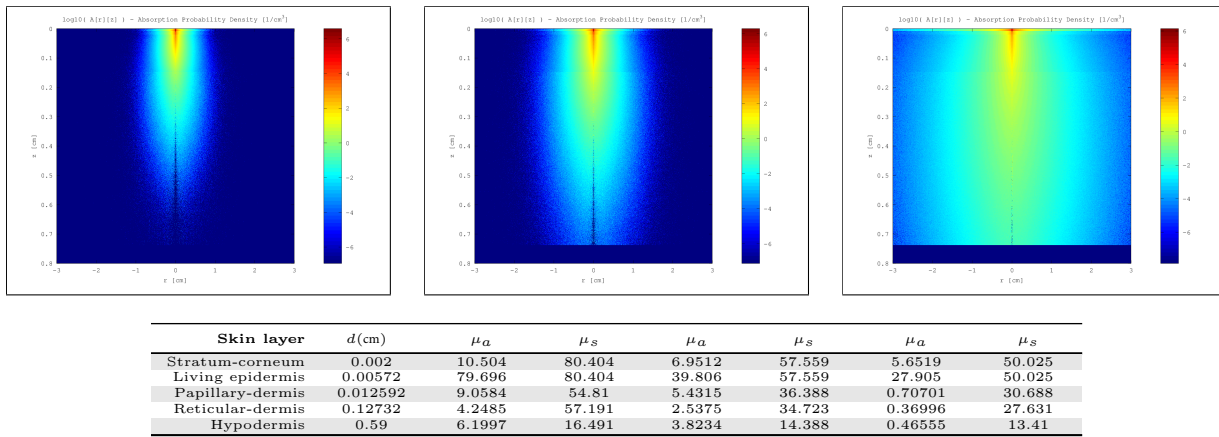
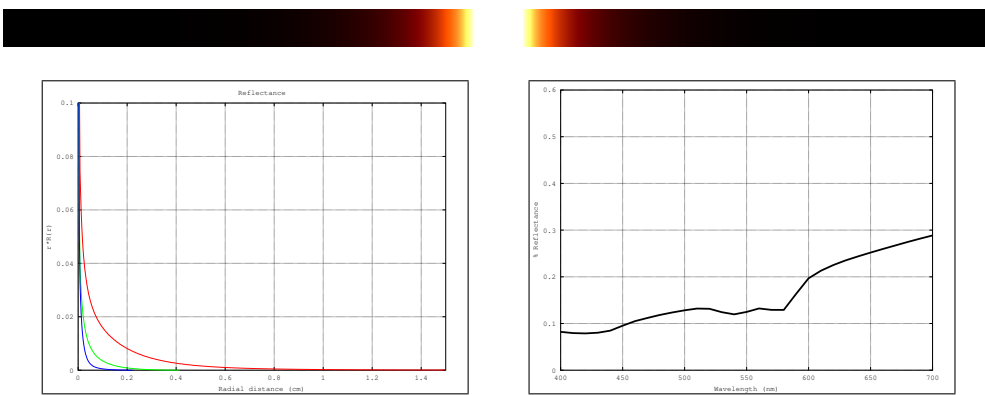


Figure 227: Top row: MonteCarlo simulations for 450nm, 550nm and 610nm. Bottom row: Resultant optical parameters (d , μ_a , μ_s') applying our skin aging model.



Fitting	R	G	B
w_i v_i RMS,AMAX	(646.425, 43.566, 6.029, 1.231, 0.246, 0.035) (0.547, 2.628, 20.526, 147.515, 1143.189, 8410.081) 1.49e-11, 1e-03f	(388.003, 36.395, 4.430, 1.130, 0.249, 0.038) (0.477, 1.870, 11.243, 53.752, 269.793, 1536.807) 2.77e-12, 3e-04f	(546.248, 56.760, 6.520, 1.928, 0.400, 0.034) (0.362, 1.301, 5.552, 19.665, 77.519, 458.327) 8.58e-11, 2e-03f

Figure 228: Top row: Diffusion profile response for a pencil light-beam. Middle-row: RGB-profiles and reflectance-per-wavelength. Bottom row: Result of fitting the RGB-profile with 6 weighted Gaussians.